

LYRA Calibration Report

1. Radiometric Model Simulation
2. Calibration Software
3. Flatfield Software
4. Off-Pointing Simulation
5. Pulsed-LED Tests
6. Noise Distribution

1. Radiometric Model Simulation

The LYRA Radiometric Model was calculated and presented on the instrument's web pages at http://lyra.oma.be/radiometric_model/radiometric_model.php

Sample values for spectral irradiance were taken from the TIMED/SEE instrument. To calculate estimated LYRA responses, values for filter transmittance and detector responsivity were taken from various BESSY campaigns in 2005 and 2006: first filter and detector values separately, then combined as the LYRA configuration was selected. The latest values of the BESSY campaign of February 2007 still have to be integrated into the model. Some entries in the web pages have to be updated:

- Although it says on the web page, "XN" is the "currently considered" filter for the Lyman alpha channels, for LYRA channel 3-1 it is "N+XN" which is stated as "now discarded".
- Although it only says "Zirconium" on the web page table, it is Zr (150nm) for channel 2-4 and Zr (300nm) for the other two.
- Although the aperture area is given as 7.06858e-08 square meter on the web page, calculations obviously were always done with 7.06858e-06, which is correct.

Purity definitions:

- The Herzberg channel is always given as 200-220 nm.
- The Zirconium channel is given as 0-20 nm or 1-20 nm.
- The Aluminium channel is given as 17-70 nm (or as "n/a") in the "LYRA" paper, ASR 2006; I used 17-80 nm, as it says on the web pages.
- The Lyman alpha channel is given as 115-125 nm or 121.6 +/- 2.5 nm in the "LYRA" paper, ASR 2006. On the web pages it just says 121.5 nm. I used a 2.5 nm interval around 121.5, i.e. 121.5 +/- 1.25 nm. On the other hand, there is only one single significant Lyman alpha value in the TIMED/SEE solar flux data, anyway.

Simulations are built on the hypothesis that filter transmittance and detector responsivity are actually zero where undefined, i.e. above or below certain physical thresholds. After the theoretical response (with filter and detector values treated separately), the response with the measured combined values were simulated.

Then I tried to figure out the "calibration" factors with which one could re-calculate the measured solar irradiance (TIMED/SEE "minimum", "maximum" and "high") from the estimated output of the various channels. In order to do this, one has to multiply the LYRA channel output signal (in Ampere) with a factor (in $W A^{-1} m^{-2}$) to estimate the solar signal in the corresponding interval (in $W m^{-2}$). This calibration factor depends on the purity (which can vary), the aperture area (which is constant), and a response factor that depends on the average filter transmittance and detector responsivity in the spectral interval corresponding to the channel (which should be more or less constant).

$$\frac{\text{LYRA signal [A]} * \text{purity [\%]} / \text{area [m}^2\text{]} / \text{response factor [A W}^{-1}\text{]}}{\text{calibration factor}} = \text{solar signal [W m}^{-2}\text{]}$$

The question is if one can deduce the calibration factor from the simulations, despite the fact that it involves an integral of various multiplied curves, and if this factor is constant.

*-1 (Lyman alpha channels +/- 121.5 nm)

The purity appears to grow linear with the irradiance, therefore the calibration factor is not constant. But maybe it can be calculated in a straightforward way, using the LYRA signal itself. (In the double-filter channel 3-1 the purity values are closer together.)

*-2 (Herzberg channels 200-220 nm)

The purity appears to be constant, and the resulting calibration factor is also constant. On the other hand, the values seem to be estimated from irradiance measurements which are completely identical, at least in the spectral interval of interest.

*-3 (Aluminium channels 17-80 nm)

The purity is heavily dependent on the solar irradiance: for high solar flux, the LYRA signal is dominated by shorter wavelengths and the purity goes towards 2-10%. Maybe the solar minimum and maximum, or flare situations, have to be treated separately.

*-4 (Zirconium channels 1-20 nm)

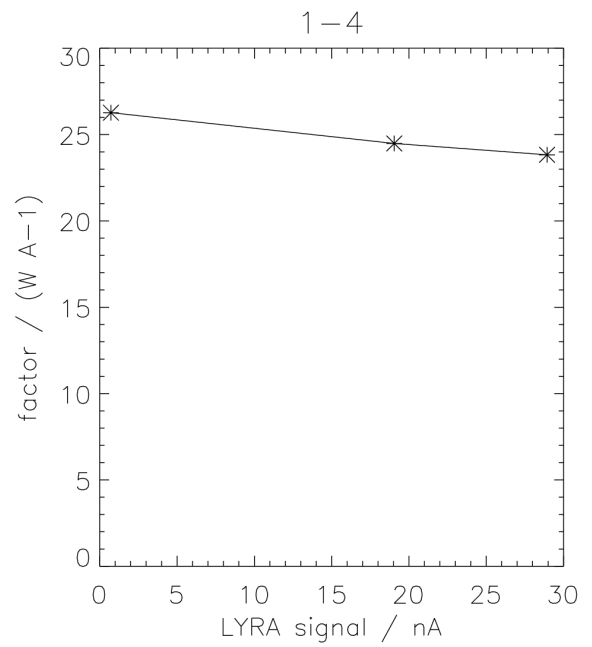
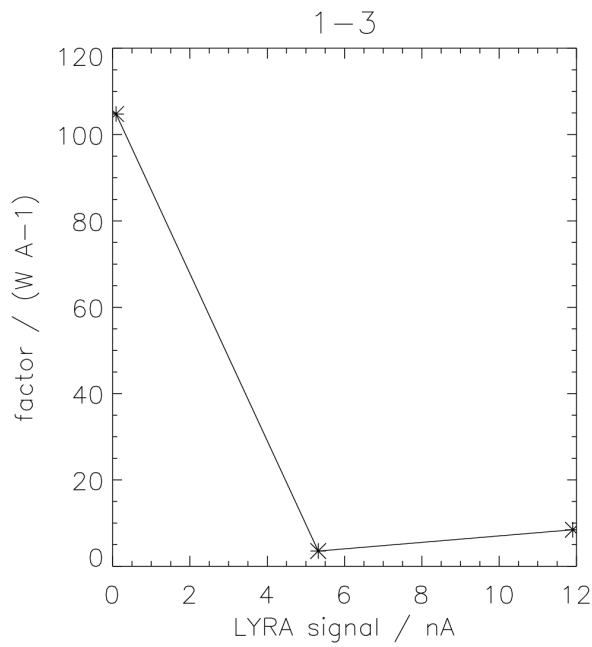
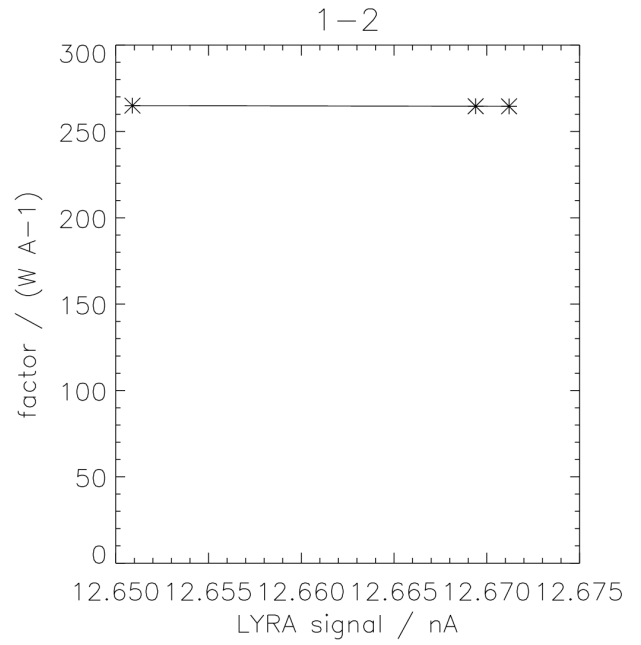
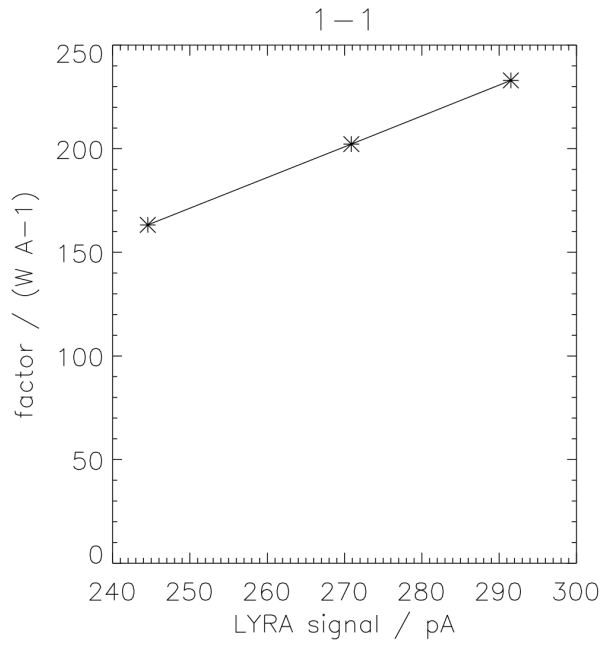
The purity is always constant in an almost ideal way (~100%), the additional influence of the double filter (channels 1-4, 3-4) being less than 0.1%. The responsivity (influence of very short wavelengths!) appears to be higher for higher irradiance, so the calibration factor declines, but in an almost linear way. Maybe it can also be calculated in a straightforward way, using the LYRA signal itself.

It would probably be useful to estimate the calibration factors with more solar irradiance samples than just the three samples from TIMED/SEE.

Head 1

ch. flux ====	LYRA signal * [A] =====	purity [%] =====	/area / [m2] ====	resp.factor = [A W-1] =====	solar signal [W m-2] =====
1-1 Ly XN + MSM12 -----					
min	244.548 pA	23.6732	/ A /	0.00145018	= 0.00564762
max	291.520 pA	33.7892	A	0.00145035	0.00960818
high	270.879 pA	29.3251	A	0.00145022	0.00774904
1-2 Herzberg + PIN10 -----					
min	12.6509 nA	83.8327	A	0.00316396	0.474210
max	12.6694 nA	83.7100	A	0.00316396	0.474210
high	12.6712 nA	83.6982	A	0.00316396	0.474210
1-3 Aluminium + MSM11 -----					
min	0.0884 nA	61.0785	A	0.00583021	0.0013105
max	11.9076 nA	4.7316	A	0.00717245	0.0111131
high	5.3192 nA	2.5320	A	0.00559629	0.0034047
1-4 Zr (300nm) + AXUV20D -----					
min	0.7201 nA	99.9920	A	0.0380640	0.0026762
max	28.9357 nA	99.9972	A	0.0419707	0.0975310
high	19.0501 nA	99.9993	A	0.0408429	0.0659849

A=7.06858e-06 m2



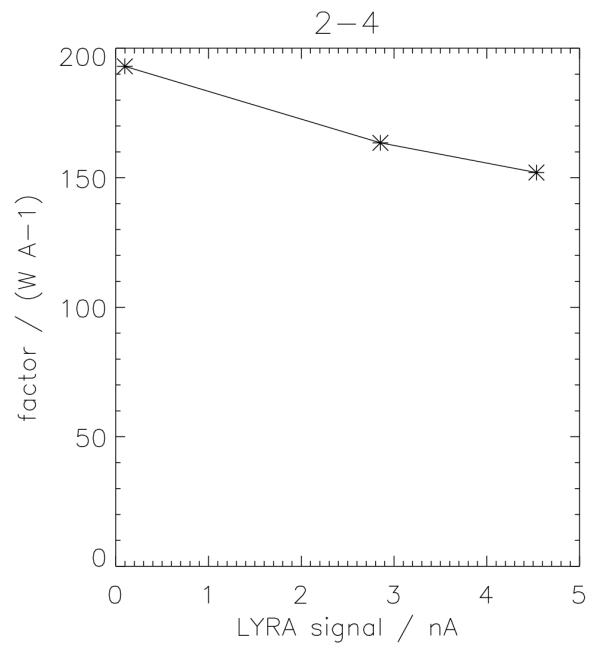
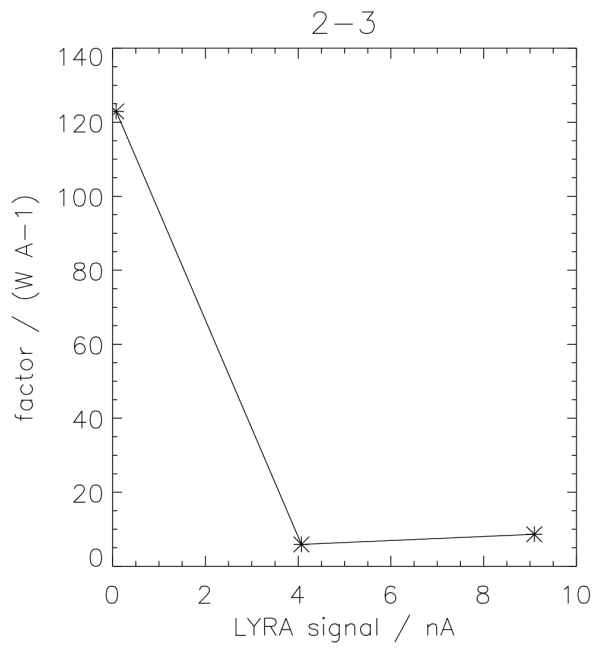
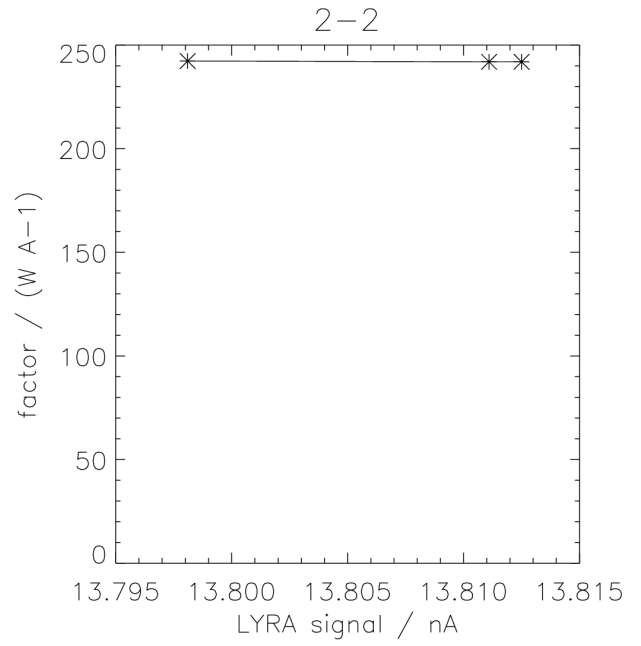
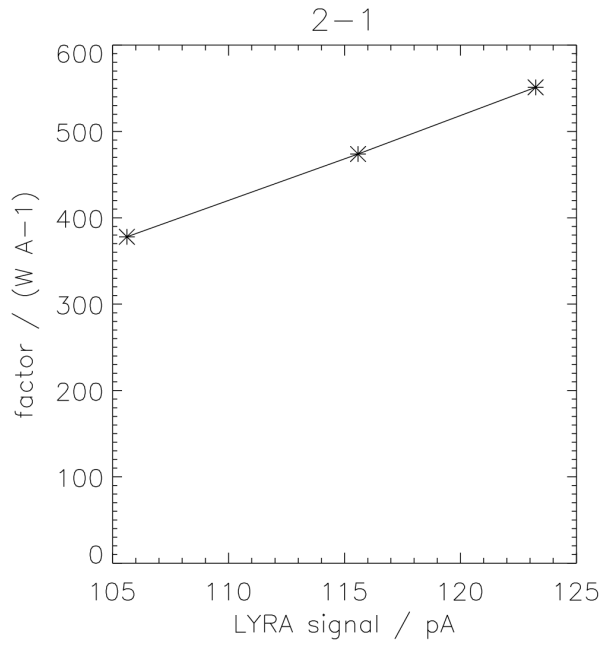
Caption for this and the following figures:

Separately for the four channels of one LYRA head, the factors are shown that are necessary to convert the simulated output signal back to the input signal of interest.

Head 2

ch.	LYRA signal *	purity	/area /	resp.factor =	solar signal
flux	[A]	[%]	[m2]	[A W-1]	[W m-2]
====	=====	=====	====	=====	=====
2-1 Ly XN + MSM21					
min	105.615 pA	* 20.4182	/ A /	0.000540186	= 0.00564762
max	123.239 pA	29.7734	A	0.000540260	0.00960818
high	115.582 pA	25.6005	A	0.000540203	0.00774904
2-2 Herzberg + PIN11					
min	13.7981 nA	84.0515	A	0.00345989	0.474210
max	13.8111 nA	83.9724	A	0.00345989	0.474210
high	13.8125 nA	83.9639	A	0.00345989	0.474210
2-3 Aluminium + MSM15					
min	0.07535 nA	62.1494	A	0.00505581	0.0013105
max	9.09185 nA	5.5091	A	0.00637630	0.0111131
high	4.06936 nA	2.7505	A	0.00465076	0.0034047
2-4 Zr (150nm) + MSM19					
min	0.09801 nA	99.9166	A	0.00517676	0.0026762
max	4.53508 nA	99.9749	A	0.00657658	0.0975310
high	2.85311 nA	99.9934	A	0.00611665	0.0659849

A=7.06858e-06 m2



Head 3

ch.	LYRA signal *	purity	/area /	resp.factor =	solar signal
flux	[A]	[%]	[m2]	[A W-1]	[W m-2]
====	=====	=====	====	=====	=====
3-1 Ly N+XN + AXUV20A					

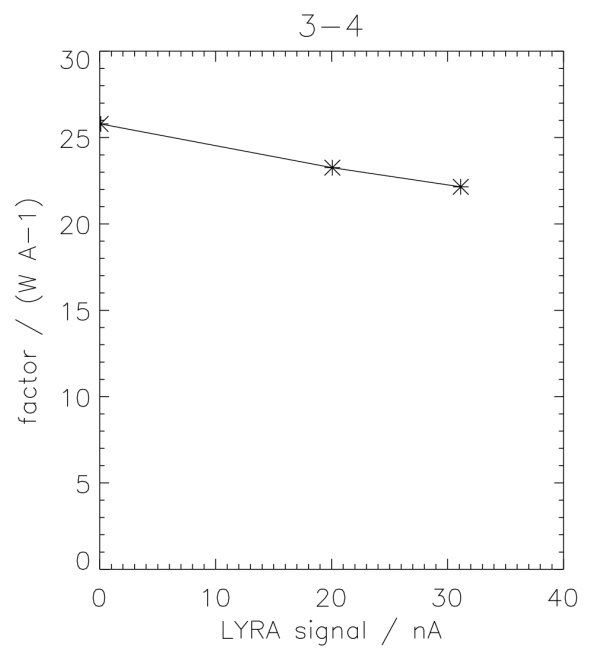
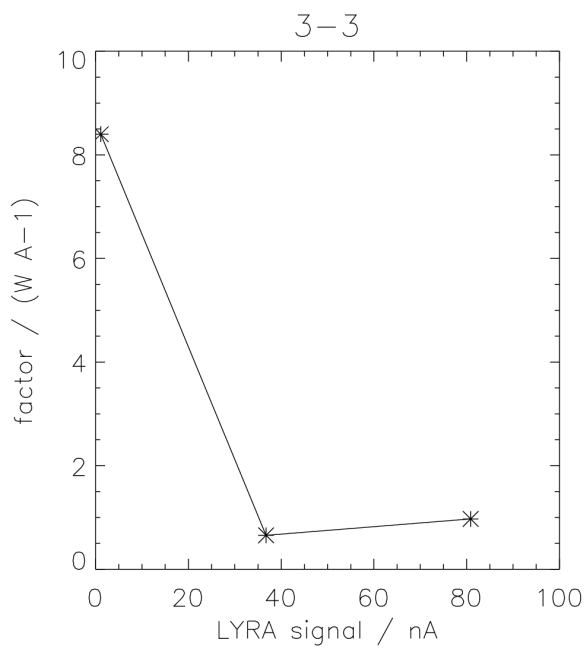
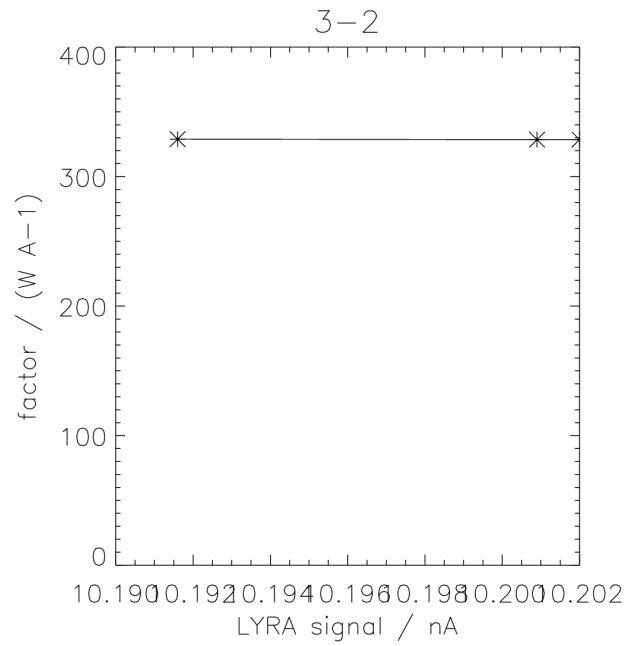
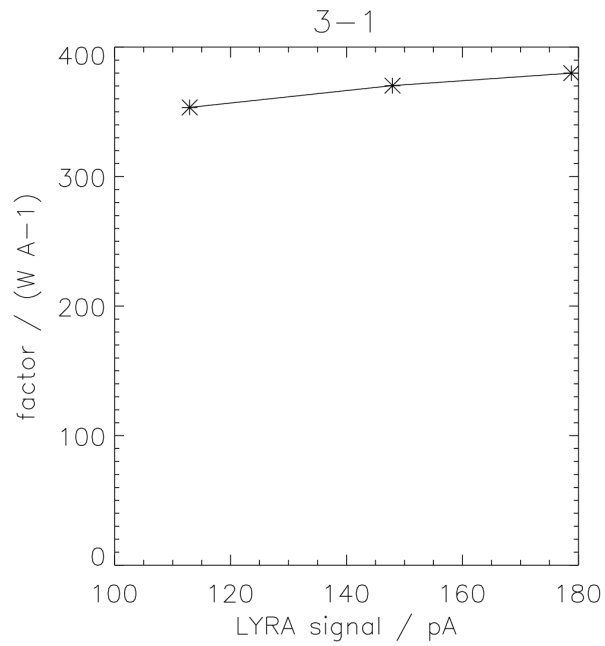
min	112.943 pA	* 79.4972	/ A /	0.00224913	= 0.00564762
max	178.780 pA	85.4482	A	0.00224930	0.00960818
high	147.934 pA	83.2798	A	0.00224919	0.00774904
3-2 Herzberg + PIN12					

min	10.1916 nA	83.7435	A	0.00254619	0.474210
max	10.2009 nA	83.6672	A	0.00254619	0.474210
high	10.2020 nA	83.6583	A	0.00254619	0.474210
3-3 Aluminium + AXUV20B					

min	1.1030 nA	74.3664	A	0.088551	0.0013105
max	80.8530 nA	10.3437	A	0.106464	0.0111131
high	36.7403 nA	5.6494	A	0.086244	0.0034047
3-4 Zr (300nm) + AXUV20C					

min	0.7335 nA	99.9909	A	0.0387750	0.0026762
max	31.1312 nA	99.9970	A	0.0451552	0.0975310
high	20.0586 nA	99.9992	A	0.0430052	0.0659849

A=7.06858e-06 m2



2. Calibration Software

In the previous chapter, it was considered how to calculate the solar signal (in absolute physical units, e.g., $W m^{-2}$) from its corresponding LYRA channel output (e.g., converted to A). It was argued that this estimation must involve the (potentially variable) purity, the (constant) aperture size, and a factor (linear or else) that combines the integrals of filter transmittance and detector responsivity in the spectral interval of interest.

Simulations showed the following: For the Lyman-alpha channels (*-1), purity grows with irradiance. For the Herzberg channels (*-2), purities and resulting calibration factors appear to be constant. For the Aluminium channels (*-3), purity varies heavily with irradiance. For the Zirconium channels (*-4), purity appears to be constant but responsivity grows with irradiance.

The question was asked if one could use the LYRA channel signal itself to calculate calibration factors that depend on the signal strength, maybe in a non-linear way. This was discussed at the LYRA meeting in Davos (05/06 Oct 2006) on the basis of the information shown in Figure 0. It was suggested to try and use information from *other* LYRA channels instead, in order to enhance the purity of certain problematic channels. In particular, it is clearly visible from the spectral responsivities of the Lyman-alpha channels that they are influenced by the neighbouring longer-wavelength continuum around 180-230 nm. Likewise, it is visible that the spectral responsivities of the Aluminium channels are influenced by the neighbouring shorter-wavelength signal around 1-10 nm. Since these disturbing signals are in fact observed and measured by LYRA via the Herzberg and Zirconium channels, respectively, it was suggested to subtract these signals in an appropriate way.

In the following, I suggest an attempt for procedures and resulting software for all twelve LYRA channels. First, in Figures 1-1 etc the measured combined responsivity is graphically presented for each channel together with three simulated spectral output signals. These signals were simulated with the help of TIMED/SEE spectral data sets called “min”, “high”, and “max”, taken on different days and representing a variety of solar irradiances to be expected. A longer-wavelength extension concerning wavelengths above 200 nm was added to the TIMED/SEE data sets; this extension does not vary. - Below these figures, the simulated values for the LYRA end signals are shown in a table: the “total” expected output signal, the “pure” signal of interest (defined by the nominal spectral interval of the channel), and the resulting difference “rest” signal (all in nA), together with the “solar” signal, i.e. the integrated input from the TIMED/SEE interval of interest (in $W m^{-2}$). - Subsequently, a method is suggested to calculate the latter from the former.

The procedures suggested here are solely based on the three data sets mentioned above, plus the assumption that zero solar input should lead to zero LYRA output. As soon as the assumed models look “reasonable”, linear interpolation between data points is suggested instead of assuming higher-order polynomial or exponential functions in the case of sublinear or superlinear relations. In other cases, simple linear factors can be used. Figures 1-1a etc show the relations between total or pure LYRA signals to the solar signal in the upper row, and – where applicable – the relation between the neighbouring channel signal and the rest signal in the lower row. The arguments are similar for all three heads (only the values vary), but different for all four channels.

In the case of higher values in the Aluminium channels (*-3), where more than 90% contamination have to be estimated and subtracted, the success appears doubtful.

As a next step, I suggest to test the model with other realistic TIMED/SEE data sets.

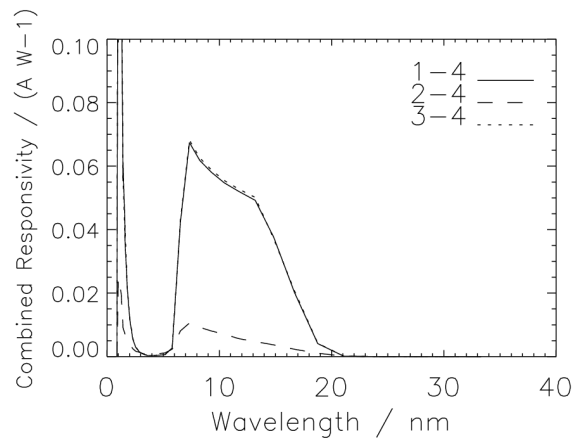
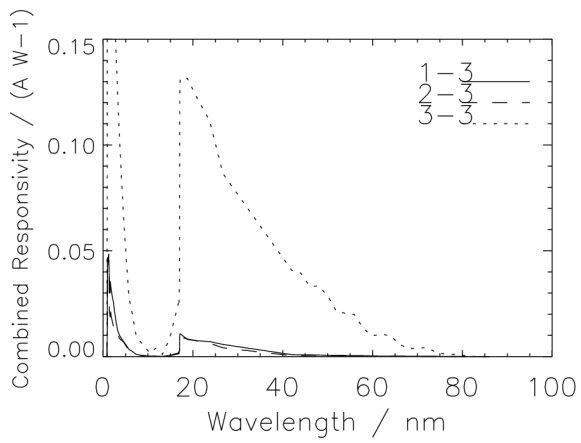
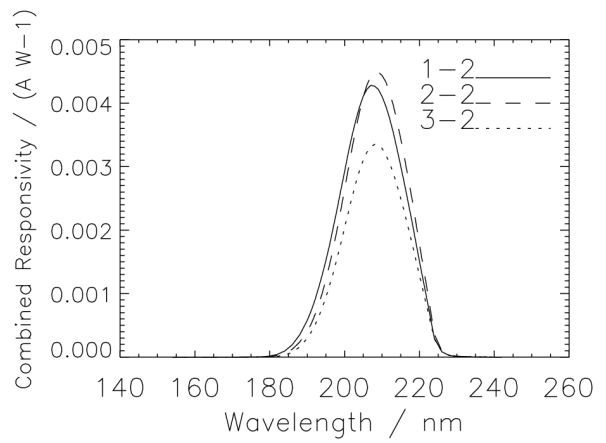
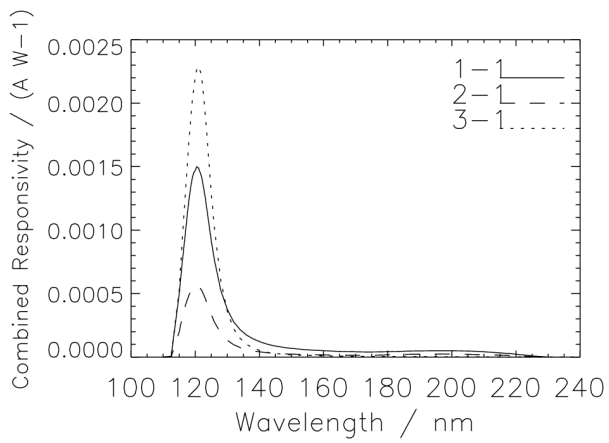


Figure 0. LYRA channel responsivities as presented at the Davos meeting: Combination of filter and detector effects measured as a function of wavelength. *-1 = Lyman-alpha channels, *-2 = Herzberg channels, *-3 = Aluminium channels, *-4 = Zirconium channels.

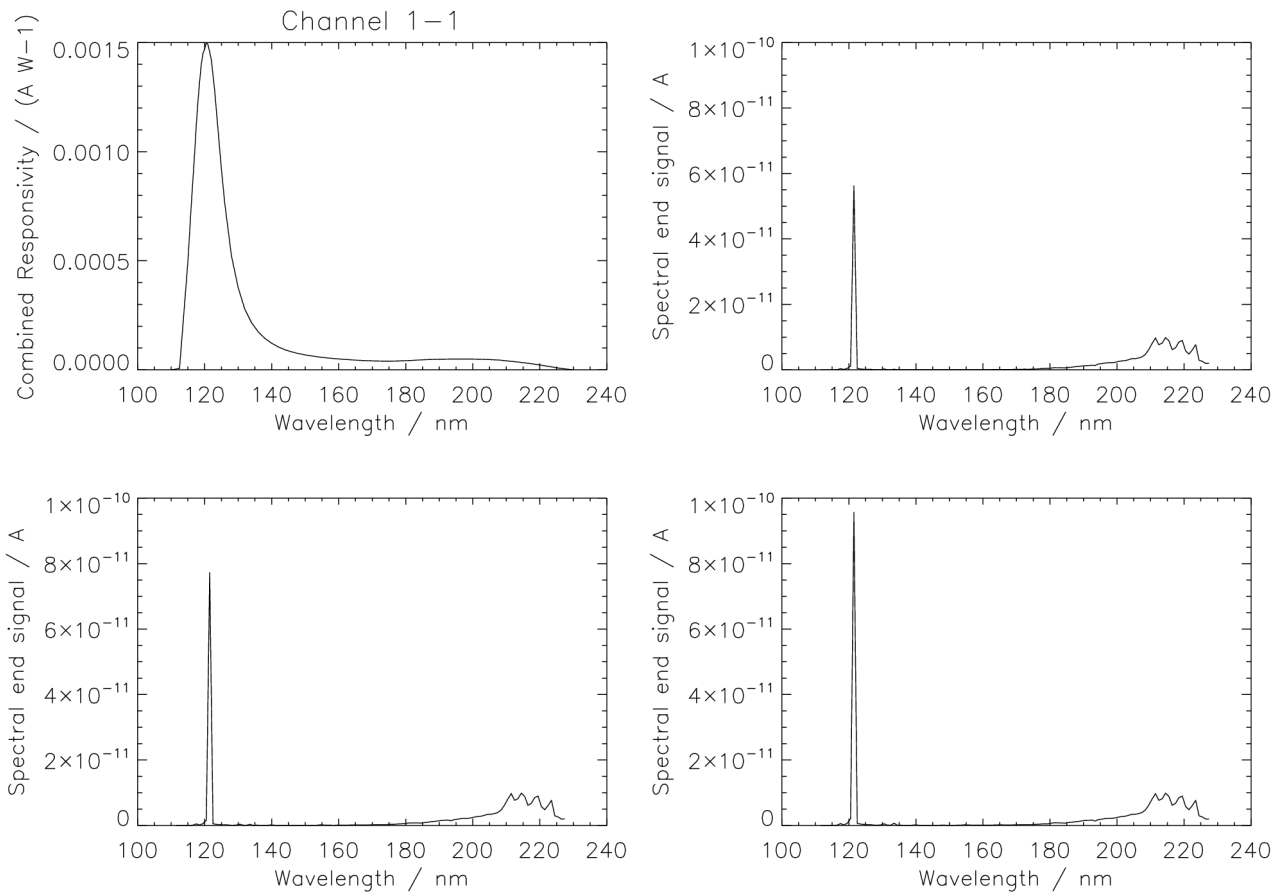


Figure 1-1. Measured responsivity and simulated output (min, high, max) for LYRA channel 1-1.

1-1: Ly XN + MSM12 (121.5 +/- nm)

sample	total	pure	rest	solar
min	0.244548 nA	0.0578922 nA (23.7%)	0.186656 nA	0.00564762 Wm ⁻²
high	0.270879 nA	0.0794356 nA (29.3%)	0.191444 nA	0.00774904 Wm ⁻²
max	0.291520 nA	0.0985021 nA (33.8%)	0.193018 nA	0.00960818 Wm ⁻²

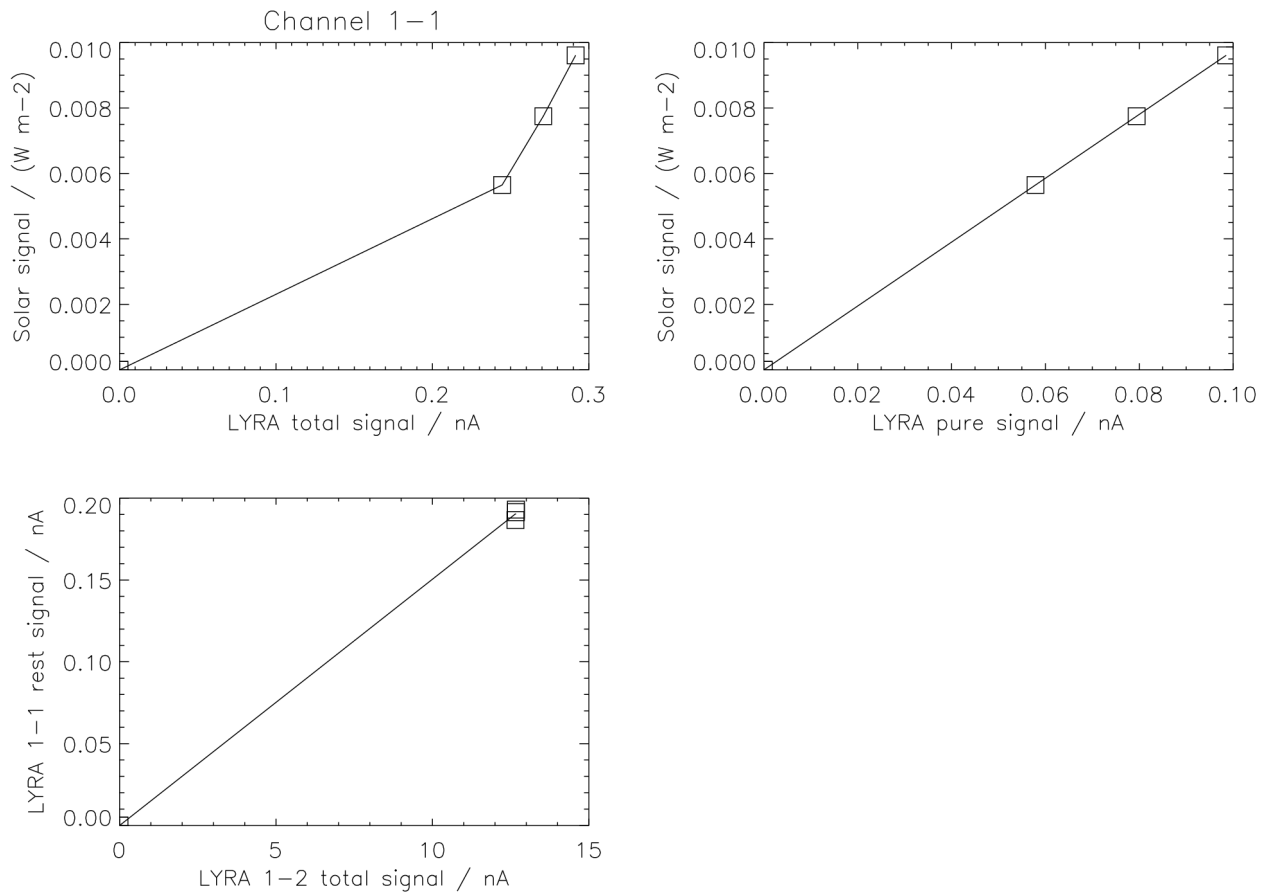


Figure 1-1a. Simulated relations between input and output for LYRA channel 1-1.

The functional relation between the solar signal and the LYRA total signal is obviously not straightforward (see upper left image). The reason is a contamination due to the influence of the interval 180-230 nm, which is not part of the nominal interval around the Lyman-alpha line. But this rest signal can obviously be estimated with the help of the output signal from LYRA channel 1-2 in a simple way (see lower image):

$$[LYRA\ 1-1\ rest\ signal / nA] = 0.015 * [LYRA\ 1-2\ total\ signal / nA]$$

The pure signal can be estimated as the difference:

$$[LYRA\ 1-1\ pure\ signal / nA] = [LYRA\ 1-1\ total\ signal / nA] - [LYRA\ 1-1\ rest\ signal / nA]$$

And the solar signal can again be estimated from the pure signal in a simple way (see upper right image):

$$[“Lyman-alpha”\ solar\ signal / (W\ m-2)] = 0.0975 * [LYRA\ 1-1\ pure\ signal / nA]$$

Remarks: Defining 2.5 nm around 121.5 nm as nominal interval leads to just three TIMED/SEE data points (120.5, 121.5, and 122.5 nm), of which only 121.5 nm is significant. This means that the simulation is essentially based on one value; a small variation of the nominal interval would not lead to different simulation results. - Due to the simple linear factors, the estimation error is within +/-5.4%.

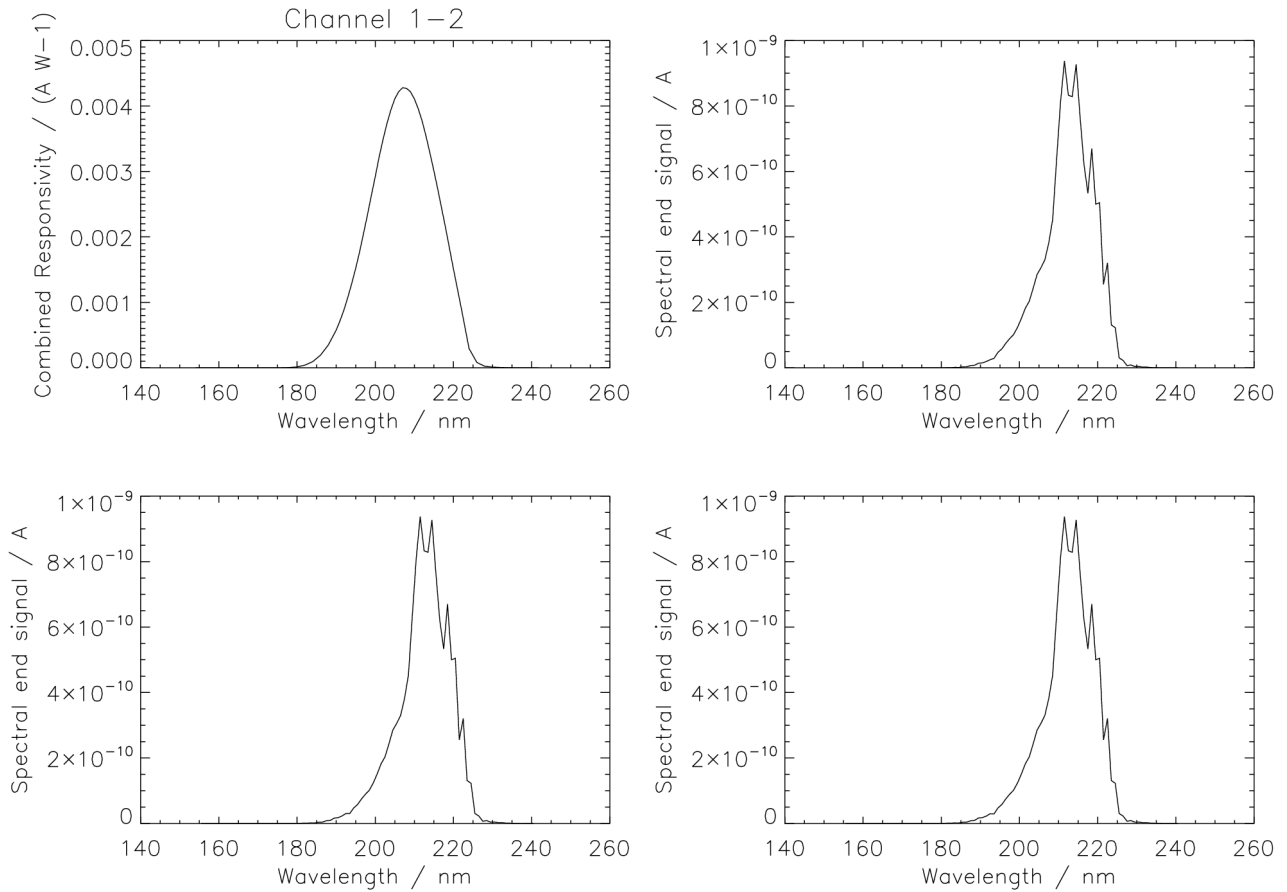


Figure 1-2. Measured responsivity and simulated output (min, high, max) for LYRA channel 1-2.

1-2: Herzberg + PIN10 (200-220 nm)

sample	total	pure	rest	solar
min	12.6509 nA	10.6056 nA (83.8%)	2.04531 nA	0.474210 Wm ⁻²
high	12.6712 nA	10.6056 nA (83.7%)	2.06564 nA	0.474210 Wm ⁻²
max	12.6694 nA	10.6056 nA (83.7%)	2.06385 nA	0.474210 Wm ⁻²

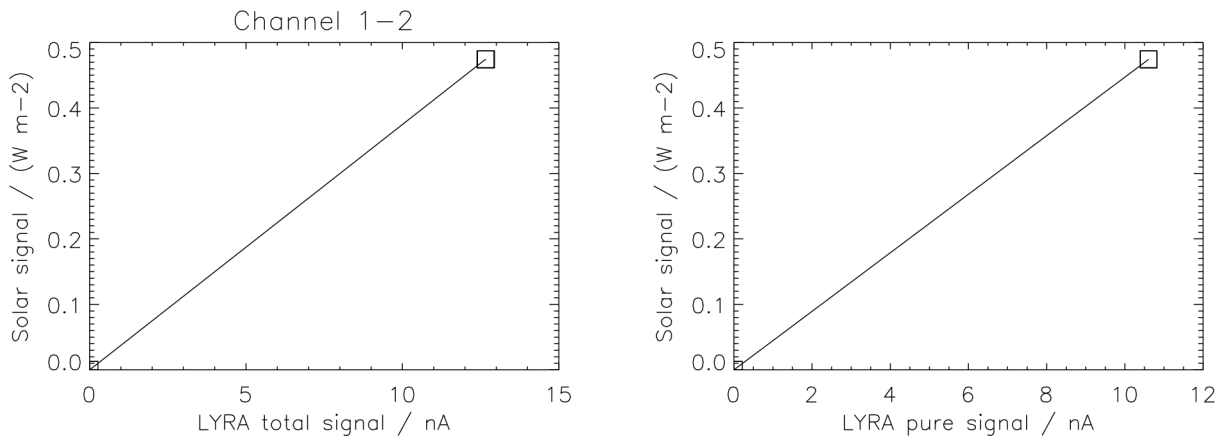


Figure 1-2a. Simulated relations between input and output for LYRA channel 1-2.

The functional relation between the solar signal and the LYRA total signal looks straightforward at first sight. No rest signal has to be calculated. The pure signal can simply be estimated by a linear factor (see table last page):

$$[LYRA\ 1-2\ pure\ signal / nA] = 0.837 * [LYRA\ 1-2\ total\ signal / nA]$$

And the solar signal can be estimated from the pure signal in a simple way (see upper right image):

$$[“Herzberg”\ solar\ signal / (W\ m-2)] = 0.0447 * [LYRA\ 1-2\ pure\ signal / nA]$$

Remarks: The estimate is actually only based on one sample instead of three, because the TIMED/SEE data extensions above 200 nm are identical. - If other limits of the nominal interval were chosen, the purity could naturally be improved (rough estimates):

200 – 220 nm => 84 % purity, 197 – 223 nm => 95 % purity, 195 – 225 nm => 98 % purity,
 190 – 230 nm => 99.5 % purity, 180 – 230 nm => 99.9 % purity.

Due to the simple linear factors, the estimation error is within +/-1%.

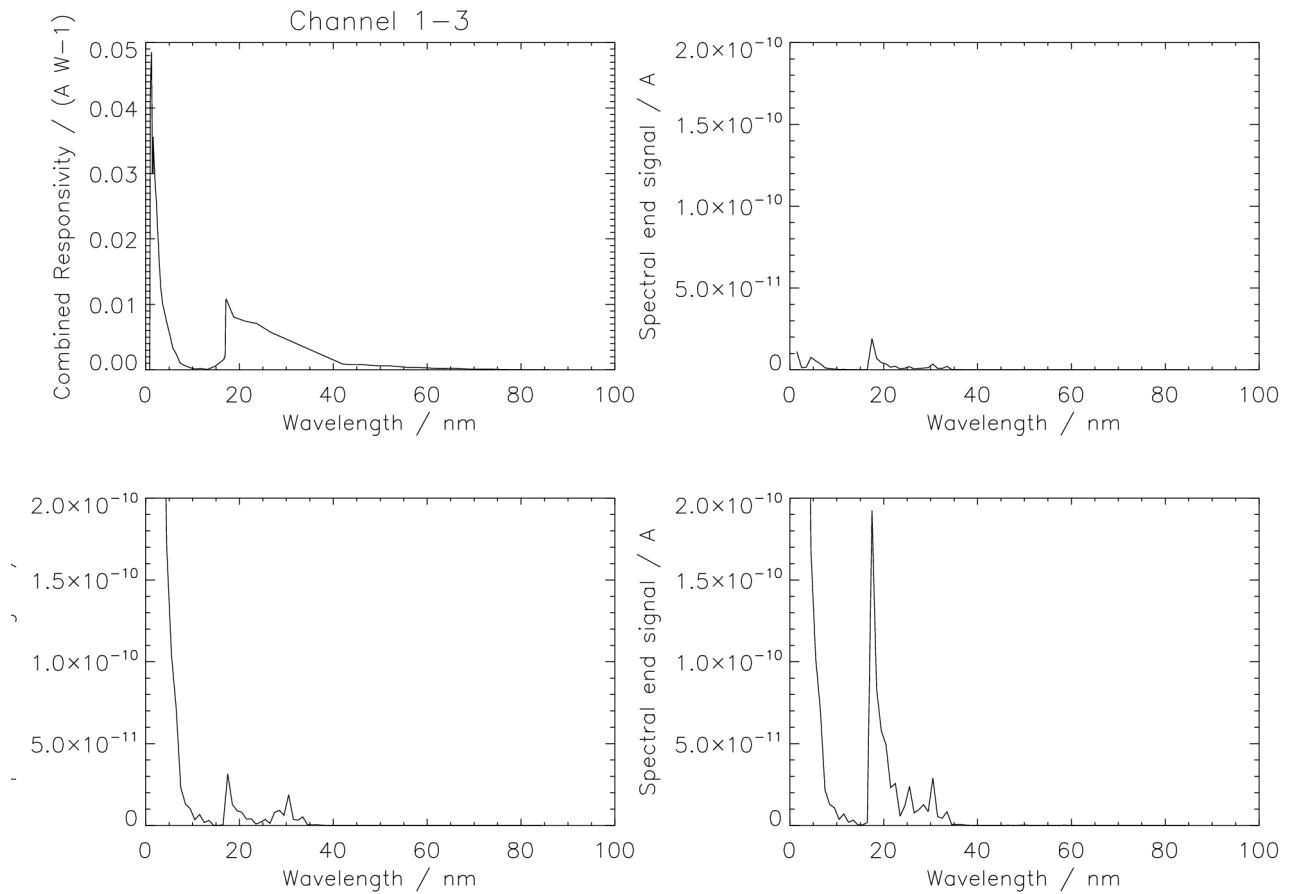


Figure 1-3. Measured responsivity and simulated output (min, high, max) for LYRA channel 1-3.

1-3: Aluminium + MSM11 (17-80 nm)

sample	total		pure		rest		solar
min	0.0884238	nA	0.0540079	nA (61.1%)	0.0344159	nA	0.00131051 Wm ⁻²
high	5.31929	nA	0.134685	nA (2.5%)	5.18460	nA	0.00340476 Wm ⁻²
max	11.9076	nA	0.563424	nA (4.7%)	11.3442	nA	0.0111131 Wm ⁻²

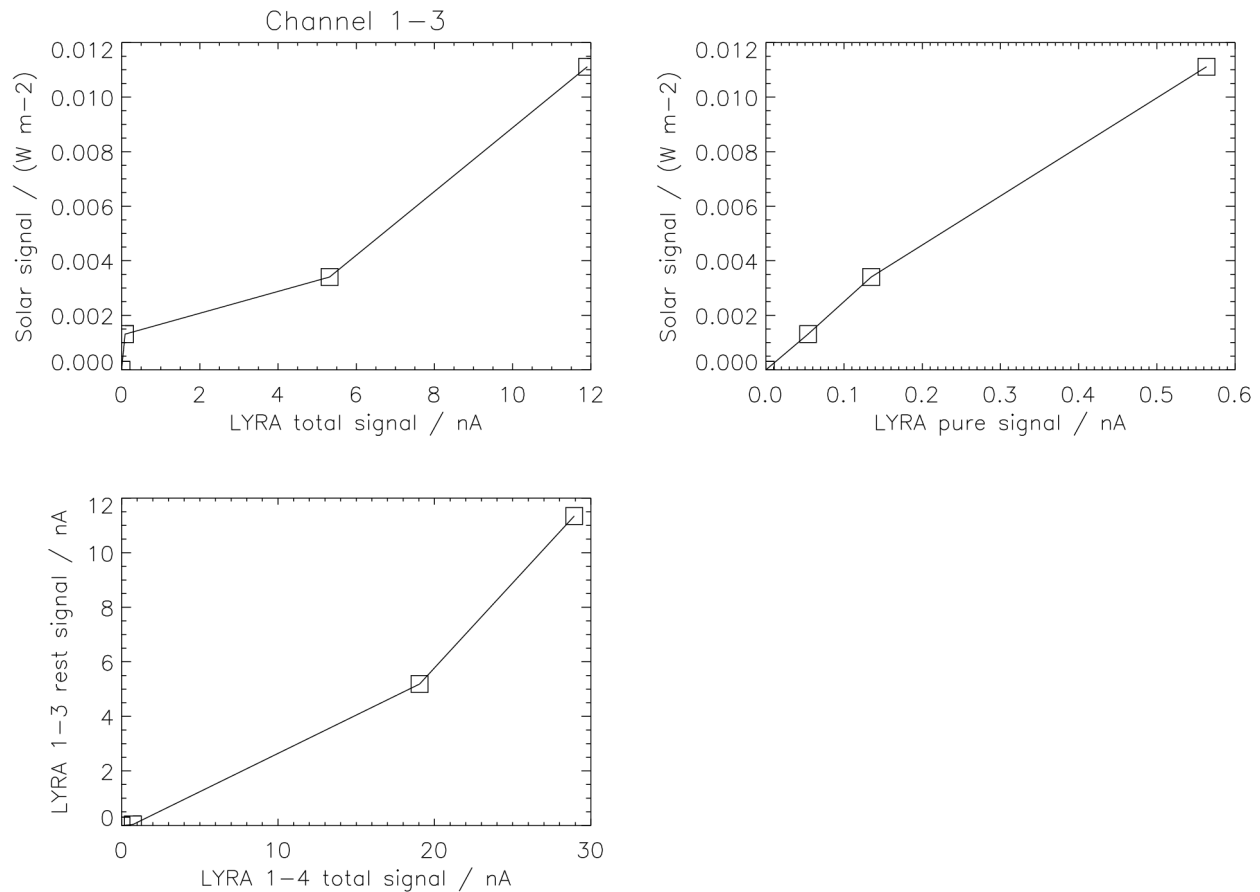


Figure 1-3a. Simulated relations between input and output for LYRA channel 1-3.

The functional relation between the solar signal and the LYRA total signal is obviously not straightforward (rather zigzag, see upper left image). The reason is a contamination due to the influence of the interval 1-10 nm, which is not part of the 17-80 nm nominal interval of the “Aluminium” channels. This rest signal can possibly be estimated with the help of the output signal from LYRA channel 1-4; not as simple as in the other cases, but with linear interpolation between the points of a superlinear relationship as visible in the lower image:

$$[LYRA\ 1-3\ rest\ signal / nA] = interp[LYRA\ 1-4\ total\ signal / nA]$$

The pure signal can be estimated as the difference:

$$[LYRA\ 1-3\ pure\ signal / nA] = [LYRA\ 1-3\ total\ signal / nA] - [LYRA\ 1-3\ rest\ signal / nA]$$

And the solar signal can be estimated from the pure signal, again not in a simple way but with linear interpolation between the points of a slightly sublinear relationship as visible in the upper right image:

$$[“Aluminium”\ solar\ signal / (W\ m-2)] = interp[LYRA\ 1-3\ pure\ signal / nA]$$

Remarks: Although the channel interval nominally reaches up to 80 nm, effectively it appears to end at 35 nm (see Figure 1-3). - If a large subset of these channels' solar signal is similar to the “high” or “max” simulation data, then the uncalibrated data (before subtraction of the substantial short-wavelength contamination) will probably not be very meaningful. - Due to the linear interpolation, the estimation error is 0%, but this is unrealistic.

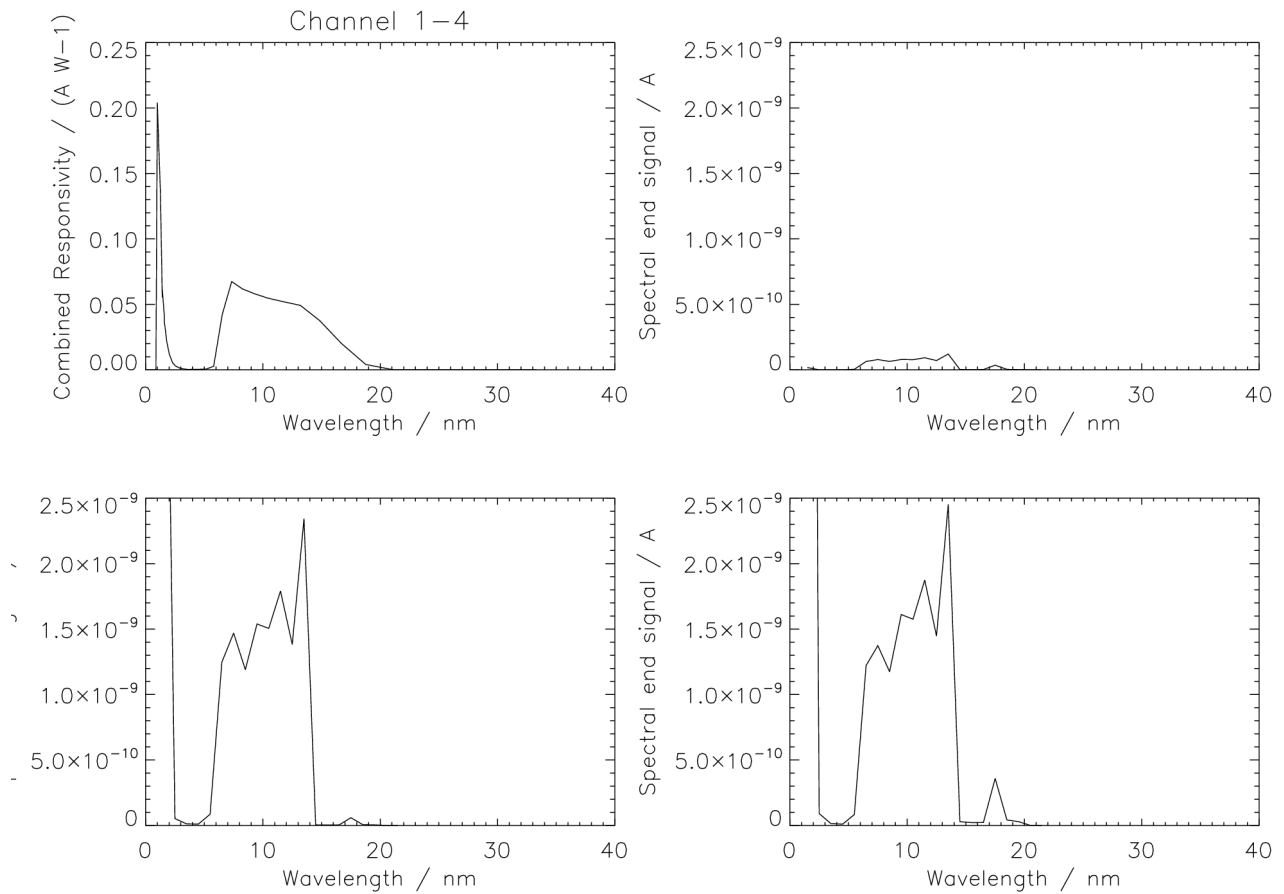


Figure 1-4. Measured responsivity and simulated output (min, high, max) for LYRA channel 1-4.

1-4: Zr(300nm) + AXUV20D (1-20 nm)

sample	total		pure		rest		solar
min	0.720131 nA		0.720074 nA	(100.%)	0.000057676 nA		0.00267627 Wm ⁻²
high	19.0501 nA		19.0500 nA	(100.%)	0.000131450 nA		0.0659849 Wm ⁻²
max	28.9357 nA		28.9349 nA	(100.%)	0.000804690 nA		0.0975310 Wm ⁻²

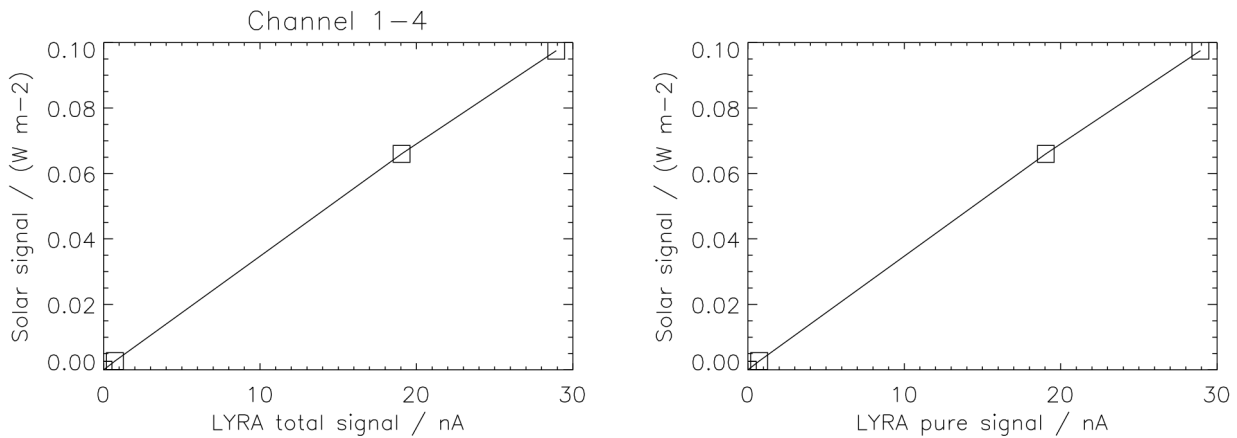


Figure 1-4a. Simulated relations between input and output for LYRA channel 1-4.

The functional relation between the solar signal and the LYRA total signal looks straightforward. No rest signal has to be calculated. Since the purity of the Zirconium channels is always around 100%, the pure signal can simply be estimated by the total signal:

$$[LYRA\ 1-4\ pure\ signal / nA] = [LYRA\ 1-4\ total\ signal / nA]$$

And the solar signal can be estimated from the pure signal with linear interpolation between the points of a slightly sublinear relationship as visible in the upper right image:

$$[“Zirconium”\ solar\ signal / (W\ m-2)] = interp[LYRA\ 1-4\ pure\ signal / nA]$$

Remarks: Application of a simple linear factor, in this case 0.00352, instead of interpolation would lead to an error of +/- 5%. Due to the linear interpolation, the estimation error is 0%, but this is unrealistic.

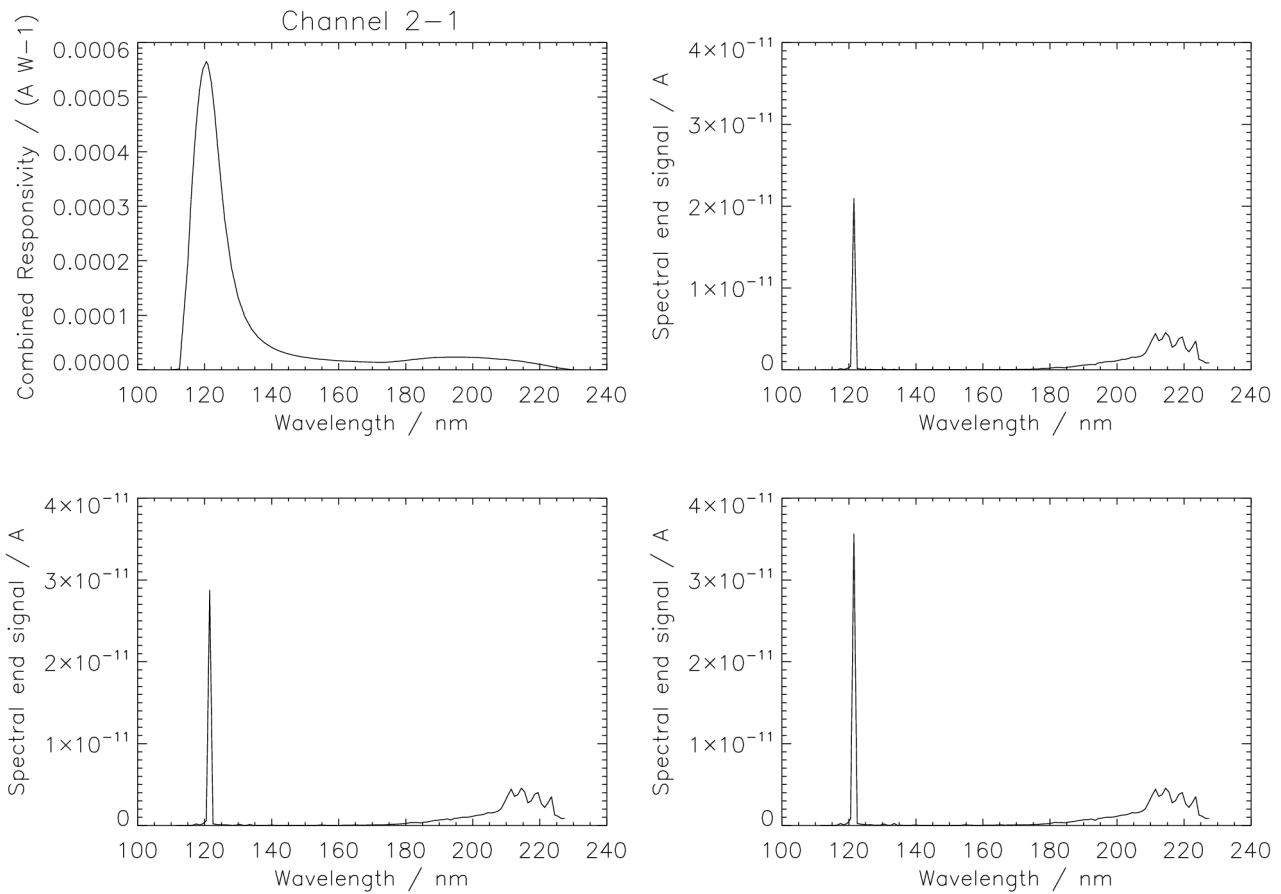


Figure 2-1. Measured responsivity and simulated output (min, high, max) for LYRA channel 2-1.

2-1: Ly XN + MSM21 (121.5 +/- nm)

sample	total	pure	rest	solar
min	0.105615 nA	0.0215646 nA (20.4%)	0.0840500 nA	0.00564762 Wm ⁻²
high	0.115582 nA	0.0295895 nA (25.6%)	0.0859923 nA	0.00774904 Wm ⁻²
max	0.123239 nA	0.0366925 nA (29.8%)	0.0865466 nA	0.00960818 Wm ⁻²

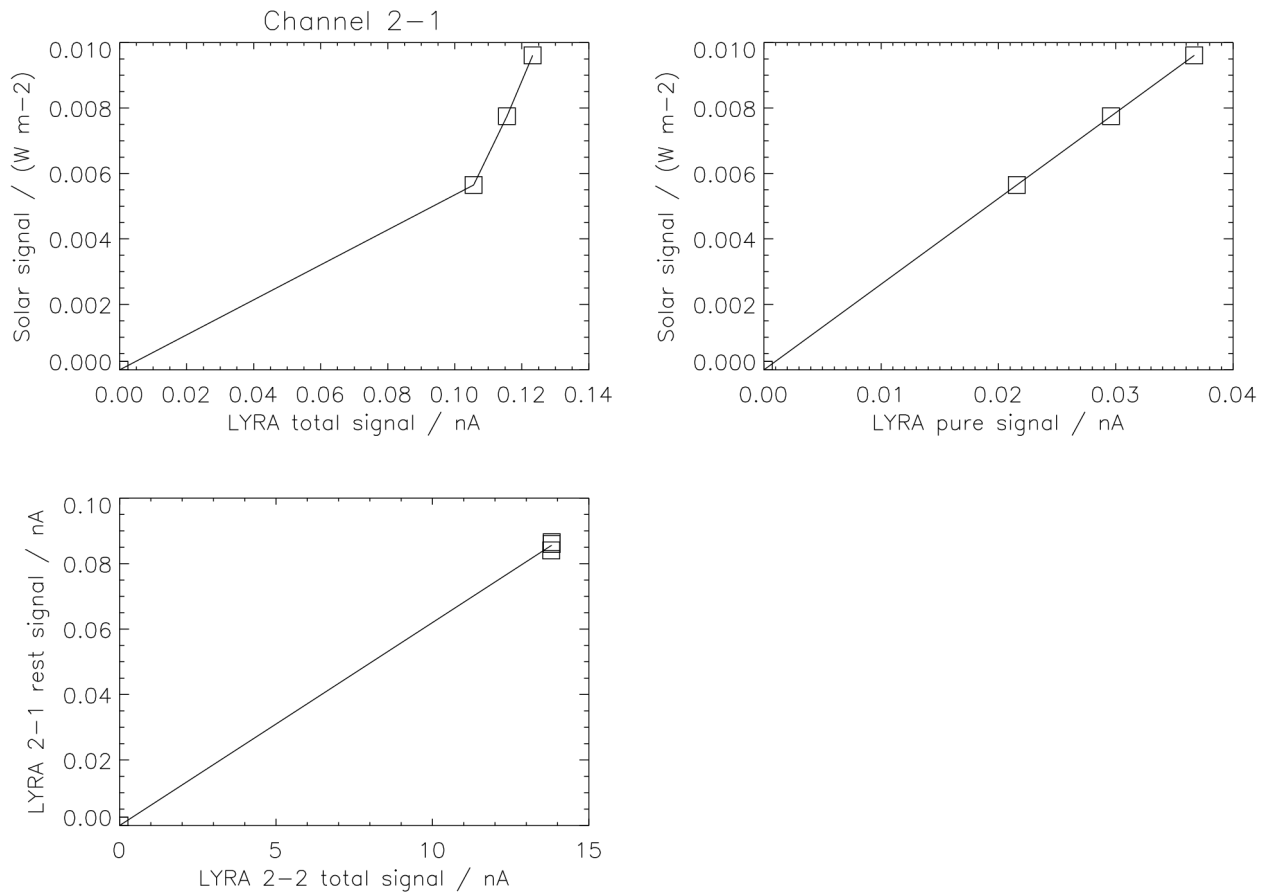


Figure 2-1a. Simulated relations between input and output for LYRA channel 2-1.

The functional relation between the solar signal and the LYRA total signal is obviously not straightforward (see upper left image). The reason is a contamination due to the influence of the interval 180-230 nm, which is not part of the nominal interval around the Lyman-alpha line. But this rest signal can obviously be estimated with the help of the output signal from LYRA channel 2-2 in a simple way (see lower image):

$$[LYRA\ 2-1\ rest\ signal / nA] = 0.0062 * [LYRA\ 2-2\ total\ signal / nA]$$

The pure signal can be estimated as the difference:

$$[LYRA\ 2-1\ pure\ signal / nA] = [LYRA\ 2-1\ total\ signal / nA] - [LYRA\ 2-1\ rest\ signal / nA]$$

And the solar signal can again be estimated from the pure signal in a simple way (see upper right image):

$$[“Lyman-alpha”\ solar\ signal / (W\ m-2)] = 0.262 * [LYRA\ 2-1\ pure\ signal / nA]$$

Remarks: Defining 2.5 nm around 121.5 nm as nominal interval leads to just three TIMED/SEE data points (120.5, 121.5, and 122.5 nm), of which only 121.5 nm is significant. This means that the simulation is essentially based on one value; a small variation of the nominal interval would not lead to different simulation results. - Due to the simple linear factors, the estimation error is within +/-6.9%.

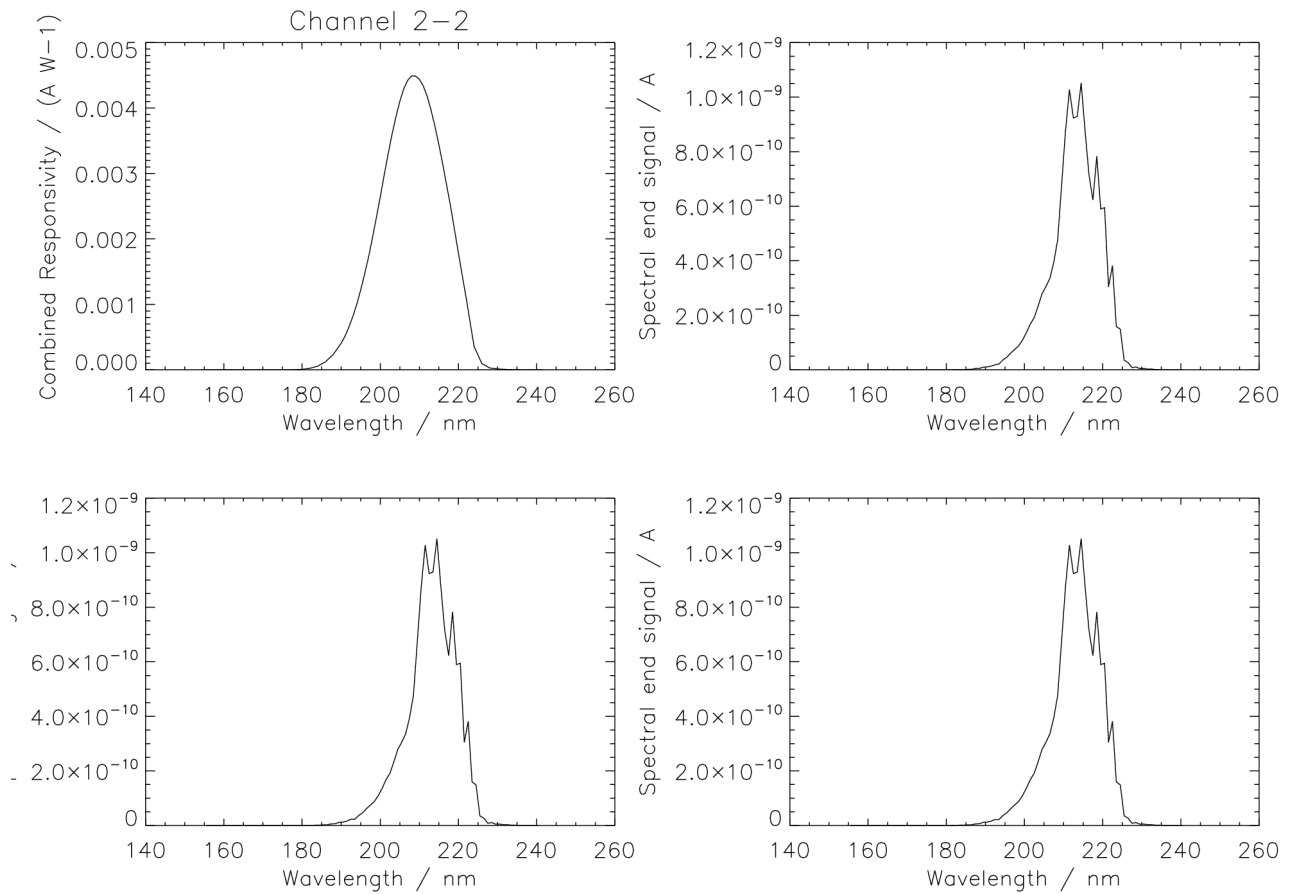


Figure 2-2. Measured responsivity and simulated output (min, high, max) for LYRA channel 2-2.

2-2: Herzberg + PIN11 (200-220 nm)

sample	total	pure	rest	solar
min	13.7981 nA	11.5975 nA (84.1%)	2.20060 nA	0.474210 Wm ⁻²
high	13.8125 nA	11.5975 nA (84.0%)	2.21499 nA	0.474210 Wm ⁻²
max	13.8111 nA	11.5975 nA (84.0%)	2.21360 nA	0.474210 Wm ⁻²

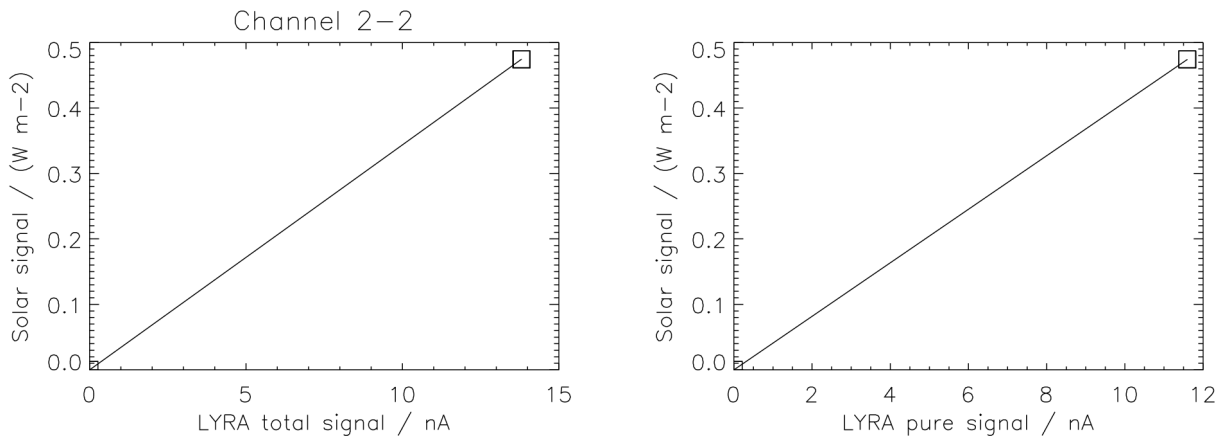


Figure 2-2a. Simulated relations between input and output for LYRA channel 2-2.

The functional relation between the solar signal and the LYRA total signal looks straightforward at first sight. No rest signal has to be calculated. The pure signal can simply be estimated by a linear factor (see table last page):

$$[LYRA\ 2-2\ pure\ signal / nA] = 0.840 * [LYRA\ 2-2\ total\ signal / nA]$$

And the solar signal can be estimated from the pure signal in a simple way (see upper right image):

$$[“Herzberg”\ solar\ signal / (W\ m-2)] = 0.0409 * [LYRA\ 2-2\ pure\ signal / nA]$$

Remarks: The estimate is actually only based on one sample instead of three, because the TIMED/SEE data extensions above 200 nm are identical. - If other limits of the nominal interval were chosen, the purity could naturally be improved (rough estimates):

200 – 220 nm => 84 % purity, 197 – 223 nm => 95 % purity, 195 – 225 nm => 98 % purity,
 190 – 230 nm => 99.5 % purity, 180 – 230 nm => 99.9 % purity.

Due to the simple linear factors, the estimation error is within +/-0.1%.

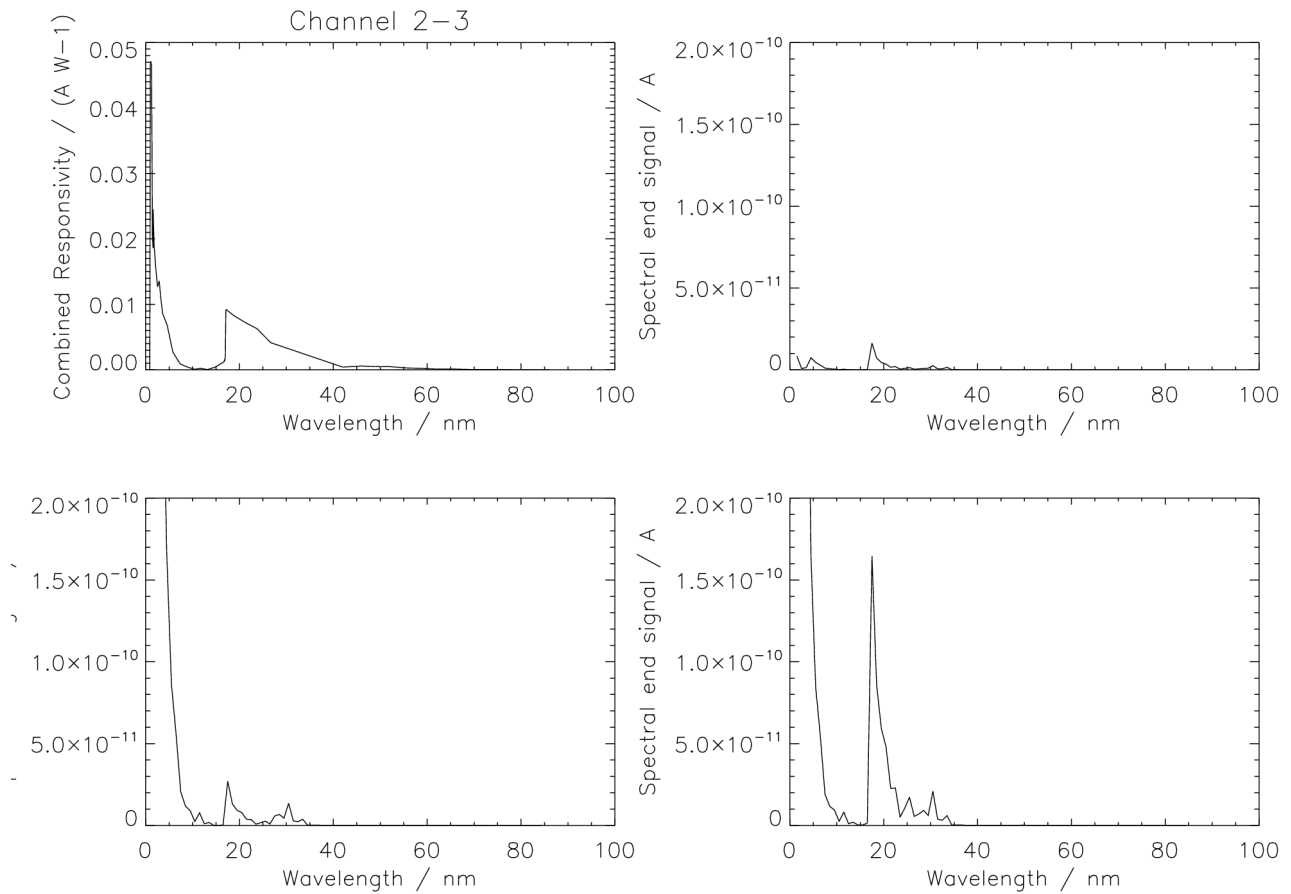


Figure 2-3. Measured responsivity and simulated output (min, high, max) for LYRA channel 2-3.

2-3: Aluminium + MSM15 (17-80 nm)

sample	total		pure		rest		solar
min	0.0753576	nA	0.0468343	nA (62.1%)	0.0285233	nA	0.00131051 Wm ⁻²
high	4.06936	nA	0.111929	nA (2.8%)	3.95743	nA	0.00340476 Wm ⁻²
max	9.09185	nA	0.500883	nA (5.5%)	8.59096	nA	0.0111131 Wm ⁻²

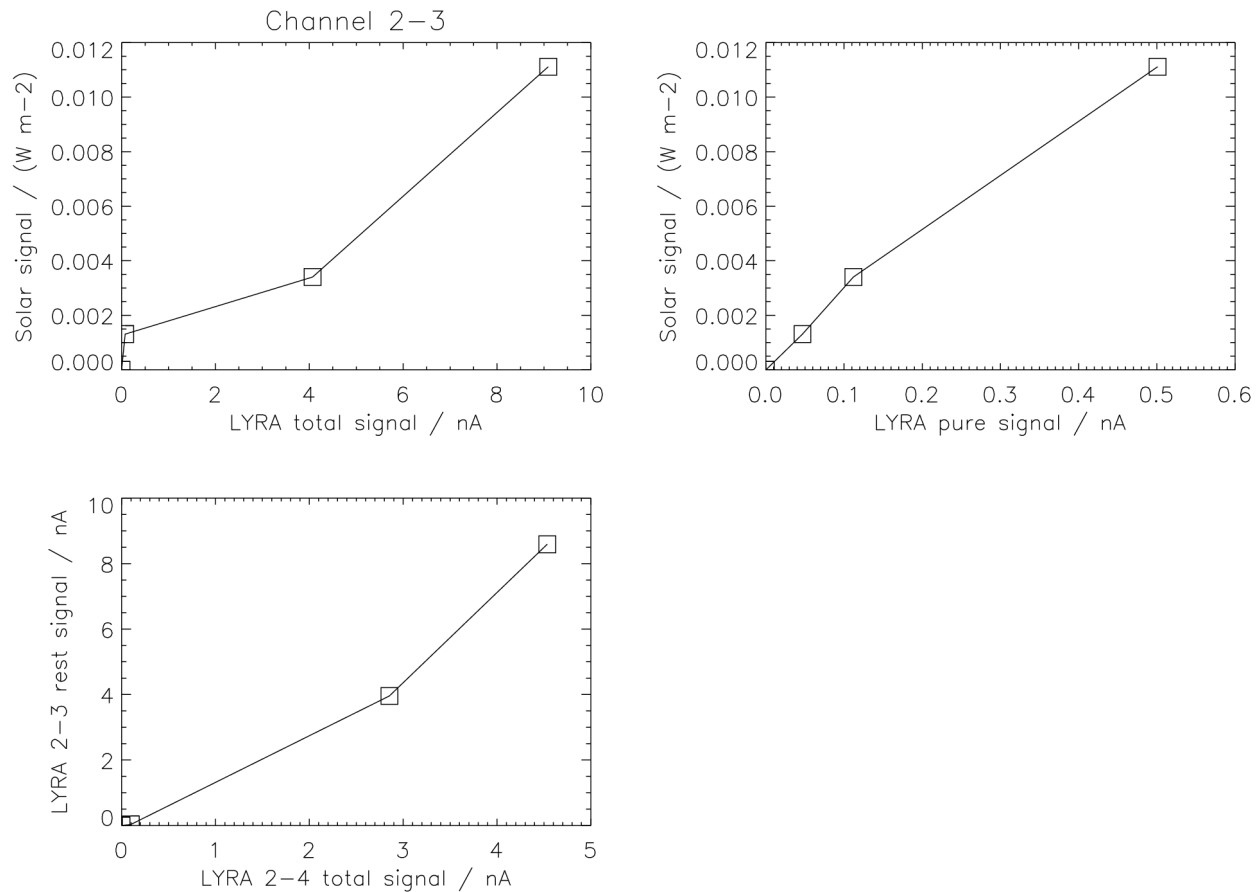


Figure 2-3a. Simulated relations between input and output for LYRA channel 2-3.

The functional relation between the solar signal and the LYRA total signal is obviously not straightforward (rather zigzag, see upper left image). The reason is a contamination due to the influence of the interval 1-10 nm, which is not part of the 17-80 nm nominal interval of the “Aluminium” channels. This rest signal can possibly be estimated with the help of the output signal from LYRA channel 2-4; not as simple as in the other cases, but with linear interpolation between the points of a superlinear relationship as visible in the lower image:

$$[LYRA\ 2-3\ rest\ signal / nA] = interp[LYRA\ 2-4\ total\ signal / nA]$$

The pure signal can be estimated as the difference:

$$[LYRA\ 2-3\ pure\ signal / nA] = [LYRA\ 2-3\ total\ signal / nA] - [LYRA\ 2-3\ rest\ signal / nA]$$

And the solar signal can be estimated from the pure signal, again not in a simple way but with linear interpolation between the points of a slightly sublinear relationship as visible in the upper right image:

$$[“Aluminium”\ solar\ signal / (W\ m-2)] = interp[LYRA\ 2-3\ pure\ signal / nA]$$

Remarks: Although the channel interval nominally reaches up to 80 nm, effectively it appears to end at 35 nm (see Figure 2-3). - If a large subset of these channels' solar signal is similar to the “high” or “max” simulation data, then the uncalibrated data (before subtraction of the substantial short-wavelength contamination) will probably not be very meaningful. - Due to the linear interpolation, the estimation error is 0%, but this is unrealistic.

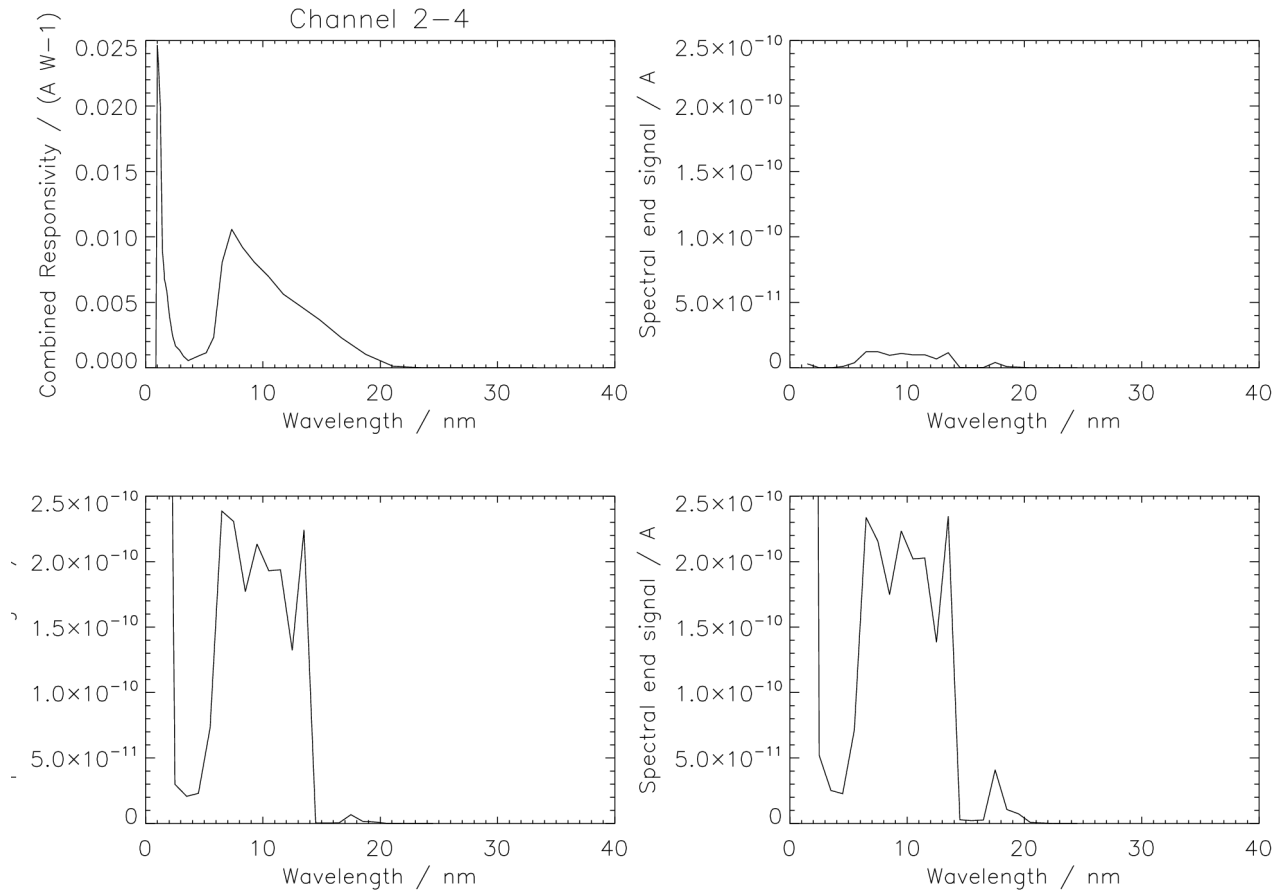


Figure 2-4. Measured responsivity and simulated output (min, high, max) for LYRA channel 2-4.

2-4: Zr(150nm) + MSM19 (1-20 nm)

sample	total		pure		rest		solar
min	0.0980128	nA	0.0979311	nA (99.9%)	0.00008175	nA	0.00267627 Wm ⁻²
high	2.85311	nA	2.85293	nA (100.%)	0.00018807	nA	0.0659849 Wm ⁻²
max	4.53508	nA	4.53394	nA (100.%)	0.00114087	nA	0.0975310 Wm ⁻²

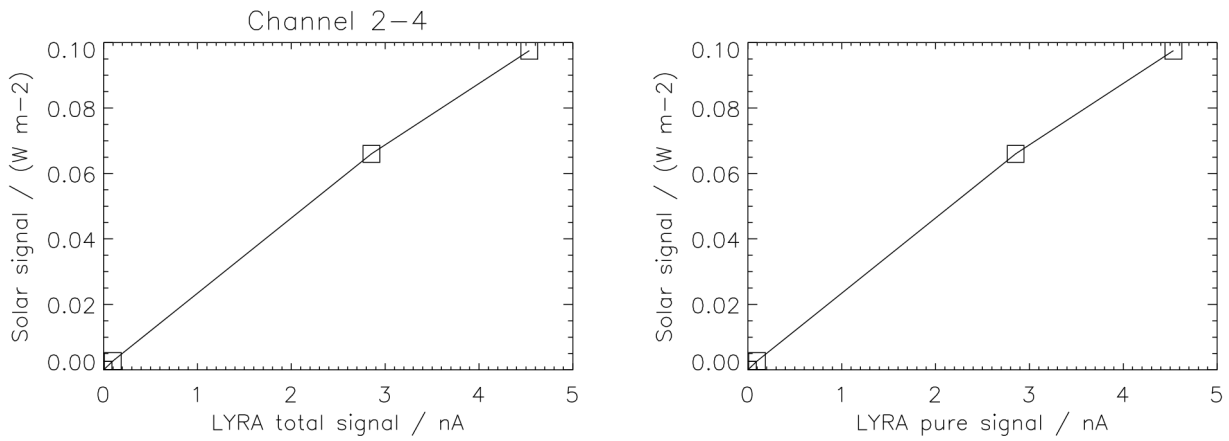


Figure 2-4a. Simulated relations between input and output for LYRA channel 2-4.

The functional relation between the solar signal and the LYRA total signal looks straightforward. No rest signal has to be calculated. Since the purity of the Zirconium channels is always around 100%, the pure signal can simply be estimated by the total signal:

$$[LYRA\ 2-4\ pure\ signal / nA] = [LYRA\ 2-4\ total\ signal / nA]$$

And the solar signal can be estimated from the pure signal with linear interpolation between the points of a slightly sublinear relationship as visible in the upper right image:

$$[“Zirconium”\ solar\ signal / (W\ m-2)] = interp[LYRA\ 2-4\ pure\ signal / nA]$$

Remarks: Application of a simple linear factor, in this case 0.0240, instead of interpolation would lead to an error of +/- 12%. - Due to the linear interpolation, the estimation error is 0%, but this is unrealistic.

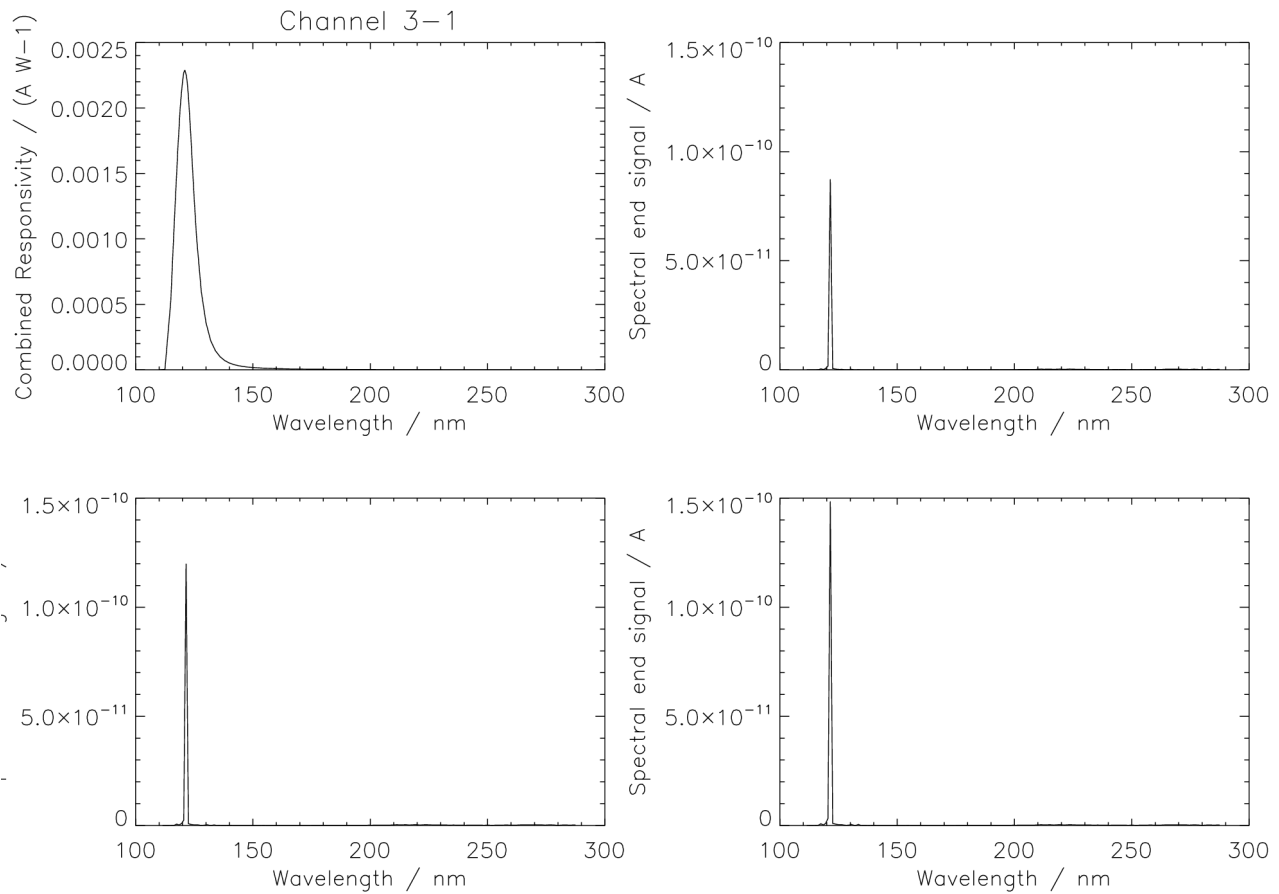


Figure 3-1. Measured responsivity and simulated output (min, high, max) for LYRA channel 3-1.

3-1: Ly N+XN + AXUV20A (121.5 +/- nm)

sample	total	pure	rest	solar
min	0.112943 nA	0.0897866 nA (79.5%)	0.0231564 nA	0.00564762 Wm ⁻²
high	0.147934 nA	0.123199 nA (83.3%)	0.0247348 nA	0.00774904 Wm ⁻²
max	0.178779 nA	0.152764 nA (85.4%)	0.0260155 nA	0.00960818 Wm ⁻²

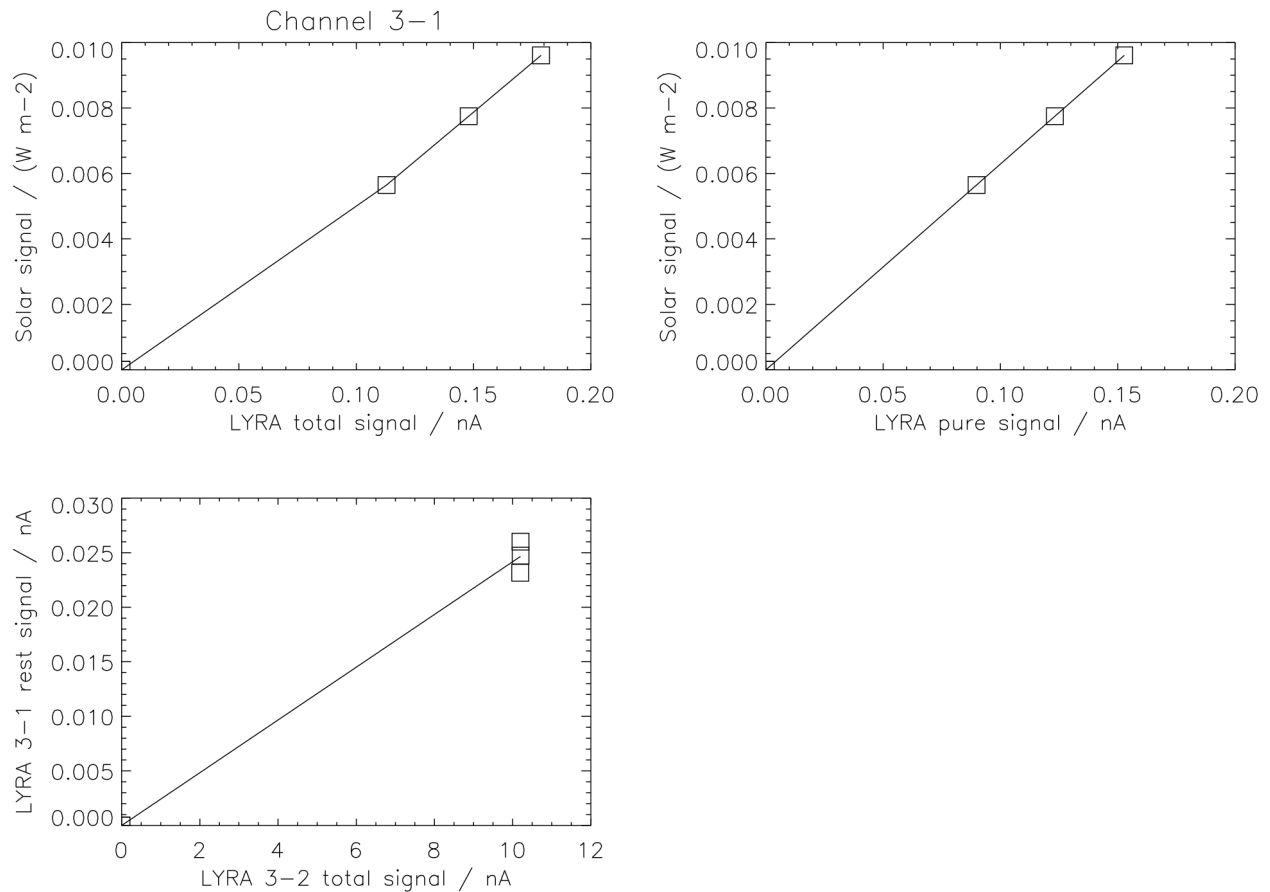


Figure 3-1a. Simulated relations between input and output for LYRA channel 3-1.

The functional relation between the solar signal and the LYRA total signal is not quite straightforward, although more so than for channels 1-1 or 2-1 (see upper left image). The reason is again a contamination due to the influence of the interval 180-230 nm, which is not part of the nominal interval around the Lyman-alpha line, but this contamination is smaller here due to the double filter, N+XN. This rest signal can obviously be estimated with the help of the output signal from LYRA channel 3-2 in a simple way (see lower image):

$$[LYRA\ 3-1\ rest\ signal / nA] = 0.0024 * [LYRA\ 3-2\ total\ signal / nA]$$

The pure signal can be estimated as the difference:

$$[LYRA\ 3-1\ pure\ signal / nA] = [LYRA\ 3-1\ total\ signal / nA] - [LYRA\ 3-1\ rest\ signal / nA]$$

And the solar signal can again be estimated from the pure signal in a simple way (see upper right image):

$$[“Lyman-alpha”\ solar\ signal / (W\ m^{-2})] = 0.0629 * [LYRA\ 3-1\ pure\ signal / nA]$$

Remarks: Defining 2.5 nm around 121.5 nm as nominal interval leads to just three TIMED/SEE data points (120.5, 121.5, and 122.5 nm), of which only 121.5 nm is significant. This means that the simulation is essentially based on one value; a small variation of the nominal interval would not lead to different simulation results. - Due to the simple linear factors, the estimation error is within +/-1.5%.

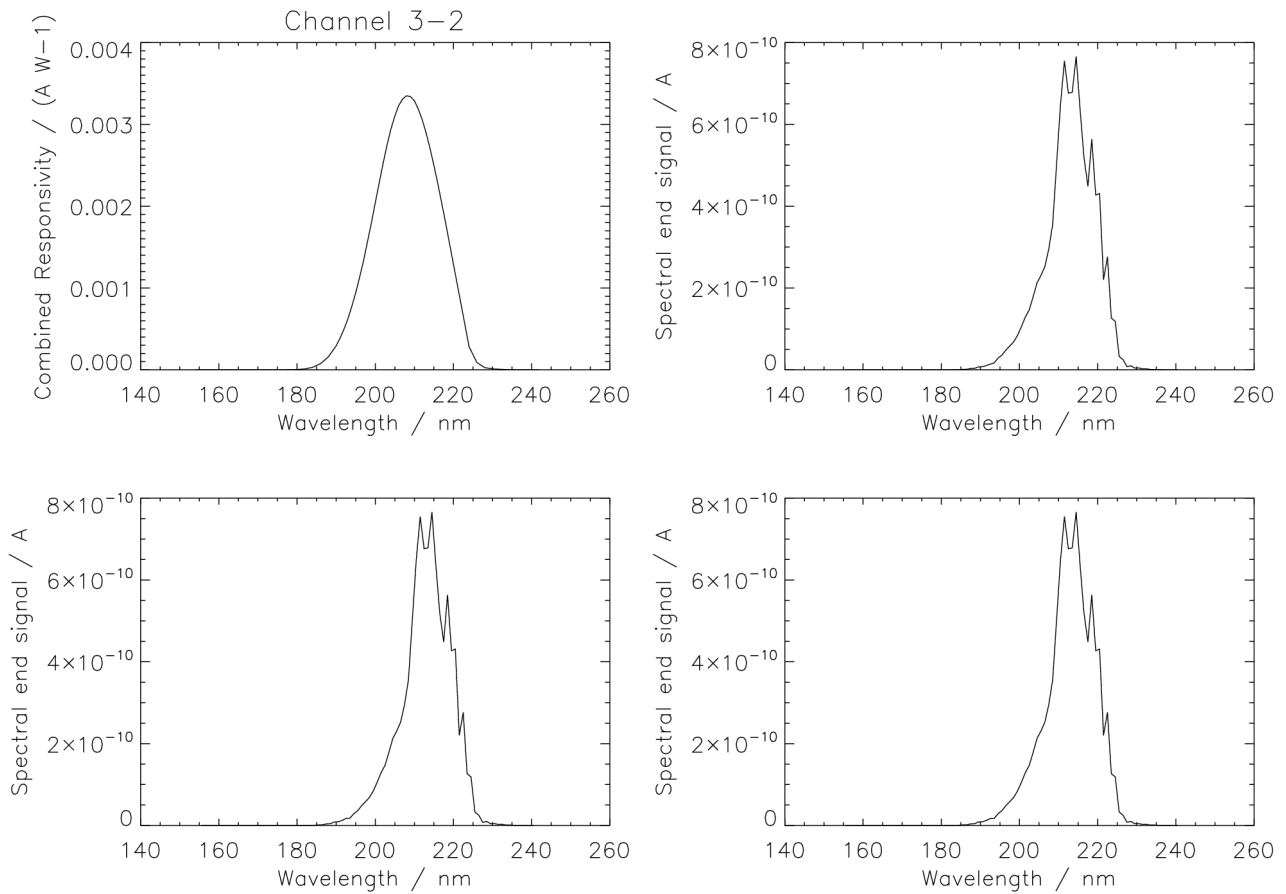


Figure 3-2. Measured responsivity and simulated output (min, high, max) for LYRA channel 3-2.

3-2: Herzberg + PIN12 (200-220 nm)

sample	total	pure	rest	solar
min	10.1916 nA	8.53481 nA (83.7%)	1.65680 nA	0.474210 Wm ⁻²
high	10.2020 nA	8.53481 nA (83.7%)	1.66717 nA	0.474210 Wm ⁻²
max	10.2009 nA	8.53481 nA (83.7%)	1.66609 nA	0.474210 Wm ⁻²

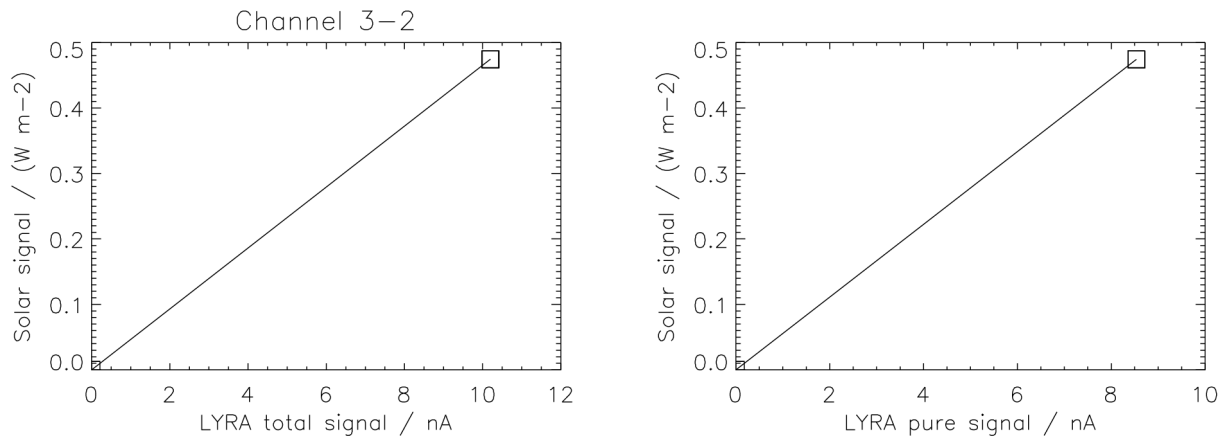


Figure 3-2a. Simulated relations between input and output for LYRA channel 3-2.

The functional relation between the solar signal and the LYRA total signal looks straightforward at first sight. No rest signal has to be calculated. The pure signal can simply be estimated by a linear factor (see table last page):

$$[LYRA\ 3-2\ pure\ signal / nA] = 0.837 * [LYRA\ 3-2\ total\ signal / nA]$$

And the solar signal can be estimated from the pure signal in a simple way (see upper right image):

$$[“Herzberg”\ solar\ signal / (W\ m-2)] = 0.0556 * [LYRA\ 3-2\ pure\ signal / nA]$$

Remarks: The estimate is actually only based on one sample instead of three, because the TIMED/SEE data extensions above 200 nm are identical. - If other limits of the nominal interval were chosen, the purity could naturally be improved (rough estimates):

200 – 220 nm => 84 % purity, 197 – 223 nm => 95 % purity, 195 – 225 nm => 98 % purity,
 190 – 230 nm => 99.5 % purity, 180 – 230 nm => 99.9 % purity.

Due to the simple linear factors, the estimation error is within +/-0.1%.

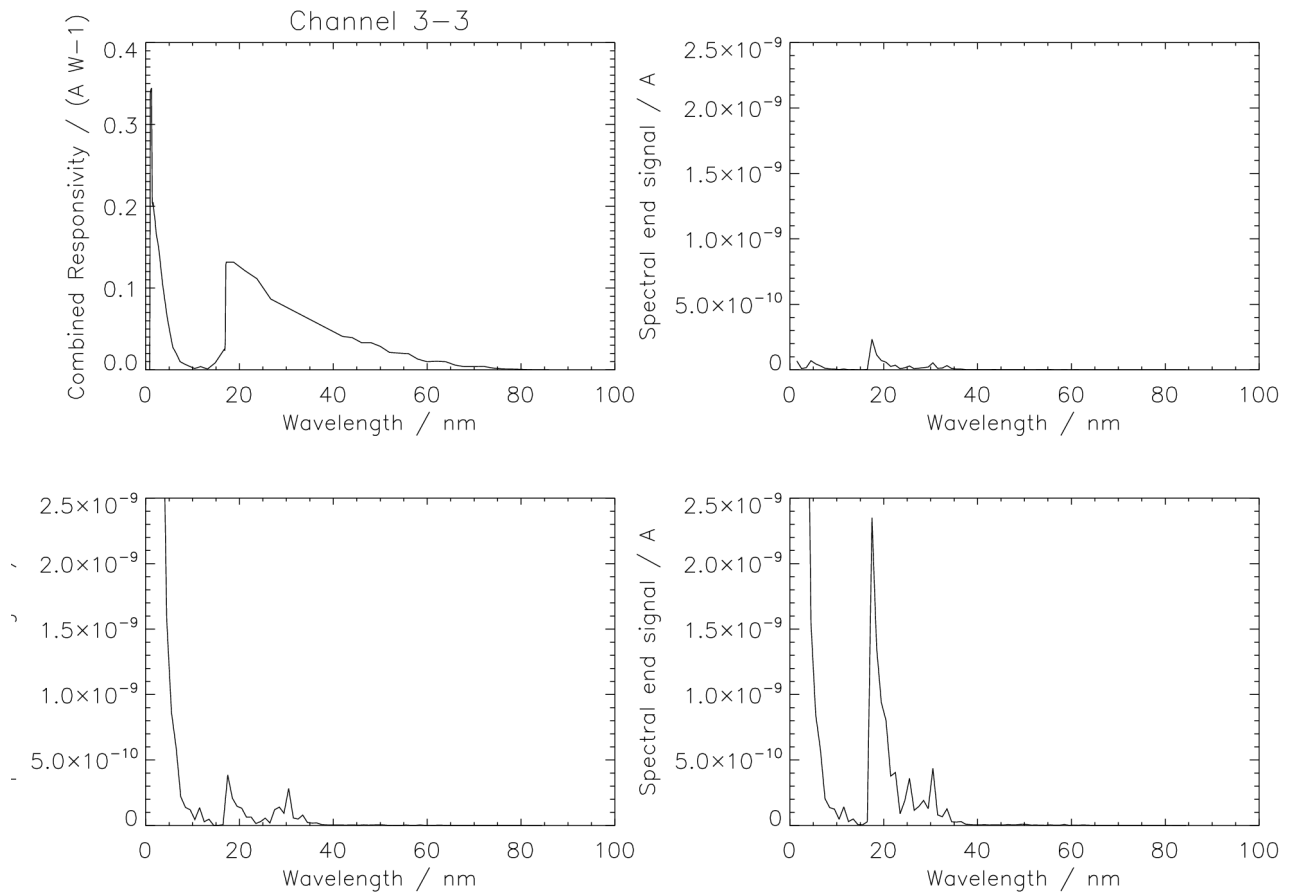


Figure 3-3. Measured responsivity and simulated output (min, high, max) for LYRA channel 3-3.

3-3: Aluminium + AXUV20B (17-80 nm)

sample	total	pure	rest	solar
min	1.10304 nA	0.820291 nA (74.4%)	0.282749 nA	0.00131051 Wm ⁻²
high	36.7403 nA	2.07564 nA (5.6%)	34.6646 nA	0.00340476 Wm ⁻²
max	80.8530 nA	8.36320 nA (10.3%)	72.4898 nA	0.0111131 Wm ⁻²

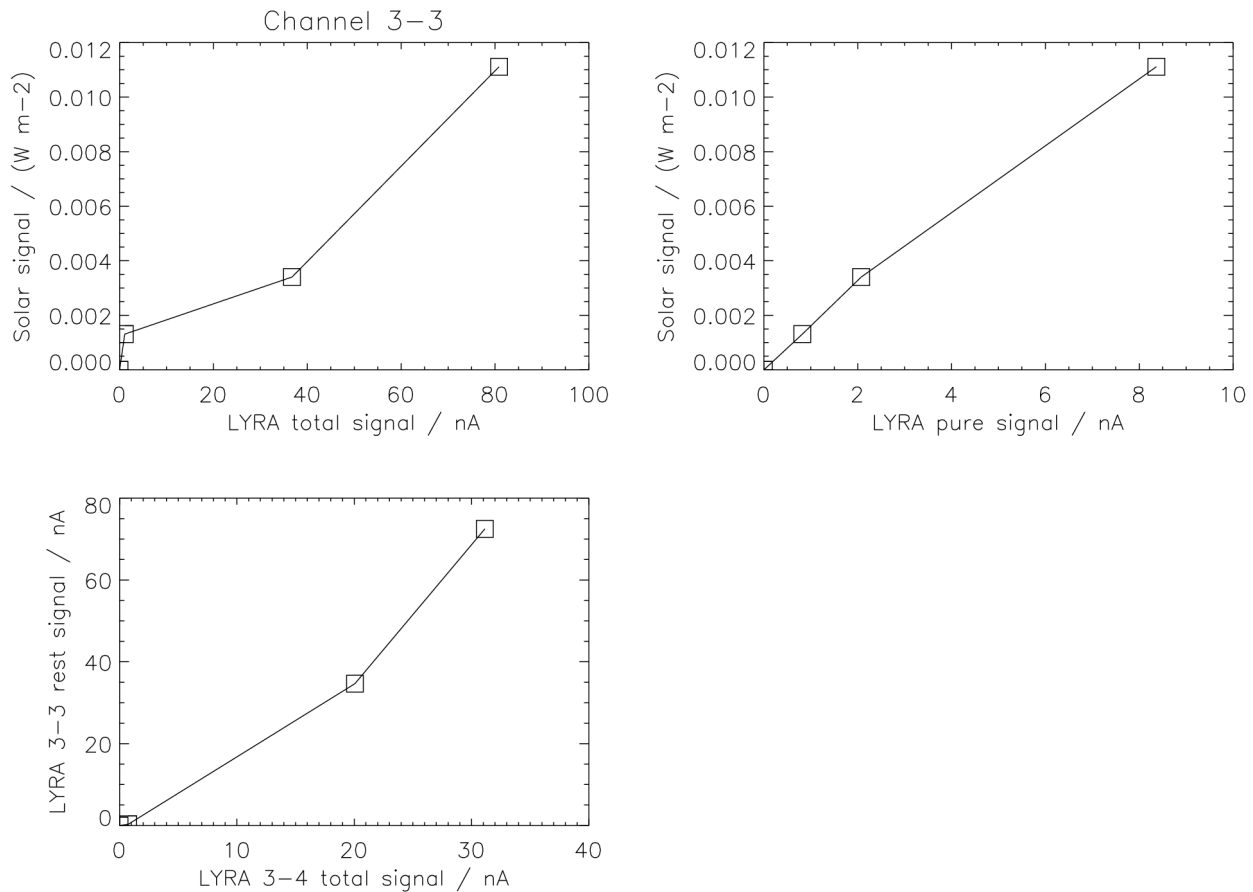


Figure 3-3a. Simulated relations between input and output for LYRA channel 3-3.

The functional relation between the solar signal and the LYRA total signal is obviously not straightforward (rather zigzag, see upper left image). The reason is a contamination due to the influence of the interval 1-10 nm, which is not part of the 17-80 nm nominal interval of the “Aluminium” channels. This rest signal can possibly be estimated with the help of the output signal from LYRA channel 3-4; not as simple as in the other cases, but with linear interpolation between the points of a superlinear relationship as visible in the lower image:

$$[LYRA\ 3-3\ rest\ signal / nA] = interp[LYRA\ 3-4\ total\ signal / nA]$$

The pure signal can be estimated as the difference:

$$[LYRA\ 3-3\ pure\ signal / nA] = [LYRA\ 3-3\ total\ signal / nA] - [LYRA\ 3-3\ rest\ signal / nA]$$

And the solar signal can be estimated from the pure signal, again not in a simple way but with linear interpolation between the points of a slightly sublinear relationship as visible in the upper right image:

$$[“Aluminium”\ solar\ signal / (W\ m-2)] = interp[LYRA\ 3-3\ pure\ signal / nA]$$

Remarks: Although the channel interval nominally reaches up to 80 nm, effectively it appears to end at 35 nm (see Figure 3-3). - If a large subset of these channels' solar signal is similar to the “high” or “max” simulation data, then the uncalibrated data (before subtraction of the substantial short-wavelength contamination) will probably not be very meaningful. - Due to the linear interpolation, the estimation error is 0%, but this is unrealistic.

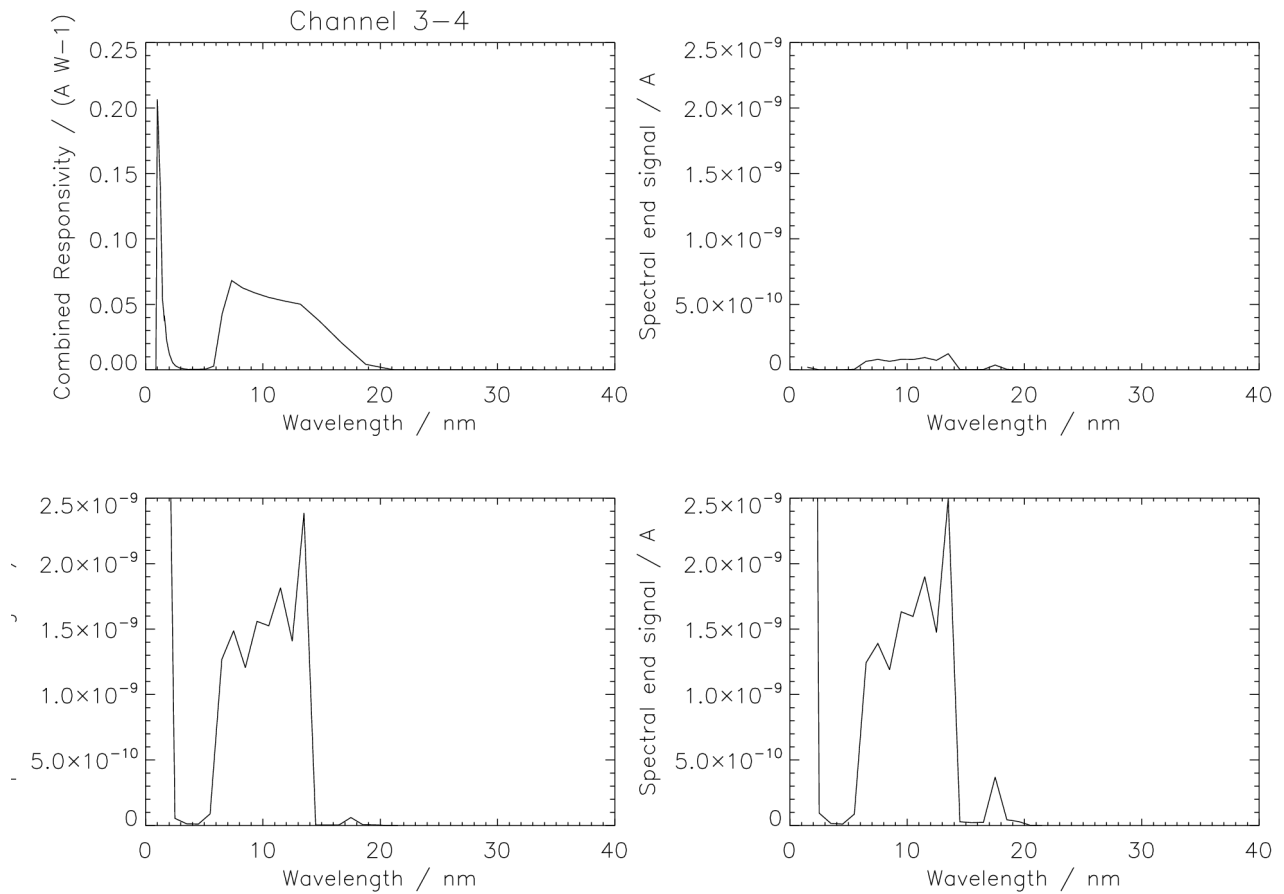


Figure 3-4. Measured responsivity and simulated output (min, high, max) for LYRA channel 3-4.

3-4: Zr(300nm) + AXUV20C (1-20 nm)

sample	total	pure	rest	solar
min	0.733590 nA	0.733524 nA (100.%)	0.00006645 nA	0.00267627 Wm ⁻²
high	20.0586 nA	20.0585 nA (100.%)	0.00015277 nA	0.0659849 Wm ⁻²
max	31.1312 nA	31.1303 nA (100.%)	0.00092371 nA	0.0975310 Wm ⁻²

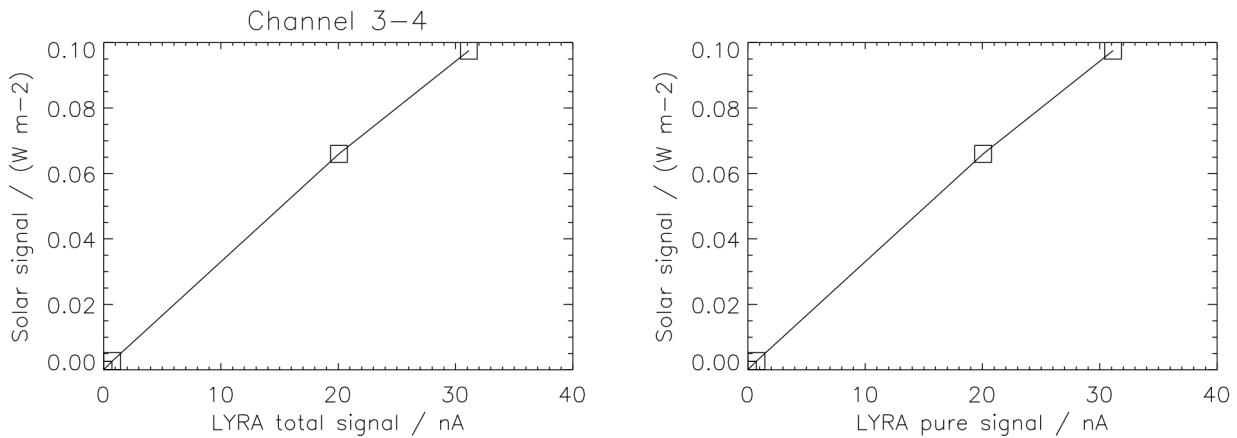


Figure 3-4a. Simulated relations between input and output for LYRA channel 3-4.

The functional relation between the solar signal and the LYRA total signal looks straightforward. No rest signal has to be calculated. Since the purity of the Zirconium channels is always around 100%, the pure signal can simply be estimated by the total signal:

$$[LYRA\ 3-4\ pure\ signal / nA] = [LYRA\ 3-4\ total\ signal / nA]$$

And the solar signal can be estimated from the pure signal with linear interpolation between the points of a slightly sublinear relationship as visible in the upper right image:

$$[“Zirconium”\ solar\ signal / (W\ m-2)] = interp[LYRA\ 3-4\ pure\ signal / nA]$$

Remarks: Application of a simple linear factor, in this case 0.00336, instead of interpolation would lead to an error of +/- 8%. - Due to the linear interpolation, the estimation error is 0%, but this is unrealistic.

```

; calc_calib.pro
; -----
; IED 14 Nov 2006
; -----
; IDL program to calculate the calibrated solar values (in four intervals:
; Lyman-alpha, Herzberg, Aluminium, Zirconium), given one LYRA head and its
; four observed (or simulated) values.
; LYRA observations below zero are set to zero and an ERROR message is printed.
; LYRA observations above the interpolation range are extrapolated, and a
; WARNING message is printed in case it is more than 20% above.
; In case a result value is below zero, an ERROR message is printed.
; -----

```

```

t11=[0.244548,0.270879,0.291520]
t12=[12.6509,12.6712,12.6694]
t13=[0.0884238,5.31929,11.9076]
t14=[0.720131,19.0501,28.9357]
t21=[0.105615,0.115582,0.123239]
t22=[13.7981,13.8125,13.8111]
t23=[0.0753576,4.06936,9.09185]
t24=[0.0980128,2.85311,4.53508]
t31=[0.112943,0.147934,0.178779]
t32=[10.1916,10.2020,10.2009]
t33=[1.10304,36.7403,80.8530]
t34=[0.733590,20.0586,31.1312]
p11=[0.0578922,0.0794356,0.0985021]
p12=[10.6056,10.6056,10.6056]
p13=[0.0540079,0.134685,0.563424]
p14=[0.720074,19.0500,28.9349]
p21=[0.0215646,0.0295895,0.0366925]
p22=[11.5975,11.5975,11.5975]
p23=[0.0468343,0.111929,0.500883]
p24=[0.0979311,2.85293,4.53394]
p31=[0.0897866,0.123199,0.152764]
p32=[8.53481,8.53481,8.53481]
p33=[0.820291,2.07564,8.36320]
p34=[0.733524,20.0585,31.1303]
s11=[0.00564762,0.00774904,0.00960818]
s12=[0.474210,0.474210,0.474210]
s13=[0.00131051,0.00340476,0.0111131]
s14=[0.00267627,0.0659849,0.0975310]
s21=[0.00564762,0.00774904,0.00960818]
s22=[0.474210,0.474210,0.474210]
s23=[0.00131051,0.00340476,0.0111131]
s24=[0.00267627,0.0659849,0.0975310]
s31=[0.00564762,0.00774904,0.00960818]
s32=[0.474210,0.474210,0.474210]
s33=[0.00131051,0.00340476,0.0111131]
s34=[0.00267627,0.0659849,0.0975310]

```

```

oncemore:
head=0
read,'LYRA Head (1,2,3) ? ',head
if ((head gt 3) or (head lt 1)) then goto,oncemore
o1=0. & o2=0. & o3=0. & o4=0.
s1=0. & s2=0. & s3=0. & s4=0.
read,'LYRA observations [in nA] # # # # ? ',o1,o2,o3,o4

if (head eq 1) then begin
  if (o1 lt 0.) then begin
    print,'ERROR: Channel 1-1 negative'
  
```

```

o1=0.
endif
if (o1 gt 1.2*max(t11)) then $
print,'WARNING: Channel 1-1 far above interpolation range'
if (o2 lt 0.) then begin
print,'ERROR: Channel 1-2 negative'
o2=0.
endif
if (o2 gt 1.2*max(t12)) then $
print,'WARNING: Channel 1-2 far above interpolation range'
if (o3 lt 0.) then begin
print,'ERROR: Channel 1-3 negative'
o3=0.
endif
if (o3 gt 1.2*max(t13)) then $
print,'WARNING: Channel 1-3 far above interpolation range'
if (o4 lt 0.) then begin
print,'ERROR: Channel 1-4 negative'
o4=0.
endif
if (o4 gt 1.2*max(t14)) then $
print,'WARNING: Channel 1-4 far above interpolation range'

s1=0.0975*(o1-0.015*o2)
if (s1 lt 0.) then begin
print,'ERROR: Result 1-1 negative'
s1=0.
endif

s2=0.0447*(0.837*o2)

r13=t13-p13
if (o4 le t14(0)) then r3=o4*r13(0)/t14(0)
if (o4 ge t14(0)) and (o4 le t14(1)) then $
r3=r13(0)+(o4-t14(0))*(r13(1)-r13(0))/(t14(1)-t14(0))
if (o4 ge t14(1)) then r3=r13(1)+(o4-t14(1))*(r13(2)-r13(1))/(t14(2)-t14(1))
p3=o3-r3
if (p3 le p13(0)) then s3=p3*s13(0)/p13(0)
if (p3 ge p13(0)) and (p3 le p13(1)) then $
s3=s13(0)+(p3-p13(0))*(s13(1)-s13(0))/(p13(1)-p13(0))
if (p3 ge p13(1)) then s3=s13(1)+(p3-p13(1))*(s13(2)-s13(1))/(p13(2)-p13(1))
if (s3 lt 0.) then begin
print,'ERROR: Result 1-3 negative'
s3=0.
endif

if (o4 le t14(0)) then s4=o4*s14(0)/t14(0)
if (o4 ge t14(0)) and (o4 le t14(1)) then $
s4=s14(0)+(o4-t14(0))*(s14(1)-s14(0))/(t14(1)-t14(0))
if (o4 ge t14(1)) then s4=s14(1)+(o4-t14(1))*(s14(2)-s14(1))/(t14(2)-t14(1))
if (s4 lt 0.) then begin
print,'ERROR: Result 1-4 negative'
s4=0.
endif

print,'LYRA Head 1 observations [in nA]
print,o1,o2,o3,o4
print,'corresponding solar values [in W m-2]
print,s1,s2,s3,s4
endif

```

```

if (head eq 2) then begin
  if (o1 lt 0.) then begin
    print, 'ERROR: Channel 2-1 negative'
    o1=0.
  endif
  if (o1 gt 1.2*max(t21)) then $
    print, 'WARNING: Channel 2-1 far above interpolation range'
  if (o2 lt 0.) then begin
    print, 'ERROR: Channel 2-2 negative'
    o2=0.
  endif
  if (o2 gt 1.2*max(t22)) then $
    print, 'WARNING: Channel 2-2 far above interpolation range'
  if (o3 lt 0.) then begin
    print, 'ERROR: Channel 2-3 negative'
    o3=0.
  endif
  if (o3 gt 1.2*max(t23)) then $
    print, 'WARNING: Channel 2-3 far above interpolation range'
  if (o4 lt 0.) then begin
    print, 'ERROR: Channel 2-4 negative'
    o4=0.
  endif
  if (o4 gt 1.2*max(t24)) then $
    print, 'WARNING: Channel 2-4 far above interpolation range'

s1=0.262*(o1-0.0062*o2)
if (s1 lt 0.) then begin
  print, 'ERROR: Result 2-1 negative'
  s1=0.
endif

s2=0.0409*(0.840*o2)

r23=t23-p23
if (o4 le t24(0)) then r3=o4*r23(0)/t24(0)
if (o4 ge t24(0)) and (o4 le t24(1)) then $
  r3=r23(0)+(o4-t24(0))*(r23(1)-r23(0))/(t24(1)-t24(0))
if (o4 ge t24(1)) then r3=r23(1)+(o4-t24(1))*(r23(2)-r23(1))/(t24(2)-t24(1))
p3=o3-r3
if (p3 le p23(0)) then s3=p3*s23(0)/p23(0)
if (p3 ge p23(0)) and (p3 le p23(1)) then $
  s3=s23(0)+(p3-p23(0))*(s23(1)-s23(0))/(p23(1)-p23(0))
if (p3 ge p23(1)) then s3=s23(1)+(p3-p23(1))*(s23(2)-s23(1))/(p23(2)-p23(1))
if (s3 lt 0.) then begin
  print, 'ERROR: Result 2-3 negative'
  s3=0.
endif

if (o4 le t24(0)) then s4=o4*s24(0)/t24(0)
if (o4 ge t24(0)) and (o4 le t24(1)) then $
  s4=s24(0)+(o4-t24(0))*(s24(1)-s24(0))/(t24(1)-t24(0))
if (o4 ge t24(1)) then s4=s24(1)+(o4-t24(1))*(s24(2)-s24(1))/(t24(2)-t24(1))
if (s4 lt 0.) then begin
  print, 'ERROR: Result 2-4 negative'
  s4=0.
endif

print, 'LYRA Head 2 observations [in nA]
print, o1, o2, o3, o4
print, 'corresponding solar values [in W m-2]

```

```

print,s1,s2,s3,s4
endif

if (head eq 3) then begin
if (o1 lt 0.) then begin
print,'ERROR: Channel 3-1 negative'
o1=0.
endif
if (o1 gt 1.2*max(t31)) then $
print,'WARNING: Channel 3-1 far above interpolation range'
if (o2 lt 0.) then begin
print,'ERROR: Channel 3-2 negative'
o2=0.
endif
if (o2 gt 1.2*max(t32)) then $
print,'WARNING: Channel 3-2 far above interpolation range'
if (o3 lt 0.) then begin
print,'ERROR: Channel 3-3 negative'
o3=0.
endif
if (o3 gt 1.2*max(t33)) then $
print,'WARNING: Channel 3-3 far above interpolation range'
if (o4 lt 0.) then begin
print,'ERROR: Channel 3-4 negative'
o4=0.
endif
if (o4 gt 1.2*max(t34)) then $
print,'WARNING: Channel 3-4 far above interpolation range'

s1=0.0629*(o1-0.0024*o2)
if (s1 lt 0.) then begin
print,'ERROR: Result 3-1 negative'
s1=0.
endif

s2=0.0556*(0.837*o2)

r33=t33-p33
if (o4 le t34(0)) then r3=o4*r33(0)/t34(0)
if (o4 ge t34(0)) and (o4 le t34(1)) then $
r3=r33(0)+(o4-t34(0))*(r33(1)-r33(0))/(t34(1)-t34(0))
if (o4 ge t34(1)) then r3=r33(1)+(o4-t34(1))*(r33(2)-r33(1))/(t34(2)-t34(1))
p3=o3-r3
if (p3 le p33(0)) then s3=p3*s33(0)/p33(0)
if (p3 ge p33(0)) and (p3 le p33(1)) then $
s3=s33(0)+(p3-p33(0))*(s33(1)-s33(0))/(p33(1)-p33(0))
if (p3 ge p33(1)) then s3=s33(1)+(p3-p33(1))*(s33(2)-s33(1))/(p33(2)-p33(1))
if (s3 lt 0.) then begin
print,'ERROR: Result 3-3 negative'
s3=0.
endif

if (o4 le t34(0)) then s4=o4*s34(0)/t34(0)
if (o4 ge t34(0)) and (o4 le t34(1)) then $
s4=s34(0)+(o4-t34(0))*(s34(1)-s34(0))/(t34(1)-t34(0))
if (o4 ge t34(1)) then s4=s34(1)+(o4-t34(1))*(s34(2)-s34(1))/(t34(2)-t34(1))
if (s4 lt 0.) then begin
print,'ERROR: Result 3-4 negative'
s4=0.
endif

```

```
print, 'LYRA Head 3 observations [in nA]
print, o1, o2, o3, o4
print, 'corresponding solar values [in W m-2]
print, s1, s2, s3, s4
endif
```

```
end
```

3. Flatfield Software

The IDL program for this purpose (see below) asks for the coordinates of the off-pointing. The solar center is assumed to be $(x,y) = (0,0)$, where the first coordinate denotes the east-west dimension, $x < 0$ being east and $x > 0$ being west; the second coordinate denotes the south-north dimension, $y < 0$ being south and $y > 0$ being north.

The program then calculates the beam of the Sun on the LYRA detector plane. The beam is limited by the precision aperture, diameter = 3 mm, distance = 27.75 mm, and also limited by the view-limiting aperture, diameter = 6.4 mm, distance = 27.75 + 70.00 mm. The location of the two images is calculated with the help of a tangens-formula, the resulting real image is the intersection of the two.

The approach was initially limited to channels *-3 and *-4, using "homogeneity" values measured during the LYRA calibration at BESSY (GI campaign, March 2006). Meanwhile, data from the NI campaign was added, thus also covering channels *-1, *-2, and *-3 at a longer wavelength. The program now asks for the LYRA channel (1-1, 1-2, ..., 3-4) and reads the measured flatfield, i.e. the geometrically distributed relative responses. The solar beam on the detector plane is weighted with this homogeneity. The resulting sum is divided by the result that would be delivered by (0,0) i.e. no off-pointing. The quotient can be called "relative" or "normalized response" of the channel.

This approach uses the documents

- "LYRA Opto-Mechanical Properties", Silvio Koller 06.02.2004
- "Off-pointings for LYRA" from P2SC wiki
- "LYRA" by Hochedez et al. ASR 2006

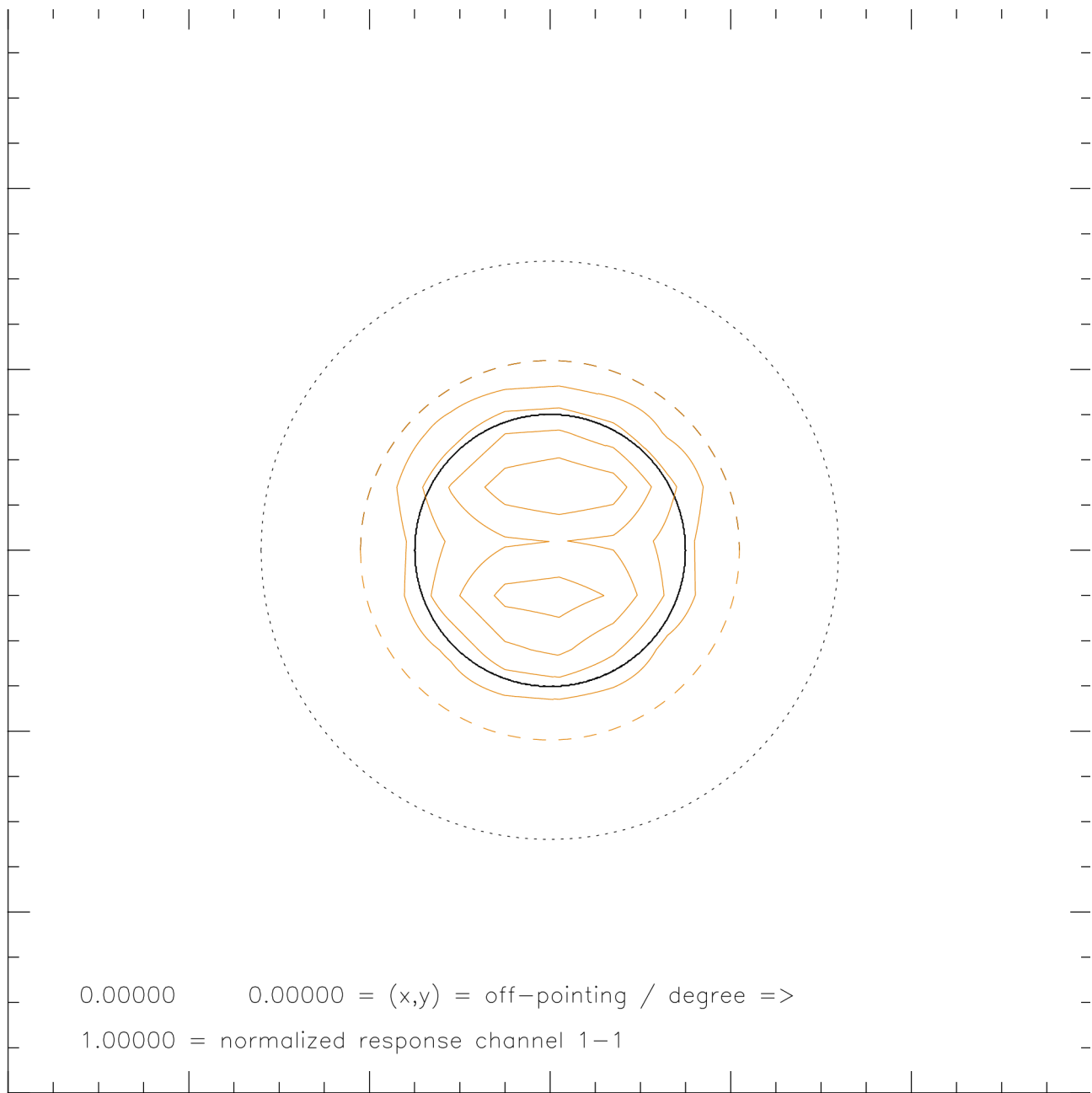
These sources contain differing values for the view-limiting aperture, 6.4 mm diameter TBC. They also contain differing values for the detector sensitive areas, but these do not matter since the actually measured values from the BESSY calibration campaign were used.

The orientation of the detector homogeneity measurements relative to their position on PROBA or their position to SWAP were also determined. With this information, together with the possible off-pointing and the possible roll angle, a general normalization factor (for absolute radiometric calibration) can be calculated. An (x,y) -map of relative responses as a function of off-pointing can be produced, given the limits of the expected pointing range. This will be the content of the next chapter.

One could think of several improvements to get better results for the "normalized response". But it has to be considered first if the greater exactness would be worth the effort:

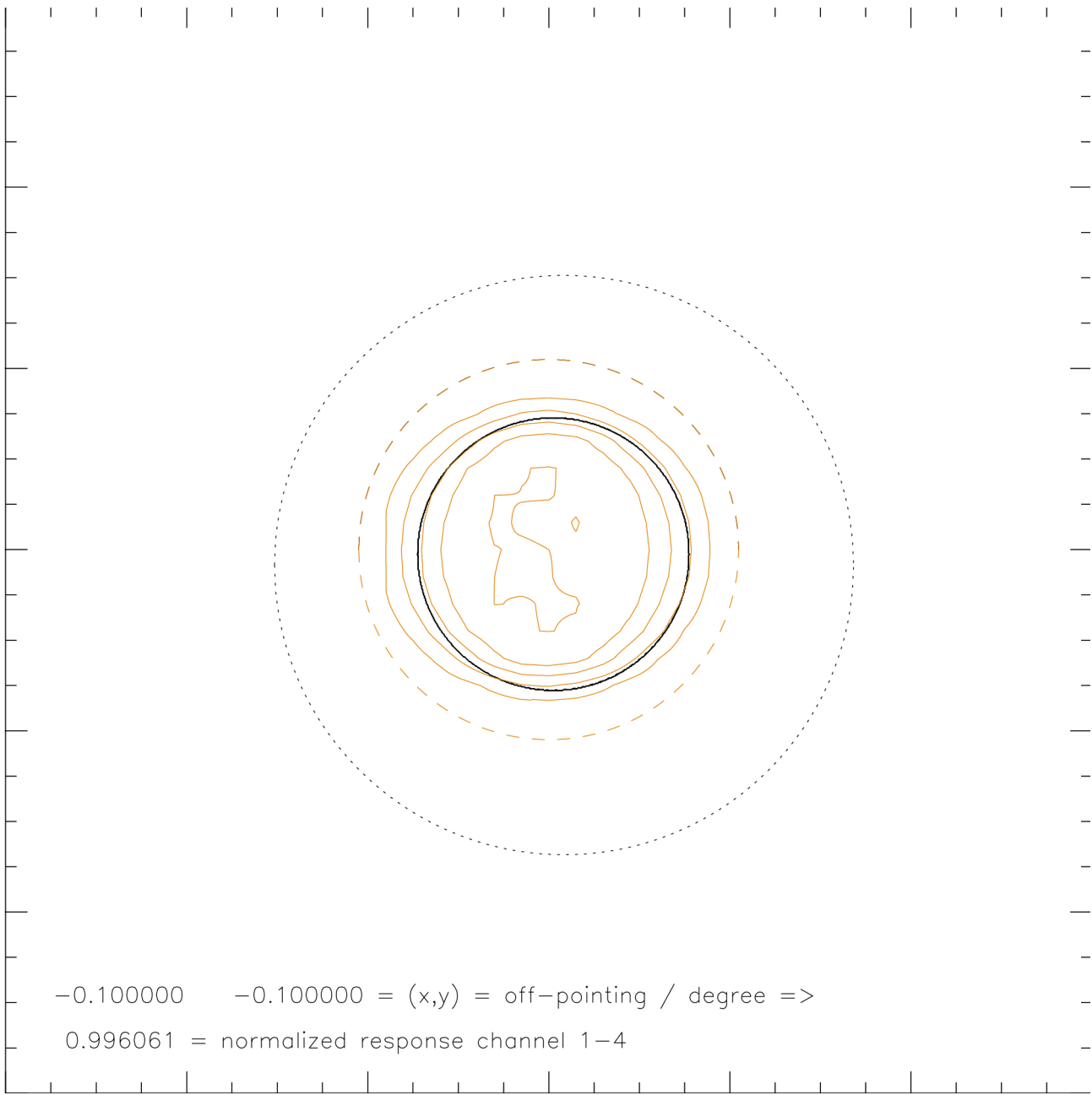
- The extension of the Sun (0.5 degree) leads to a halfshadow on both sides of the border of the solar images; this is, so far, not implemented.
- The resolution used for the numerical calculation of the solar images' intersection is 0.01 mm and could be made smaller.

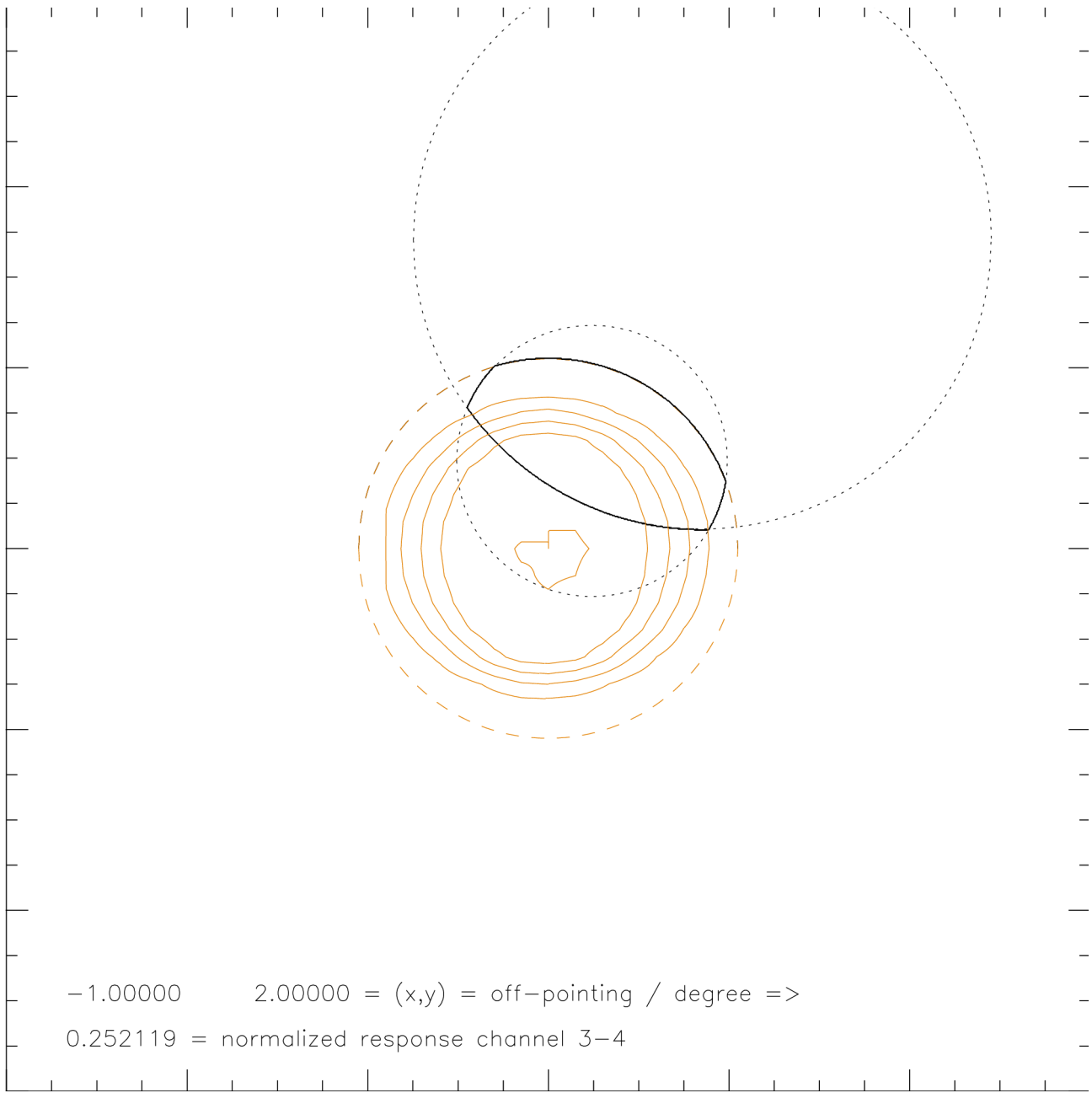
Below: Figures with five examples (various channels, various off-pointing), and IDL program listing.

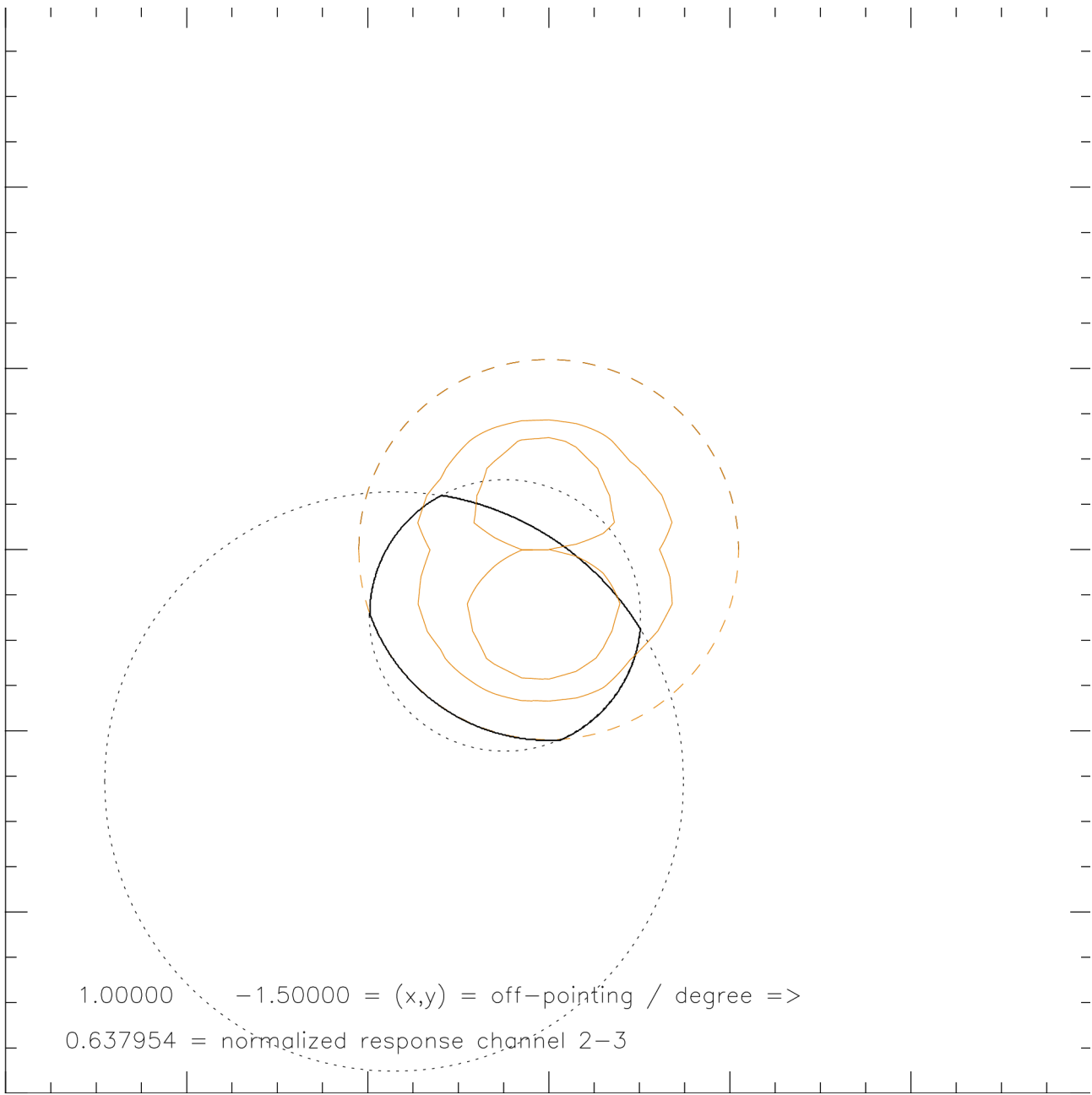


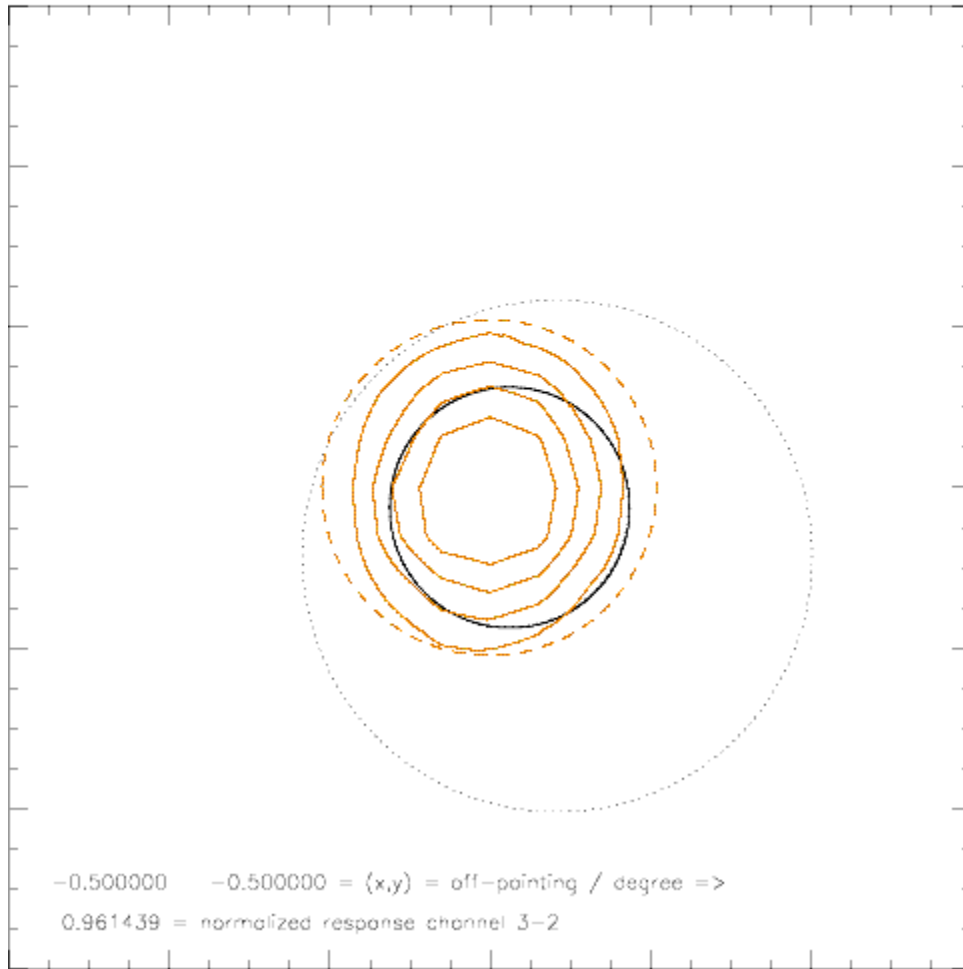
Caption for this and the following figures

- 12 mm x 12 mm extension in detector plane
- red, dashed: detector limits
- red, solid: detector flatfield contour
- black, larger, dotted: image of Sun through 6.4 mm view-limiting aperture
- black, smaller, dotted: image of Sun through 3 mm precision aperture
- black, thick solid: intersection, resulting image of Sun in detector plane









```

; plot_detim_offp.pro
;-----
; IED 25 Apr 2007
;-----
; IDL program to calculate the beam of the Sun on a LYRA detector with 4.2 mm
; diameter, given an off-pointing.
; Coordinates (x=east-west, y=south-north) of solar center = (0,0),
; coordinates of pointing in degrees east x<0, west x>0, south y<0, north y>0
; Aperture with diameter 3 mm at 27.75 mm distance,
; aperture with diameter 6.4 mm at 27.75 + 70.00 mm distance.
; After calculating the beam, the program asks for a LYRA channel (1-1,...,3-4),
; reads the measured homogeneity values, plots them, and calculates the
; normalized detector response.
; Update: Homogeneity values (flatfields) from NI campaigns added,
; values from GI campaigns with coordinate transformations.
; !! .run read_allflatfields.pro first !!
;-----

chpr=0
loadct,3
read,'print .PS (Y=1) ? ',chpr
if (chpr eq 1) then begin
  set_plot,'ps'
  ;device,/portrait,xoffset=1,yoffset=7,xsize=19,ysize=19,bits=8,/color
  device,/portrait,xoffset=1,yoffset=7,xsize=17,ysize=17,bits=8,/encapsulated,/color
  endif else begin
  set_plot,'x'
  window,xsize=600,ysize=600,retain=2
  endelse
xoff=0. & yoff=0.
read,'off-pointing in degree (east-west,south-north) #,# ? ',xoff,yoff
dist=2775.
dist2=dist+7000.
ximgoff=-dist*tan(xoff/180.*!pi)
yimgoff=dist*tan(yoff/180.*!pi)
ximgoff2=-dist2*tan(xoff/180.*!pi)
yimgoff2=dist2*tan(yoff/180.*!pi)
print,ximgoff,yimgoff
print,ximgoff2,yimgoff2
!xmin=-600 & !xmax=600 & !ymin=-600 & !ymax=600
ddet=420
rdet=ddet/2.
dpra=300
rpra=dpra/2.
dvla=640
rvla=dvla/2.
xdet=findgen(ddet+1)-rdet
ydet=sqrt(rdet*rdet-xdet*xdet)
plot,xdet,ydet,linestyle=2,charsize=0.01
loadct,4
oplot,xdet,ydet,linestyle=2,color=200
oplot,xdet,-ydet,linestyle=2,color=200
loadct,0
ximg=findgen(dpra+1)-rpra
ximg2=findgen(dvla+1)-rvla
yimg=sqrt(rpra*rpra-ximg*ximg)
yimg2=sqrt(rvla*rvla-ximg2*ximg2)
oplot,ximg+ximgoff,yimg+yimgoff,linestyle=1
oplot,ximg+ximgoff,-yimg+yimgoff,linestyle=1
oplot,ximg2+ximgoff2,yimg2+yimgoff2,linestyle=1

```

```

oplot,ximg2+ximgoff2,-yimg2+yimgoff2,linestyle=1
detimg=fltarr(1201,1201)
for i=0,ddet do begin
  xco=0>(round(xdet(i))+600)<1200
  yco1=0>(round(-ydet(i))+600)<1200
  yco2=0>(round(ydet(i))+600)<1200
  detimg(xco,yco1:yco2)=detimg(xco,yco1:yco2)+1.
endfor
for i=0,dpra do begin
  xco=0>(round(ximg(i)+ximgoff)+600)<1200
  yco1=0>(round(-yimg(i)+yimgoff)+600)<1200
  yco2=0>(round(yimg(i)+yimgoff)+600)<1200
  detimg(xco,yco1:yco2)=detimg(xco,yco1:yco2)+1.
endfor
for i=0,dvla do begin
  xco=0>(round(ximg2(i)+ximgoff2)+600)<1200
  yco1=0>(round(-yimg2(i)+yimgoff2)+600)<1200
  yco2=0>(round(yimg2(i)+yimgoff2)+600)<1200
  detimg(xco,yco1:yco2)=detimg(xco,yco1:yco2)+1.
endfor
!xmin=0 & !xmax=0 & !ymin=0 & !ymax=0
detimg(0,* )=0
detimg(1200,* )=0
detimg(*,0)=0
detimg(*,1200)=0
detimg(where(detimg lt 3))=0.
detimg=detimg/3.
ok=''
read,'ok ? ',ok
contour,detimg,/noerase,charsize=0.01

ch=''
print,'(NI2006:) 11,12,13n, ,21,22,23n, ,31,32,33n, '
print,'(GI2006:) , ,13g,14, , ,23g,24, , ,33g,34'
read,'channel ## ? ',ch
detff=fltarr(1201,1201)

if (ch eq '11') then begin
  ffhom=ni6_ff11
  ffhom00=congrid(ffhom,600,480,/interp)
  ;detff(600-250,600-210)=ffhom00
  ;detff(600-270,600-210)=ffhom00
  detff(600-290,600-230)=ffhom00
  norm00=43166.0
endif

if (ch eq '12') then begin
  ffhom=ni6_ff12
  ffhom00=congrid(ffhom,540,540,/interp)
  ;detff(600-250,600-290)=ffhom00
  detff(600-240,600-240)=ffhom00
  norm00=49028.9
endif

if (ch eq '13n') then begin
  ffhom=ni6_ff13
  ffhom00=congrid(ffhom,600,600,/interp)
  ;detff(600-260,600-250)=ffhom00
  detff(600-270,600-270)=ffhom00
  norm00=48482.6
endif

```

```
if (ch eq '13g') then begin
ffhom=gi6_ff13t
ffhom00=congrid(ffhom,390,390,/interp)
;detff(600-180,600-170)=ffhom00
detff(600-180,600-180)=ffhom00
norm00=48165.6
endif
```

```
if (ch eq '14') then begin
ffhom=gi6_ff14t
ffhom00=congrid(ffhom,390,390,/interp)
;detff(600-180,600-170)=ffhom00
detff(600-180,600-180)=ffhom00
norm00=59970.8
endif
```

```
if (ch eq '21') then begin
ffhom=ni6_ff21
ffhom00=congrid(ffhom,450,450,/interp)
;detff(600-250,600-160)=ffhom00
;detff(600-200,600-200)=ffhom00
detff(600-220,600-200)=ffhom00
norm00=34516.1
endif
```

```
if (ch eq '22') then begin
ffhom=ni6_ff22
ffhom00=congrid(ffhom,540,540,/interp)
;detff(600-250,600-290)=ffhom00
detff(600-240,600-240)=ffhom00
norm00=49171.4
endif
```

```
if (ch eq '23n') then begin
ffhom=ni6_ff23
ffhom00=congrid(ffhom,600,600,/interp)
;detff(600-280,600-240)=ffhom00
detff(600-270,600-270)=ffhom00
norm00=48197.0
endif
```

```
if (ch eq '23g') then begin
ffhom=gi6_ff23t
ffhom00=congrid(ffhom,390,390,/interp)
;detff(600-180,600-180)=ffhom00
detff(600-180,600-180)=ffhom00
norm00=66855.6
endif
```

```
if (ch eq '24') then begin
ffhom=gi6_ff24t
ffhom00=congrid(ffhom,390,390,/interp)
;detff(600-180,600-180)=ffhom00
detff(600-180,600-180)=ffhom00
norm00=70408.6
endif
```

```
if (ch eq '31') then begin
ffhom=ni6_ff31
ffhom00=congrid(ffhom,540,540,/interp)
```



```

;detff(600-250,600-240)=ffhom00
;detff(600-240,600-240)=ffhom00
detff(600-260,600-260)=ffhom00
norm00=53151.3
endif

if (ch eq '32') then begin
ffhom=ni6_ff32
ffhom00=congrid(ffhom,540,540,/interp)
;detff(600-250,600-300)=ffhom00
detff(600-240,600-240)=ffhom00
norm00=49321.3
endif

if (ch eq '33n') then begin
ffhom=ni6_ff33
ffhom00=congrid(ffhom,600,600,/interp)
;detff(600-310,600-240)=ffhom00
detff(600-270,600-270)=ffhom00
norm00=52200.3
endif

if (ch eq '33g') then begin
ffhom=gi6_ff33t
ffhom00=congrid(ffhom,390,390,/interp)
;detff(600-195,600-175)=ffhom00
detff(600-180,600-180)=ffhom00
norm00=56904.9
endif

if (ch eq '34') then begin
ffhom=gi6_ff34t
ffhom00=congrid(ffhom,390,390,/interp)
;detff(600-180,600-210)=ffhom00
detff(600-180,600-180)=ffhom00
norm00=59571.6
endif

loadct,4
contour,detff,/noerase,color=200,xstyle=4,ystyle=4,charsize=0.01
loadct,0
detimgff=total(detimg*detff)
print,detimgff,'=> normalized: ',detimgff/norm00
chstr=strmid(ch,0,1)+'-'+strmid(ch,1,1)
xyouts,0,100,string(xoff)+string(yoff)+' = (x,y) = off-pointing / degree =>'
xyouts,0,50,string(detimgff/norm00)+' = normalized response channel '+chstr
if (chpr eq 1) then begin
device,/close
;spawn,'lpr -P lpsidc idl.ps'
set_plot,'x'
endif

loadct,0
end

```

4. Off-Pointing Simulations

The LYRA team collected four sets of detector flatfield measurements, performed in four BESSY campaigns:

- “crosses” from NI 2005 for channels *-1, *-2, *-3
- “crosses” from GI 2005 for channels *-3, *-4
- “surfaces” from NI 2006 for channels *-1, *-2, *-3
- “surfaces” from GI 2006 for channels *-3, *-4

(for parameters, see Tables 1, 2, 3, 4.)

New flatfield measurements from the campaign of February 2007 have yet to be integrated in this report (TBD).

“Cross” means that only two scans, rectangular to each other, were done; “surface” means that a 2D field was scanned.

The monitored coordinates are not absolute. The measurements were made relative to a different coordinate system each time. Apart from that, the scan resolution was different each time, varying from 0.15, 0.2, 0.3, 0.5, to 0.6 mm. Results were sometimes given in V, sometimes normalized to maximum or to center value. The measurements in the GI campaigns are rotated 90 degrees compared to the NI campaigns, i.e. horizontal and vertical axes are swapped. On the other hand, channels *-3 are measured in both NI and GI, although using different wavelengths.

Therefore, the exact position of the flatfields within the detector area, or the exact position of the solar beam through the 3 mm precision hole, cannot be determined. In other words, it is not known whether the center of the scan (cross or surface) is identical to the center of the detector, or whether it is identical to the center of the solar beam. Nevertheless, the results of the “crosses” were compared with the “surfaces”, and the position of the flatfields relative to each other (i.e. their orientation on the detector plane) was confirmed.

Assuming

- a linear offset between NI 2005 and NI 2006 such that the center of the cross coincides, in average, with the center of the surface,
- rotation and offset between NI 2005 and GI 2005 such that the centers of the cross of channel 2-3 coincide,
- coordinates for GI 2006 such that the center of the surface coincides with the center of the cross from GI 2005,

then the locations of the various observations can be marked on the detector plane, in coordinates of NI 2006, as demonstrated in Figure 1 (following Tables 1,...,4).

Table 1: NI 2005 (crosses)

ch.	wave.	hor.scan	at vert.pos.	resol.	vert.scan	at hor.pos.	resol.	/ mm
1-1	121nm	1.0, ..., 7.0	@88.0	21*0.3	85.0, ..., 91.0	@4.0	21*0.3	
1-2	210nm	1.0, ..., 7.0	@101.0	21*0.3	98.0, ..., 104.0	@4.0	21*0.3	
1-3	60nm	14.0, ..., 20.0	@88.0	21*0.3	85.0, ..., 91.0	@17.0	21*0.3	
2-1	121nm	1.0, ..., 7.0	@149.0	21*0.3	146.0, ..., 152.0	@4.0	21*0.3	
2-2	210nm	1.0, ..., 7.0	@162.0	21*0.3	159.0, ..., 165.0	@4.0	21*0.3	
2-3	60nm	12.5, ..., 21.5	@149.0	31*0.3	146.0, ..., 152.0	@17.0	21*0.3	
3-1	121nm	1.0, ..., 7.0	@210.0	21*0.3	207.0, ..., 213.0	@4.0	21*0.3	
3-2	210nm	1.0, ..., 7.0	@223.0	21*0.3	220.0, ..., 226.0	@4.0	21*0.3	
3-3	60nm	13.0, ..., 19.0	@210.0	21*0.3	207.0, ..., 213.0	@16.0	21*0.3	

Channel 2-3 is indeed the only one to be scanned with 31 steps in horizontal direction. Measured is “abs. signal (V), offset corrected”. The vertical position of the horizontal scan is not explicitly given; it is assumed to be in the middle of the vertical scan, and vice versa.

Table 2: GI 2005 (crosses)

ch.	wave.	hor.scan	at vert.pos.	resol.	vert.scan	at hor.pos.	resol.	/ mm
2-3	1nm	-10.00, ..., -4.90	@81.30	35*0.15	79.00, ..., 83.50	@-7.87	31*0.15	
2-3	18nm	-10.50, ..., -5.40	@81.31	35*0.15	79.00, ..., 83.65	@-8.09	32*0.15	
2-4	1nm	2.50, ..., 7.15	@81.34	32*0.15	79.00, ..., 83.65	@4.86	32*0.15	
2-4	10nm	2.50, ..., 9.55	@81.31	48*0.15	79.00, ..., 84.10	@4.86	35*0.15	
3-3	1nm	50.00, ..., 55.60	@81.34	29*0.2	79.00, ..., 83.80	@53.00	25*0.2	
3-3	18nm	51.00, ..., 55.05	@81.37	28*0.15	79.00, ..., 84.55	@52.94	38*0.15	
3-4	1nm	62.00, ..., 68.20	@81.23	32*0.2	79.00, ..., 84.20	@65.92	28*0.2	
3-4	10nm	63.50, ..., 68.45	@81.23	34*0.15	79.00, ..., 83.95	@65.65	34*0.15	

Measured is “Signal (V)”. The vertical position of the horizontal scan is explicitly given, and vice versa.

Table 3: **NI 2006 (surfaces)**

ch.	wave.	horizontal scan	resol.	vertical scan	resol.	/ mm
1-1	121.6nm	0.9, ..., 6.3	10*0.6	86.9, ..., 91.1	8*0.6	
1-2	210.0nm	0.9, ..., 5.7	9*0.6	99.1, ..., 103.9	9*0.6	
1-3	50.0nm	13.8, ..., 19.2	10*0.6	86.5, ..., 91.9	10*0.6	
2-1	121.6nm	0.2, ..., 4.2	9*0.5	148.4, ..., 152.4	9*0.5	
2-2	210.0nm	0.9, ..., 5.7	9*0.6	160.1, ..., 164.9	9*0.6	
2-3	50.0nm	13.6, ..., 19.0	10*0.6	147.6, ..., 153.0	10*0.6	
3-1	121.6nm	0.9, ..., 5.7	9*0.6	208.6, ..., 213.4	9*0.6	
3-2	210.0nm	0.9, ..., 5.7	9*0.6	221.0, ..., 225.8	9*0.6	
3-3	50.0nm	13.3, ..., 18.7	10*0.6	208.6, ..., 214.0	10*0.6	

Measured is the relative response, $U(\text{Diode})/I(\text{Ring})$ with 3, 12, 24, 50, 100% aperture size, offset corrected, and normalized by the maximum signal. For comparison, the 100% values were used. The horizontal axis of channel 2-1 might be wrong by 0.7 mm.

Table 4: **GI 2006 (surfaces)**

ch.	wave.	horizontal scan	resol.	vertical scan	resol.	/ mm
1-3	18nm	-1.8, ..., 1.8	13*0.3	-1.8, ..., 1.8	13*0.3	
1-4	10nm	-1.8, ..., 1.8	13*0.3	-1.8, ..., 1.8	13*0.3	
2-3	18nm	-1.8, ..., 1.8	13*0.3	-1.8, ..., 1.8	13*0.3	
2-4	10nm	-1.8, ..., 1.8	13*0.3	-1.8, ..., 1.8	13*0.3	
3-3	18nm	-1.8, ..., 1.8	13*0.3	-1.8, ..., 1.8	13*0.3	
3-4	10nm	-1.8, ..., 1.8	13*0.3	-1.8, ..., 1.8	13*0.3	

Measured is the relative responsivity, normalized to the value of the center point. The coordinates of the center points are set to zero in all cases, so their relative positions are not given.

NI/GI 2005/06

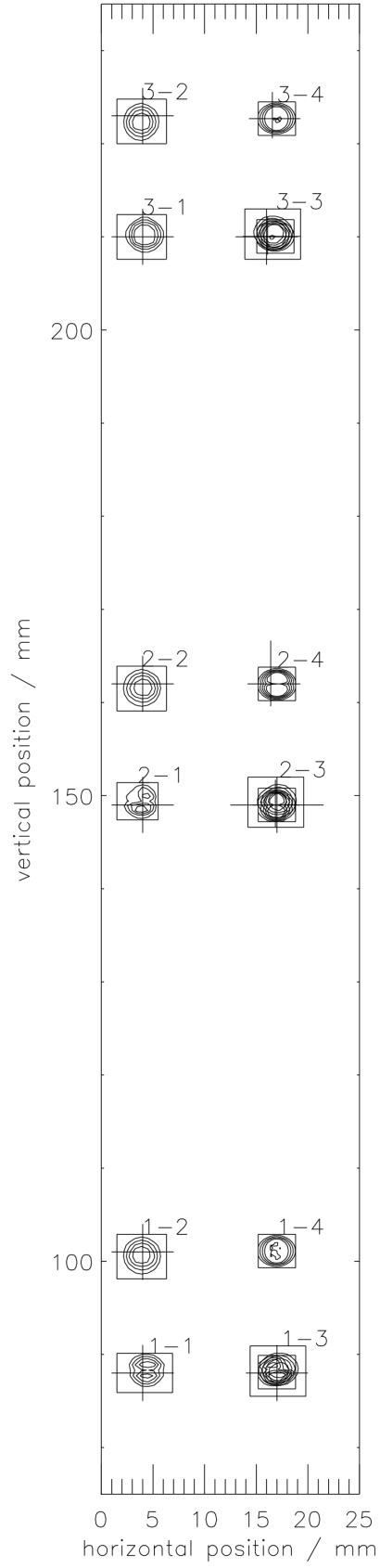


Figure 1.

Based on this common orientation, reactions to off-pointing can be simulated as described in the previous chapter. Additionally, off-pointing has been simulated here covering a whole range of possible values, namely from -1 degree to +1 degree, in east-west as well as in north-south direction. This grid of simulations leads to a surface of normalized responses as shown in the next four sample Figures 2, 3, 4, and 5, below. It is assumed that north is up (i.e. on the upper side of the detector plane as shown in the previous figure.) A possible roll angle should be implemented in the simulation software (TBD). - Numbers within the images show the variations in the correction factor (maximum and minimum for +/- 1 degree off-pointing, and for +/- 5 arcmin off-pointing around the center position).

It is not claimed here that the in-flight reaction of LYRA will be exactly like the simulations. The real positions of the various detectors on the plane might be slightly different, the nominal pointing might not be exactly centered, the response to the real solar beam might differ from the BESSY test situation in many ways (small beam size, fixed wavelength). Nevertheless, the simulation technique presented here may help to interpret in-flight findings during the commissioning phase.

It is suggested to test various off-pointing positions during the commissioning phase in co-operation with SWAP, in order to get – for each LYRA channel - a grid of relative responses comparable to the simulations described here. In the most favourite case, the simulated grids can be confirmed, maybe with a linear offset. Combining the simulations and the in-flight tests, there should emerge a tabled function of relative responses - for each channel - with pointing coordinates and roll angle as input, and a correction factor around 1.0 (= nominal pointing) as output.

Simulations show that +/- 1 degree off-pointing leads to approx. 25% reduction from the nominal response. Off-pointing in the order of the nominal jitter of PROBA2 (5 arcmin, TBC) leads to fluctuations of approx. +/- 1% around the nominal response. Off-pointing in the order of the promised maximal offset between SWAP and LYRA (10 or 20 arcsec, TBC) will therefore not be detectable.

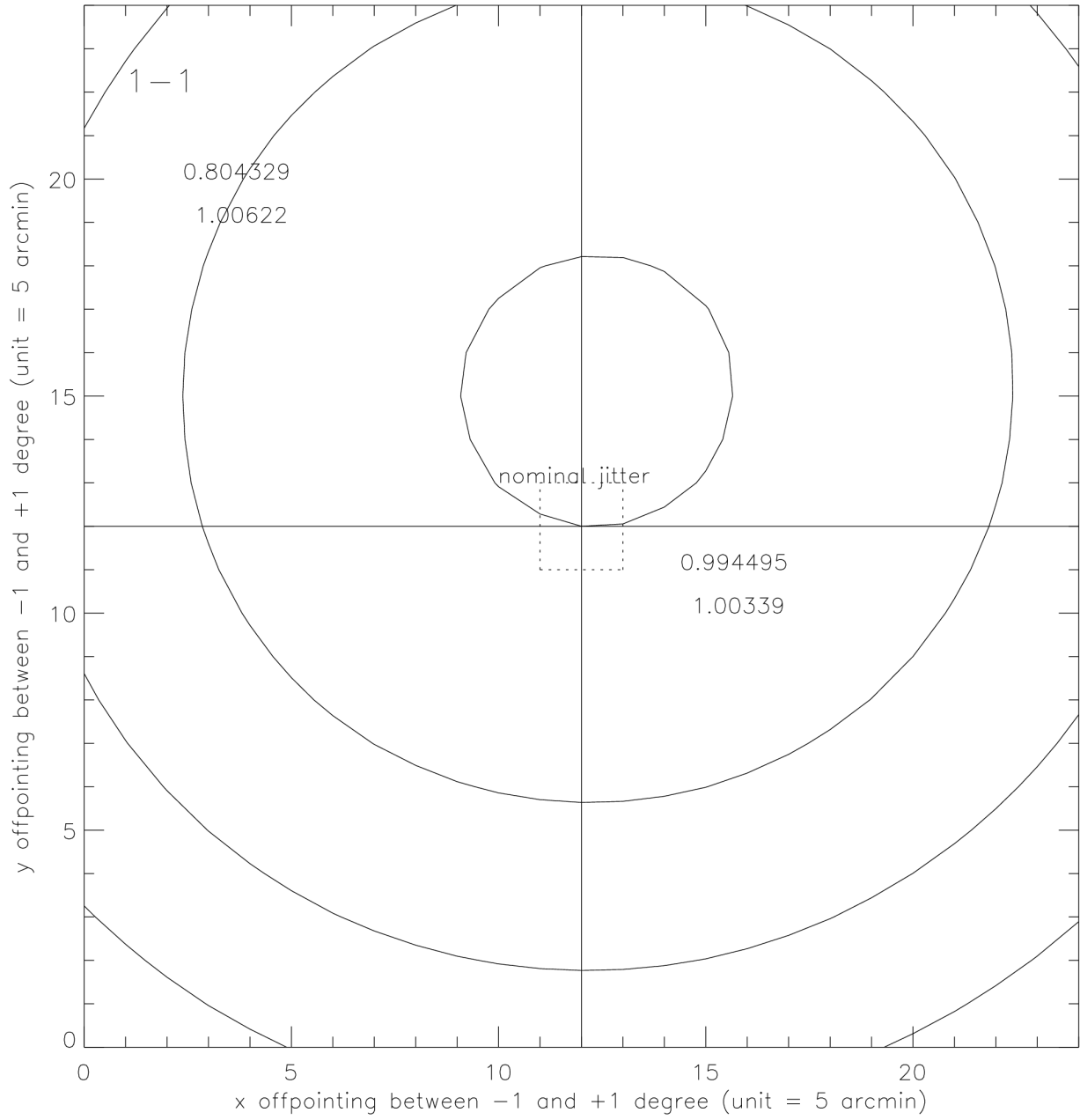


Figure 2.

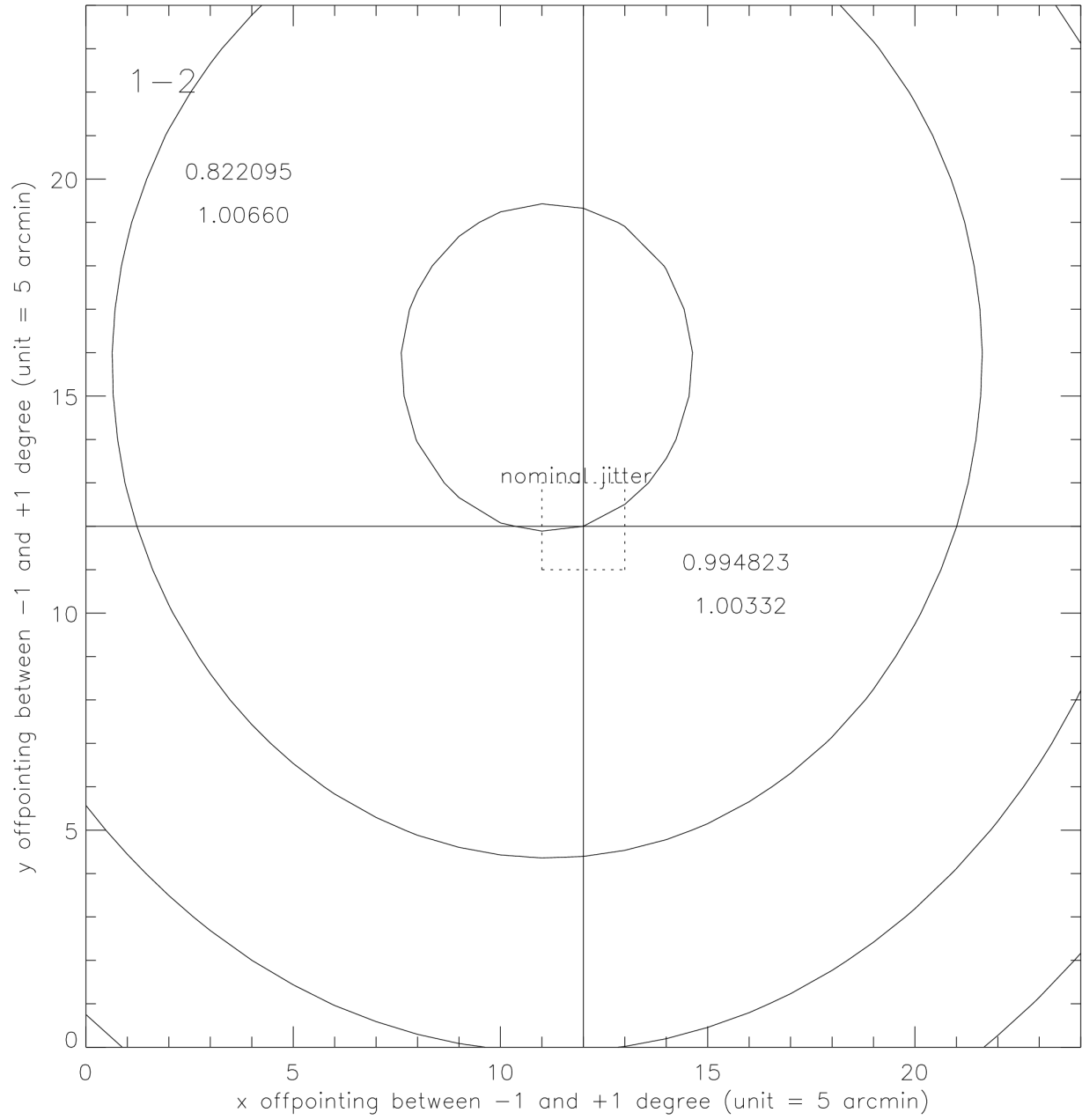


Figure 3.

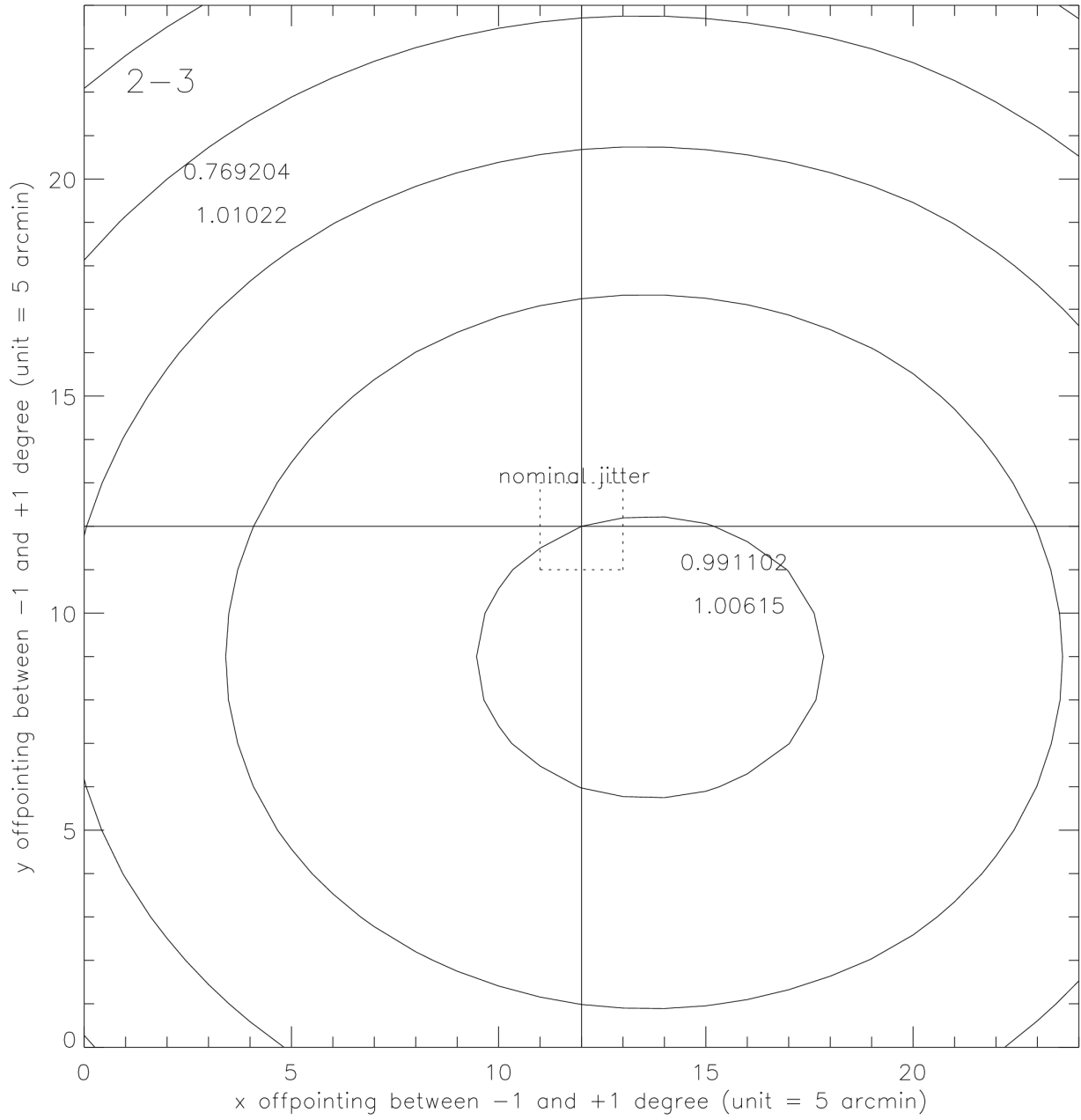


Figure 4.

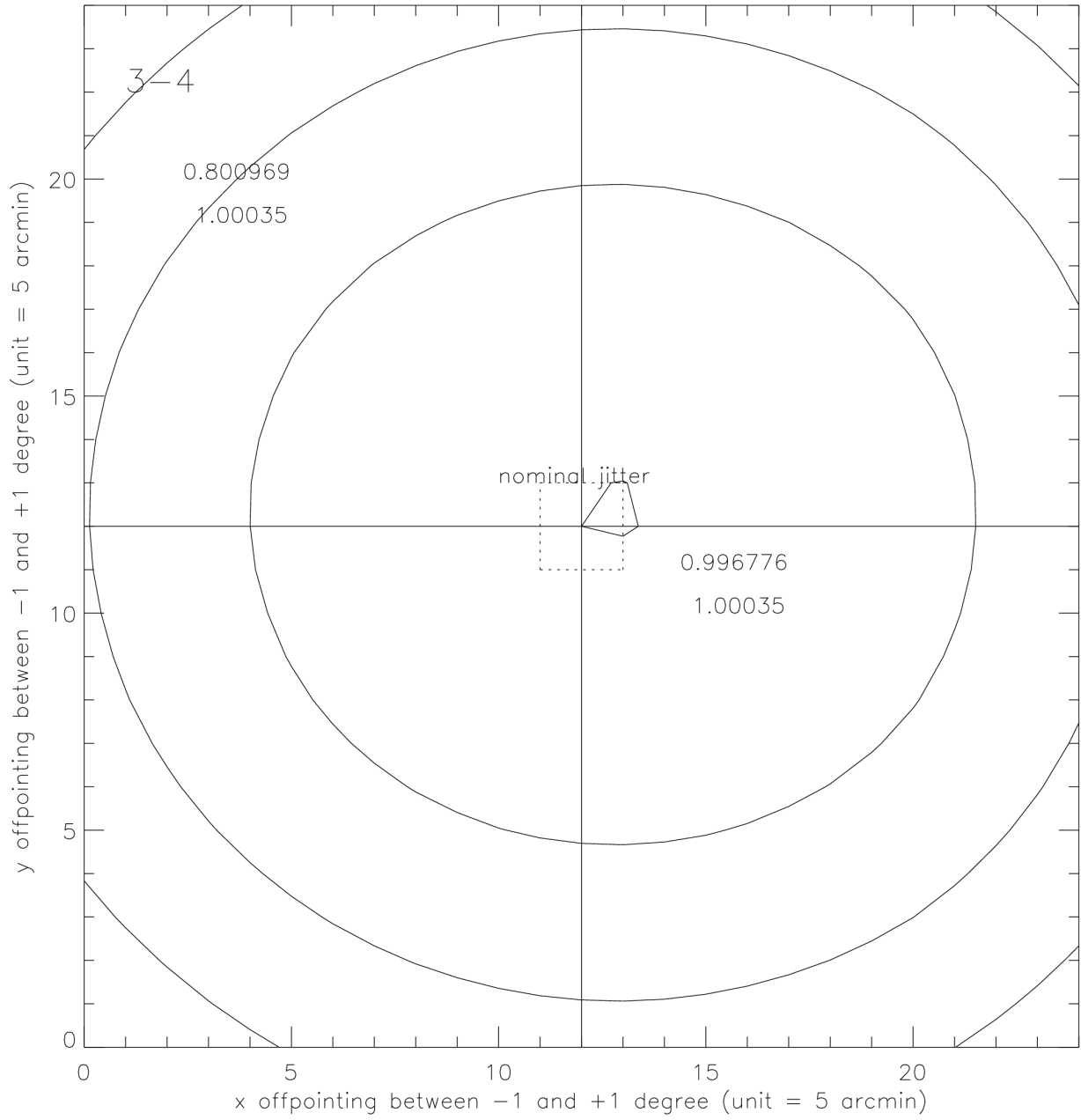


Figure 5.

5. Pulsed-LED Tests

Test Description

On 30 Nov 2006, the LYRA team at ROB received several test data files from Silvio Koller (PMOD/WRC, Davos). We were informed that LYRA had been put in their vacuum chamber, and measurements regarding temperature and LED pulsing were performed.

It was reported that the commanding by the EGSE software had not been very accurate, and thus the LED on/off temporal behaviour had quite a jitter. The serial link together with the EGSE software was too slow to acquire data with 100 Hz. Therefore, data were sampled with 50 Hz, or 20 ms integration time.

The LED frequency was roughly 3.7 Hz, i.e., the LEDs were commanded on/off approx. every 270 ms. This leads to 13 or 14 steps of 20 ms integration per cycle, one half of the cycle being recorded with LEDs “on” and the other half with LEDs “off”.

The LED field - column 13 of the Telecommand Packet containing binary number PUV1, PUV2, PUV3, PVIS - changes from “0000” (off) to “1111” (on), which usually means that all LEDs, ultraviolet and visual, are switched on and off simultaneously; in this test set, the command was used although there was no power supply available for the ultraviolet LEDs, thus *only* the effect of *visual* LEDs was recorded.

Two test runs were performed: the first one starting 30 Nov 2006 15:47:29, testing LYRA heads 1 and 2 in parallel, the second one starting 15:49:04 the same day, testing heads 2 and 3 in parallel. The tests consisted of approx. 200 on/off-cycles each, thus taking less than 1 minute.

Pulsing of LEDs appears to be a suitable tool for calibration, because several parameters can be tested without facing some of the drawbacks, like long-term drifts. This applies for MSM and AXUV detectors which displayed reliable parameters during the tests. The situation for PIN detectors appears to be more complicated.

Pulse Examples

Figures 1a and 1b show examples of some typical pulses taken 7 or 8 seconds after test start. Red lines mark the telecommands that switch the LEDs on and off, black lines mark the various resulting detector reactions, versus observation time in seconds. LYRA output signals are displayed in kHz, which – at this low activity level – appears more suitable than measuring currents in Ampere (often showing bad numerical resolution, and negative values occurring due to the voltage-frequency converters).

The general behaviour can be clearly observed: Overshooting reactions after LEDs are switched on, steady decline until they are switched off again, drop and sometimes undershoot after switch-off, more or less stable levels of dark current. Only the PIN detectors (channels *-2) behave differently: First they *drop* after switch-on, then they recover more or less fast. Their reaction signal is not very significant, but rather close to the dark current level instead.

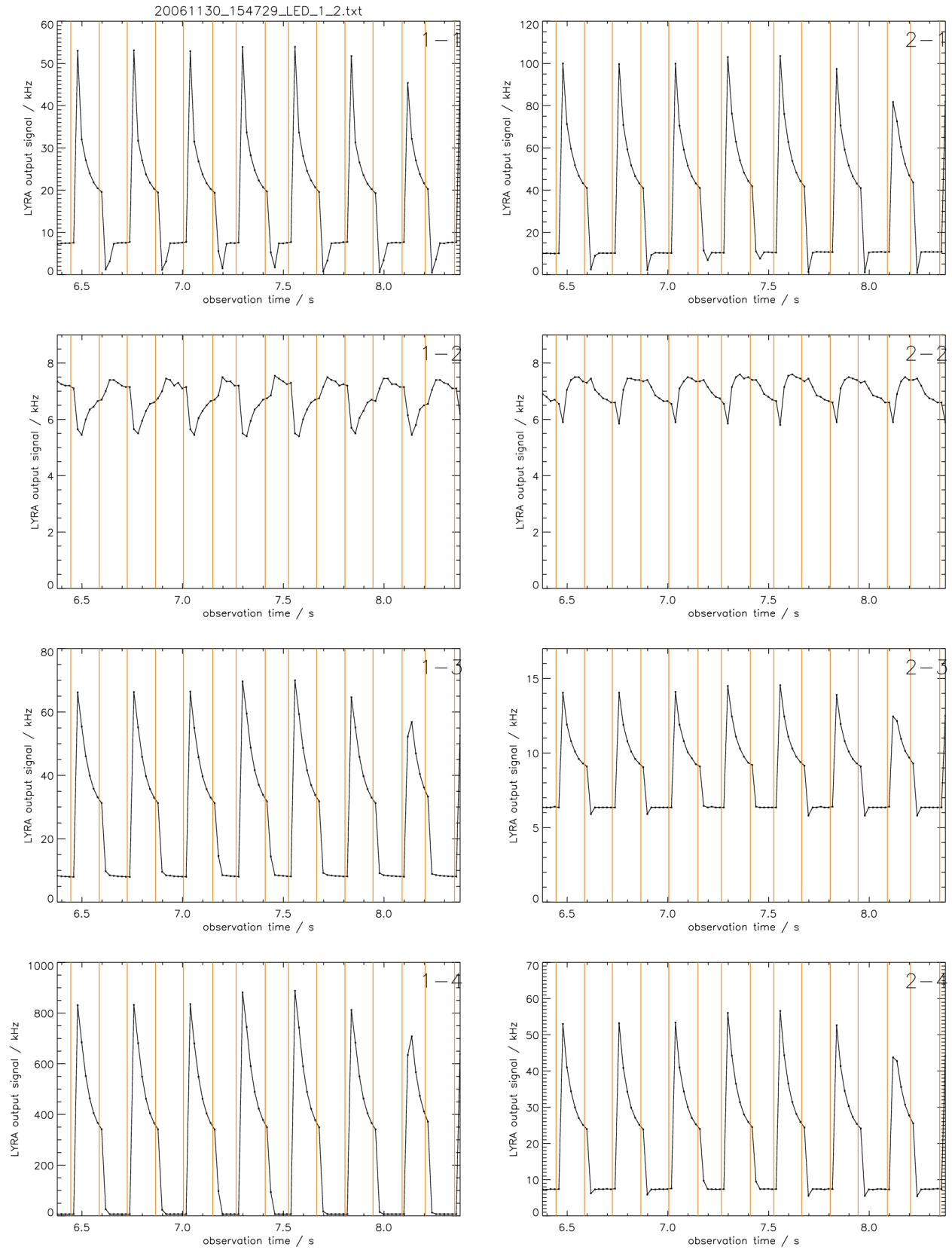


Figure 1a: Sample pulses from first test (heads 1 and 2)

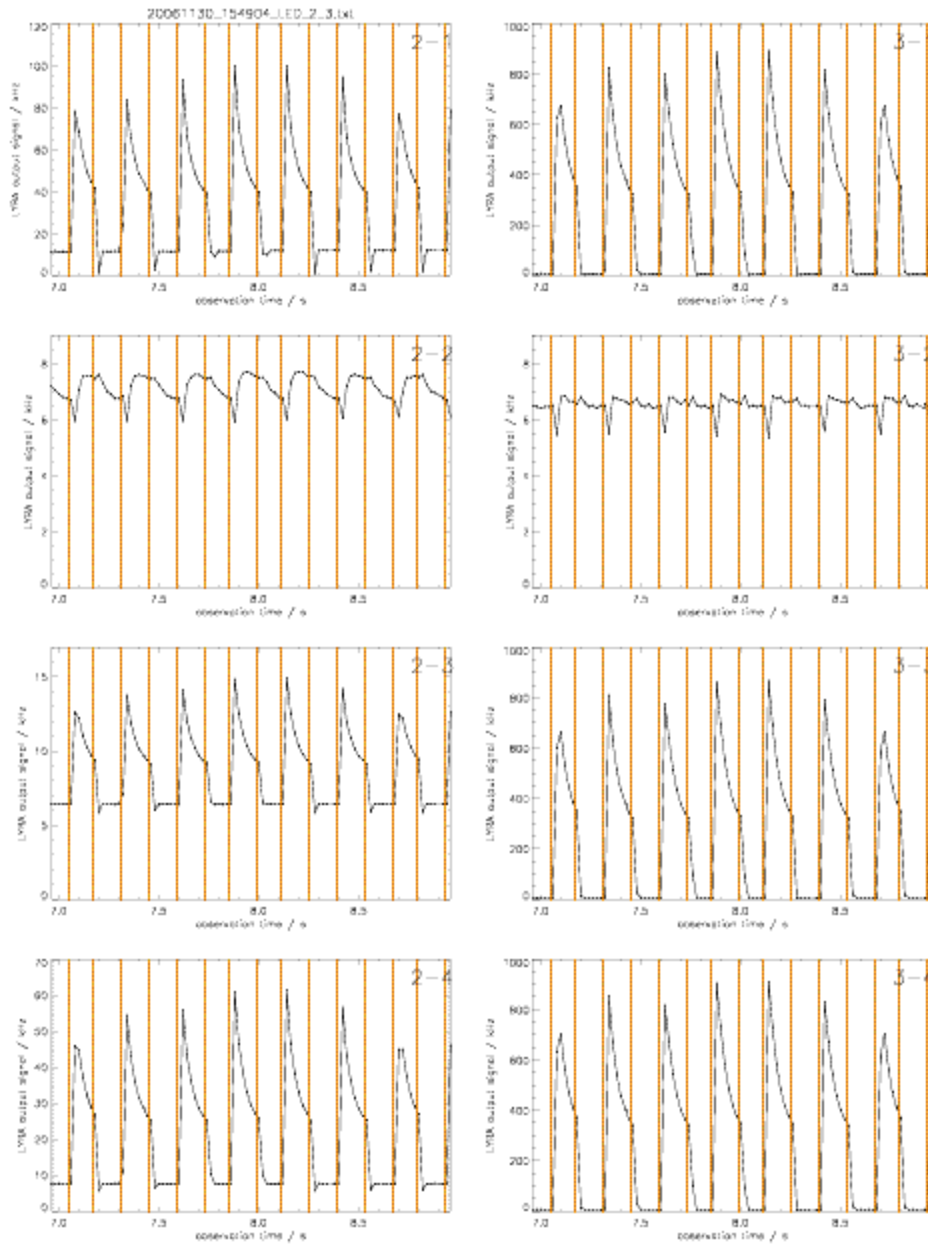


Figure 1b: Sample pulses from second test (heads 2 and 3)

Detailed Behaviour

Figures 2a and 2b show the average detailed behaviour of the pulses as recorded by the various detectors. The first (0.00 s) red line marks the time instant of the “switch on” telecommand (LED field = 1111). According to the LYRA Software User Manual, the time stamp corresponds to the instant when the packet was *put on line*. The second (0.135 s) and third (0.27 s) red line correspond to the average time instant of the “switch off” telecommand (LED field = 0000), and the following switch on of the next cycle.

The 14 asterisks mark the average LYRA output signals within the LED cycle; the 14th value occurs only in roughly half of the approx. 200 cycles. The dotted lines mark the extent of the standard deviation. The output signals are delivered in the Science Packets; according to the LYRA Software User Manual, the millisecond counter corresponds to the instant when the packet *came in* completely.

Therefore, the first averaged data point consists of observations received immediately after the switch on was commanded. Taking into account that its integration must have started 20 ms earlier, plus possible time delays for Telecommand and Science Packets, the first data point will most probably not be influenced by LEDs, and indeed shows roughly the same level as the last point of the cycle. The next 6 values are influenced by LED signals.

The next 7 values following thereafter reflect the phase of LEDs being switched off. Most detectors reach their dark current level within a decreasing phase lasting one or two steps of 20 ms integration.

Of the 14 LED cycle values, #2 and #8 – and, to a lesser extent, #3 and #9 – have a greater variance. This could be caused by the fact that in some of the cycles, #2 is partly integrated before the switch on, and #8 is partly integrated before the switch off, depending on their temporal distance to the respective telecommand.

From their behaviour, the channels can be separated into three groups that clearly depend on their detector type:

Channels 1-1, 1-3, 2-1, 2-3, 2-4 (MSM):

They display a relatively fast increase after switch on (all but channel 1-3 peak in value #2), with an overshoot; a negative exponential decay; a one-, two-, or three-step decrease after switch off, sometimes with an undershoot (1-1, 2-1); and an almost flat dark current in the last four or five values. The peaks usually vary between 40 and 85 kHz, channel 2-3 being an exception at 13 kHz.

Channels 1-4, 3-1, 3-3, 3-4 (AXUV):

They display a slower increase after switch on (all channels peak in value #3), also with an overshoot; a negative exponential decay; a two-step decrease after switch off; and an almost flat dark current in the last five values. The peaks vary closely around 700 kHz.

Channels 1-2, 2-2, 3-2 (PIN):

They display a *decrease* after switch on, with a minimum at value #2 or, even slower, at value #3; afterwards they rise again, channel 1-2 again being the slowest; after switch-off they slowly approach their dark current level again. All values stay closely around 5 to 8 kHz.

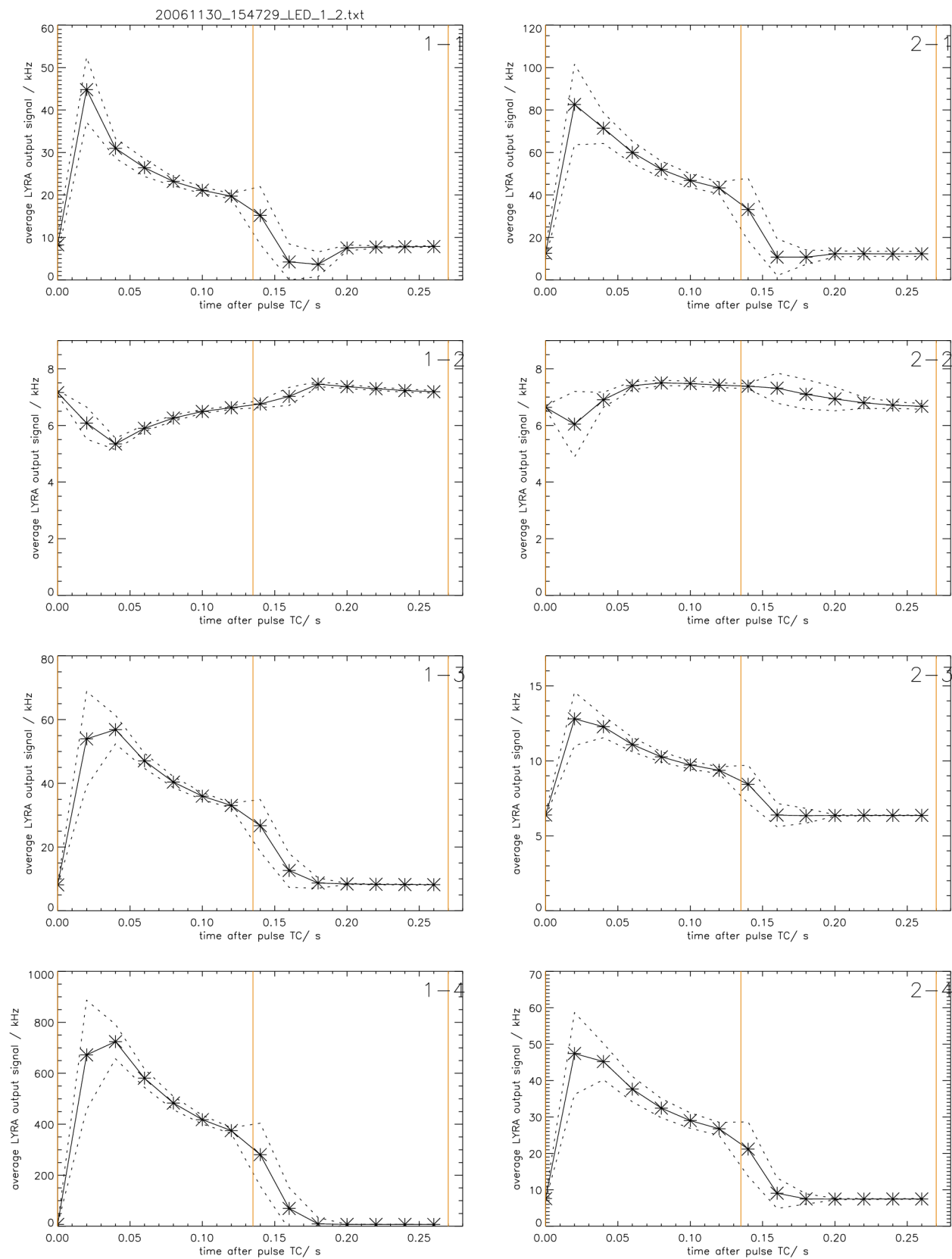


Figure 2a: Average pulses from first test (heads 1 and 2)

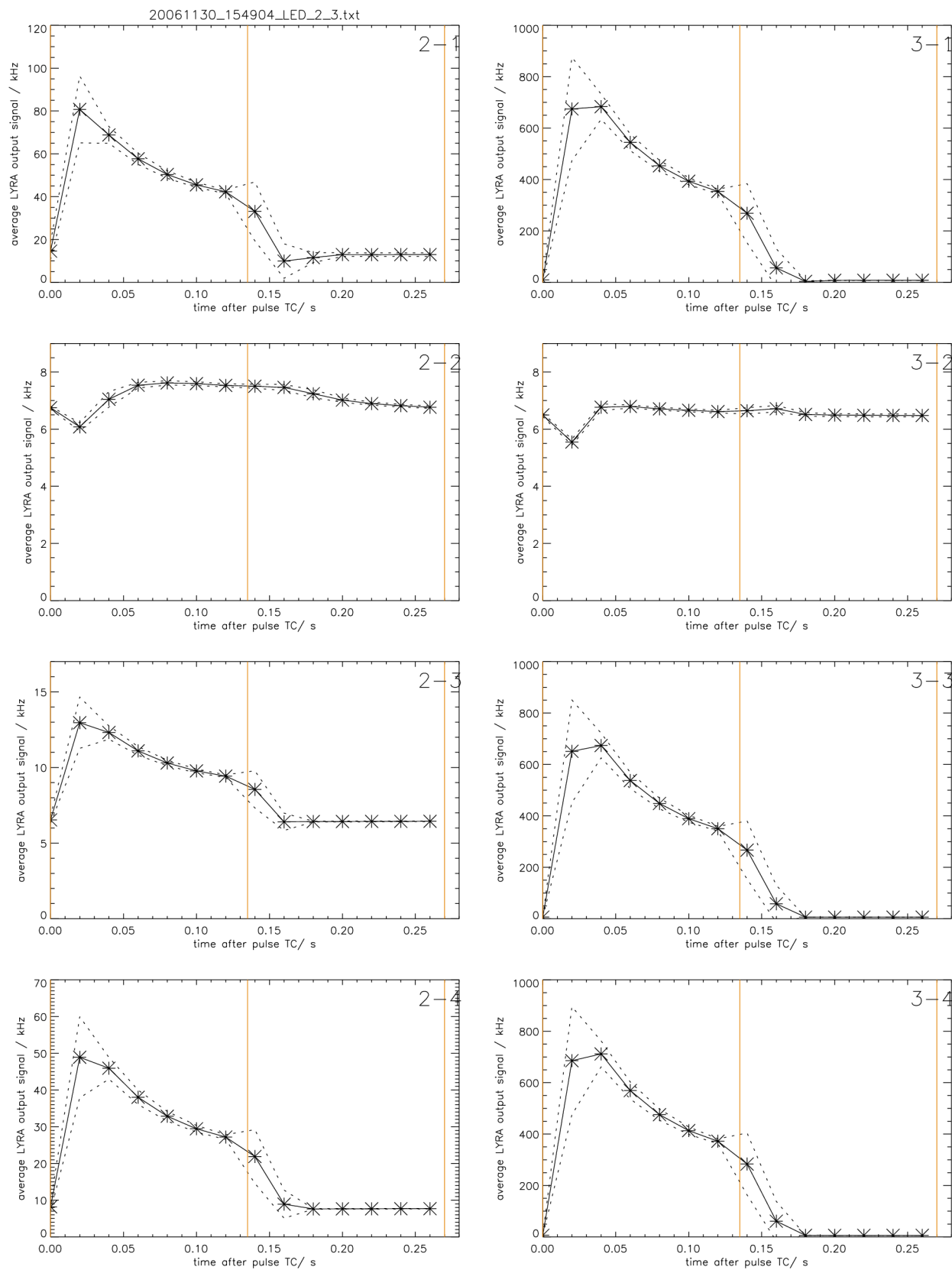


Figure 2b: Average pulses from second test (heads 2 and 3)

Pulse Fitting

In previous campaigns, other LED tests were performed: without pulses, but exposing the detectors to visual, ultraviolet, or both LEDs, constantly for 200 to 300 s instead of 0.135 s, and with an integration time of 500 ms instead of 20 ms. To make the short pulses comparable with longer LED exposures (details of those will be subject of another report, TBD), the decay phase was fitted to estimate the longer term (500 ms) expected behaviour.

Since value #1 is apparently not influenced by LEDs and value #2 may be influenced by partial exposure, values #3 to #7 were selected; these average signal values of the decay phase were fitted to a negative exponential function plus an offset value N1, since the offset obviously is not zero:

$$N(t) = N1 + N0 * \exp(-\lambda * t) , t=1,2,3,\dots$$

where t is the number of 20-ms-integration times that have passed since cycle start (the scale is arbitrary, though). All MSM and AXUV channels could be fitted well to this function.

When the fit is integrated from step 1 to step 25 (i.e., 25 times 20 ms), the resulting value should correspond to a value observed with 500 ms integration time; in reality, the integrated fit is mostly an over-estimation (see below). An additional problem for comparison also remains: The long-term tests do not reach their plateau value immediately, so the fitted integral should correspond to an “early” response in the rising phase. This is not yet a well-defined value (TBD). - Signal output values are in kHz. - Since the behaviour of the PIN detectors appears to be more complicated, they could not be fitted in this way.

Parameters resulting for fittings of the first test (heads 1 and 2):

ch.	detect.	N1	ln(N0)	lambda	peak	integr.
1-1	MSM12	16.7	3.44047	-0.390777	37.8090	19.3102
1-2	PIN10					
1-3	MSM11	27.0	4.19763	-0.400151	71.5885	32.4080
1-4	AXUV20D	286.	6.88130	-0.399094	939.410	365.421
2-1	MSM21	35.9	4.35720	-0.392950	88.7220	42.3847
2-2	PIN11					
2-3	MSM15	8.63	2.09247	-0.399472	14.0657	9.29019
2-4	MSM19	22.1	3.94645	-0.402322	56.7096	26.2793

Parameters resulting for fittings of the second test (heads 2 and 3):

ch.	detect.	N1	ln(N0)	lambda	peak	integr.
2-1	MSM21	36.0	4.31767	-0.413608	85.6036	41.8572
2-2	PIN11					
2-3	MSM15	8.77	2.10687	-0.420774	14.1683	9.39868
2-4	MSM19	22.9	3.97593	-0.419727	57.9298	26.9877
3-1	AXUV20A	277.	6.84147	-0.417142	893.666	349.319
3-2	PIN12					
3-3	AXUV20B	275.	6.82147	-0.416800	879.662	345.958
3-4	AXUV20C	292.	6.86724	-0.413912	926.811	366.915

Figures 3a and 3b show the original data averages and the fits, calculated as described above.

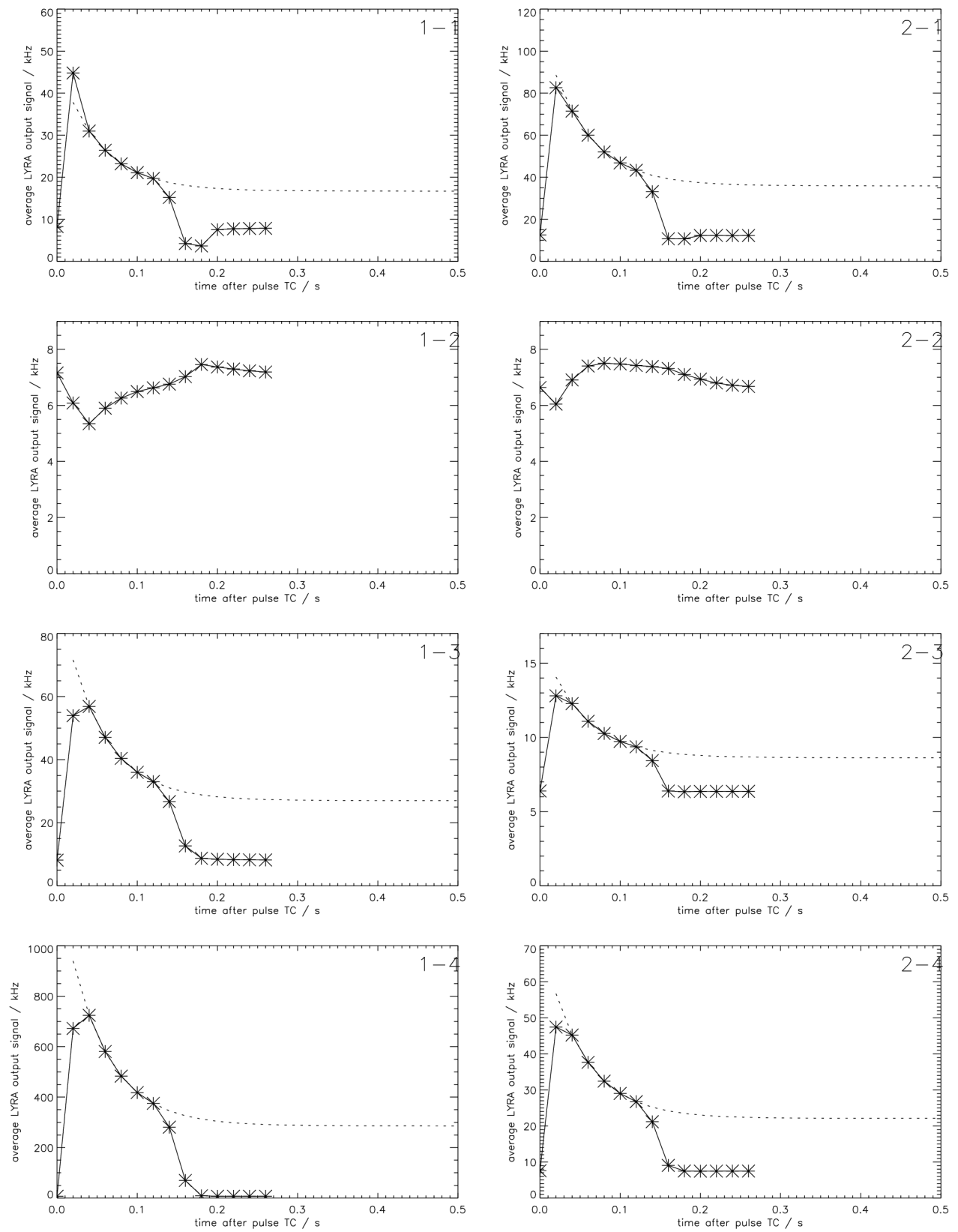


Figure 3a: Average pulses and fits of their decay phase from first test (heads 1 and 2)

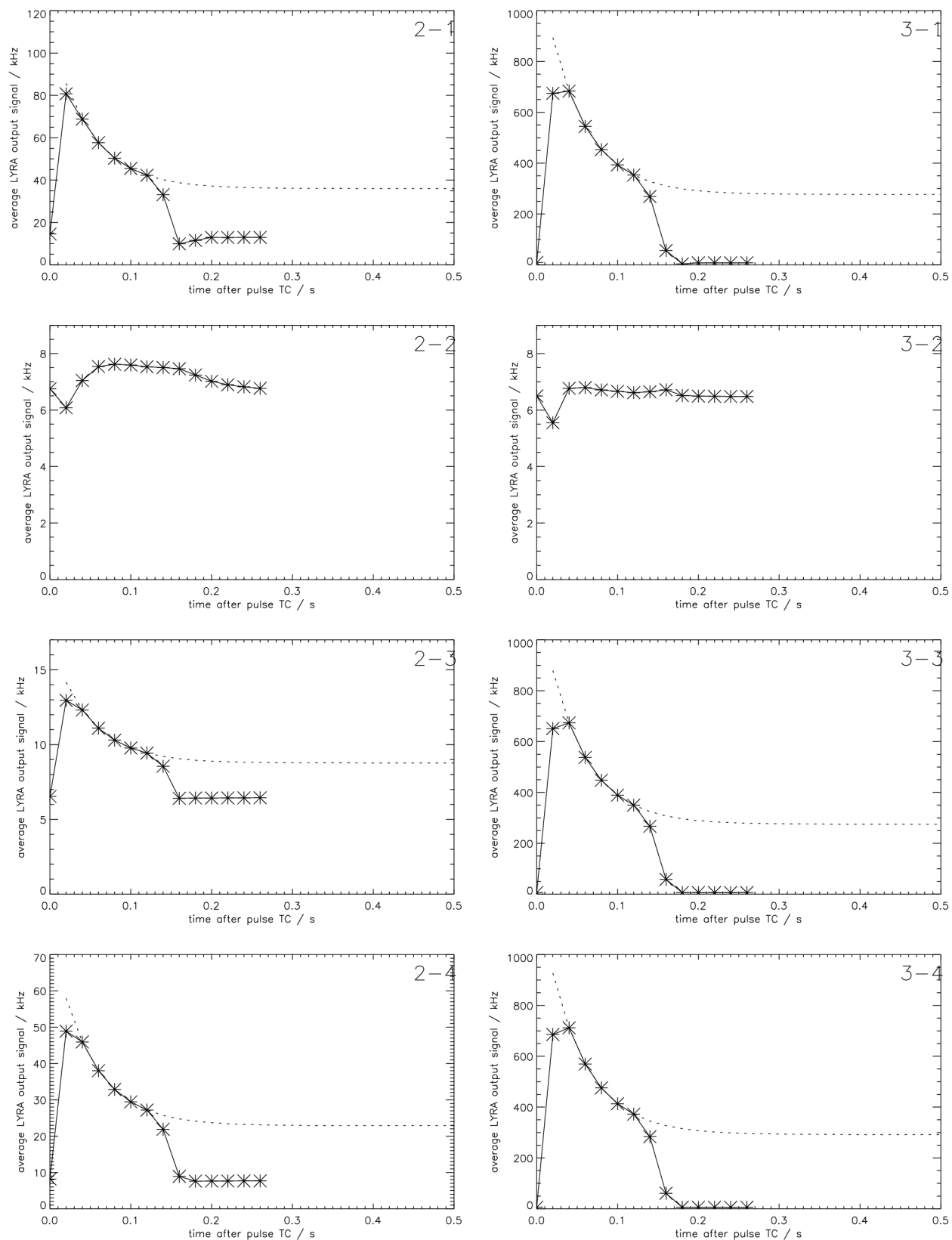


Figure 3b: Average pulses and fits of their decay phase from second test (heads 2 and 3)

The curve fits quantitatively confirm the qualitative descriptions of the MSM and AXUV detectors as stated in the preceding section. AXUV channels are more sensitive than the rest, they are more similar within their group, and their fitted peaks are always higher than their observed ones. But while they differ significantly concerning their response level, all fitted detectors show a similar decay-time constant λ between 0.39 and 0.42, which leads to a half-life period $\ln(2)/\lambda$ that corresponds to 0.035 and 0.033 s. Apparently, λ is also influenced by the test situation, since in the first test all values are between 0.39 and 0.40, and in the second test between 0.41 and 0.42.

Dark current values generally show quite similar values around 7 kHz, except for channel 2-1 which starts at the same level but then displays an upward drift.

In the following tables, the observed dark currents as well as the fitted integrals and plateau values (N1) shall be compared to previous tests that, similarly, involved observations with visual LEDs being switched on/off simultaneously. - In the case of PIN detectors, there are no fits to be compared. - Signal output values again are in kHz.

ch. detect.	other d.curr. observations	pulsLED d.curr.	other visLED observations	pulsLED integr.	pulsLED N1
1-1 MSM12	11.1658, 9.22659 10.6844, 10.6269 10.3702, 10.4285	7.86285	23.3795, 22.8930 19.1523, 18.5131 19.1358, 18.7857	19.3102	16.7
1-2 PIN10	6.44996, 6.59550 6.63115, 6.66208 6.65890, 6.65697	7.18899	6.67447, 6.86322 6.84703, 6.85157 6.92472, 6.92376		
1-3 MSM11	6.78523, 6.72557 6.80128, 6.85230 6.80939, 6.81642	8.18120	26.5878, 26.3113 26.3990, 26.2870 26.4411, 26.3905	32.4080	27.0
1-4 AXUV20D	7.39418, 7.35195 7.42589, 7.45969 7.43740, 7.44233	6.96560	273.841, 274.501 273.682, 273.114 273.601, 273.439	365.421	286.
2-1 MSM21	9.23316, 11.1333 15.0305, 15.2642	12.6185	40.3351, 42.8437 40.0283, 40.4900	41.1210	36.0
2-2 PIN11	6.48632, 6.28414 7.26520, 7.25548	6.72115	7.20643, 6.99099 7.94379, 7.96931		
2-3 MSM15	6.53941, 6.60026 5.50406, 7.32362	6.40228	8.72980, 8.58040 9.31379, 9.94156	9.34444	8.70
2-4 MSM19	9.81032, 10.1347 14.7513, 15.1552	7.58307	23.9713, 23.4299 32.7083, 30.7159	26.6335	22.5
3-1 AXUV20A	12.9890, 13.0470 19.8355	8.23991	262.668, 263.144 265.986	349.319	277.
3-2 PIN12	6.21992, 6.22710 7.07478	6.48114	6.78283, 6.55599 7.41072		
3-3 AXUV20B	6.28770, 6.28072 4.94285	6.35307	253.398, 253.004 248.342	345.958	275.
3-4 AXUV20C	5.94563, 5.93051 6.13887	6.31553	274.385, 274.090 272.047	366.915	292.

Parameters observed or fitted in the pulsed-LED tests are averages of approx. 200 cycles of 20 ms integration time. Parameters are taken from the first test for head 1, from the second test for head 3, and averaged from both tests for head 2. They are compared to 500 ms observations of dark currents and LED levels as recorded on 17 and 29 Mar 2006 during BESSY campaigns. Appropriate intervals were selected for comparison: visual LEDs switched on, but

no beam signal; approx. 200 values averaged from plateau phase, if possible.

Several of these previous observations are listed to demonstrate the variability, or - in some cases - the reliability of the tests.

For the table above, the final values (#14) of the LED-test averages are taken as estimates for the dark current. In the case of PIN detector 1-2, this is probably an over-estimate, because this channel has not finished its decline phase yet. Other cases are more complicated and involve drifts or possible temperature effects. This can be analyzed further, if necessary.

In most cases, the plateau values (N1) of the fits – rather than the integrals - correspond better with the LED values from the other tests and are therefore used for comparison in the following table. To compare the net effect of LEDs quantitatively, the various dark current levels have been subtracted (“diff” columns). For simplicity reasons, values were averaged and rounded to one decimal digit. - Values are in kHz:

ch.	detect.	d.c. obs.	d.c. fit.	LED obs.	LED fit.	diff obs.	diff fit.
1-1	MSM12	10.4	7.9	20.3	16.7	9.9	8.8
1-2	PIN10	6.6	7.2	6.9		0.3	
1-3	MSM11	6.8	8.2	26.4	27.0	19.6	18.8
1-4	AXUV20D	7.4	7.0	273.7	286.0	266.3	279.0
2-1	MSM21	12.7	12.6	40.9	36.0	28.2	23.4
2-2	PIN11	6.9	6.7	7.5		0.6	
2-3	MSM15	6.5	6.4	9.1	8.7	2.6	2.3
2-4	MSM19	12.5	7.6	27.7	22.9	15.2	15.3
3-1	AXUV20A	15.3	8.2	263.9	277.0	248.6	268.8
3-2	PIN12	6.5	6.5	6.9		0.4	
3-3	AXUV20B	5.8	6.4	251.6	275.0	245.8	268.6
3-4	AXUV20C	6.0	6.3	273.5	292.0	267.5	285.7

As a result, it can be observed that the fits of the pulsed tests...

- usually estimate the dark current levels well, around 7 kHz
- follow the trend of the dark current level and estimate it correctly in the case of channel 2-1
- do not follow the trend and thus underestimate it in the case of channels 1-1, 2-4, and 3-1
- tend to underestimate the net LED effect (dark current subtracted) in the case of the MSM detectors: -11%, -4%, -17%, -12%, 0%
- tend to overestimate the net LED effect in the case of the AXUV detectors: +5%, +8%, +9%, +7%, relative to the long-term observations.

For PIN detectors, LED pulsing apparently cannot be used to estimate exact values of decay time constants, or LED output signals, but this kind of test can nevertheless be used to estimate the overall reaction level (e.g., to measure degradation or temperature effects).

Documents used:

BRUSAG: LYRA Software Manual (SUM), Version 1.04 of 15 Mar 2005

Files used:

20061130_154729_LED_1_3.txt
 20061130_154904_LED_2_3.txt

6. Noise Distribution

Three data sets were analyzed to study the effects of different integration times on LYRA response. There are additional tests from the BESSY NI campaign in March 2006, but the following appeared most suitable:

20060317_134432_H2C3_SignalvsIntegTime.txt was observed during the BESSY GI campaign in March 2006. It contains signals from head 2, with a beam signal applied to channel 2-3. The integration time was stepped down through all possible LYRA values: 10 s, 5 s, 2 s, 1 s, 0.5 s, 0.2 s, 0.1 s, 0.05 s, 0.02 s, 0.01 s. The general behaviour is demonstrated in Figure 1.

20060317_173337_H3C3_SIGNALvsIntegTime.txt was observed during the same campaign. It contains signals from head 3 and head 2 in parallel, with a beam signal applied to channel 3-3. The integration time was stepped as above, see Figure 2.

20061213_084925_test_IT.txt was observed in Davos in December 2006. It contains dark-current signals from head 1. The integration time was stepped from long to short and back to long, 10 s,..., 0.01 s,..., 10 s, see Figure 3.

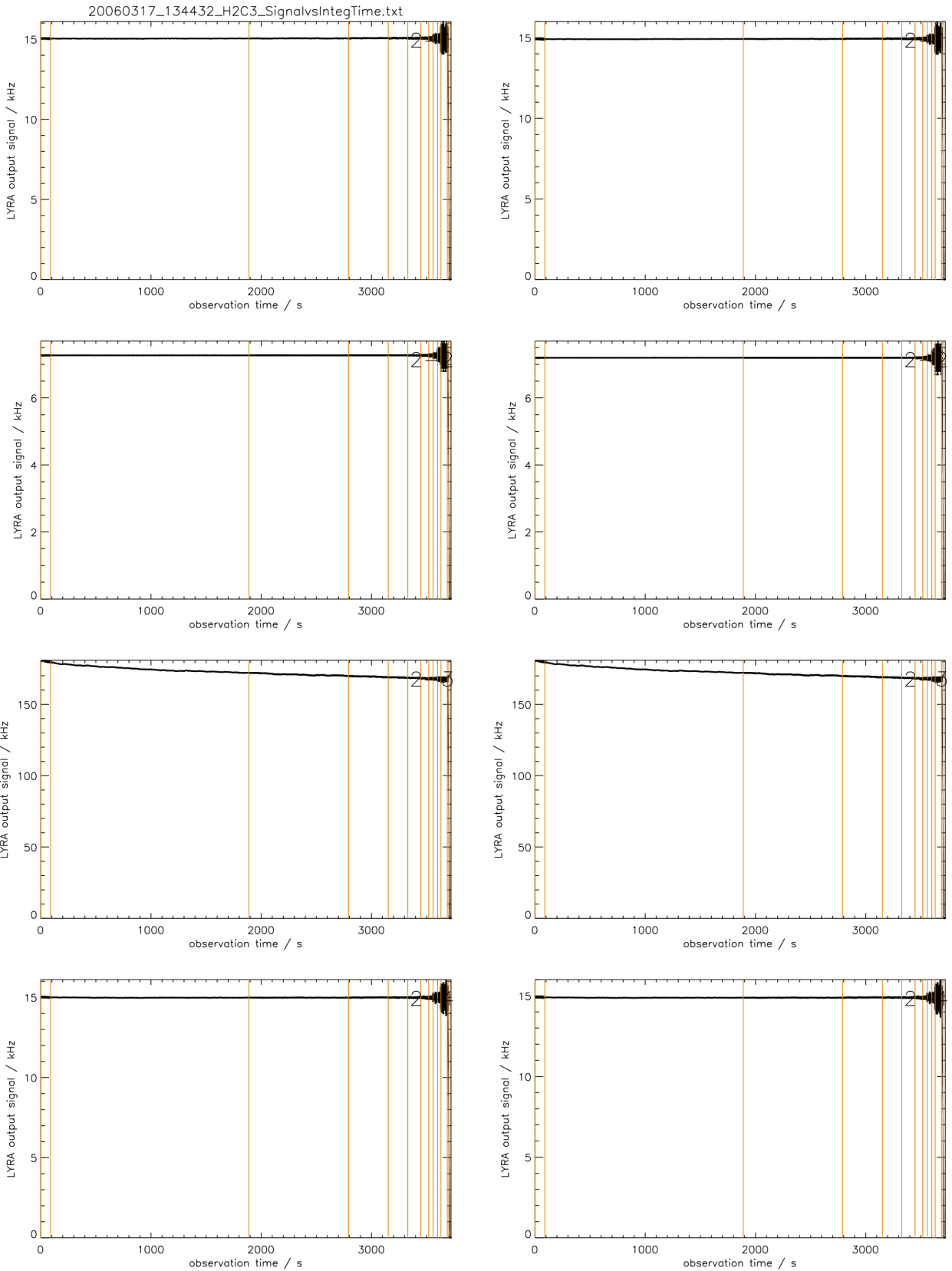


Figure 1: Signal vs. integration time for head 2; BESSY beam on channel 2-3, dark currents otherwise. Red lines mark changes of integration time, which is stepped down from 10 s to 0.01 s.

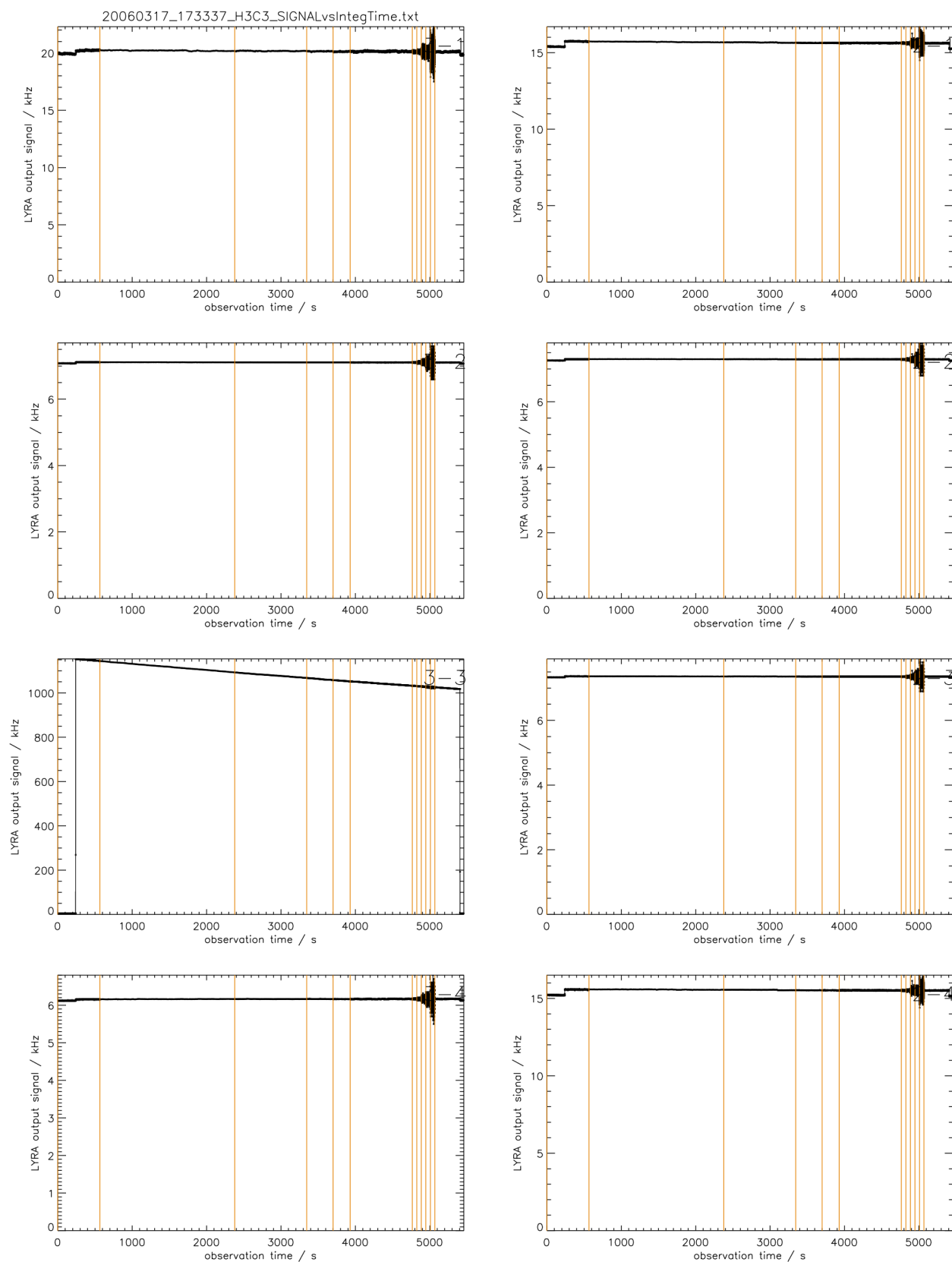


Figure 2: Signal vs. integration time for heads 3 and 2; BESSY beam on channel 3-3, dark currents otherwise. Red lines mark changes of integration time, which is stepped down from 10 s to 0.01 s.

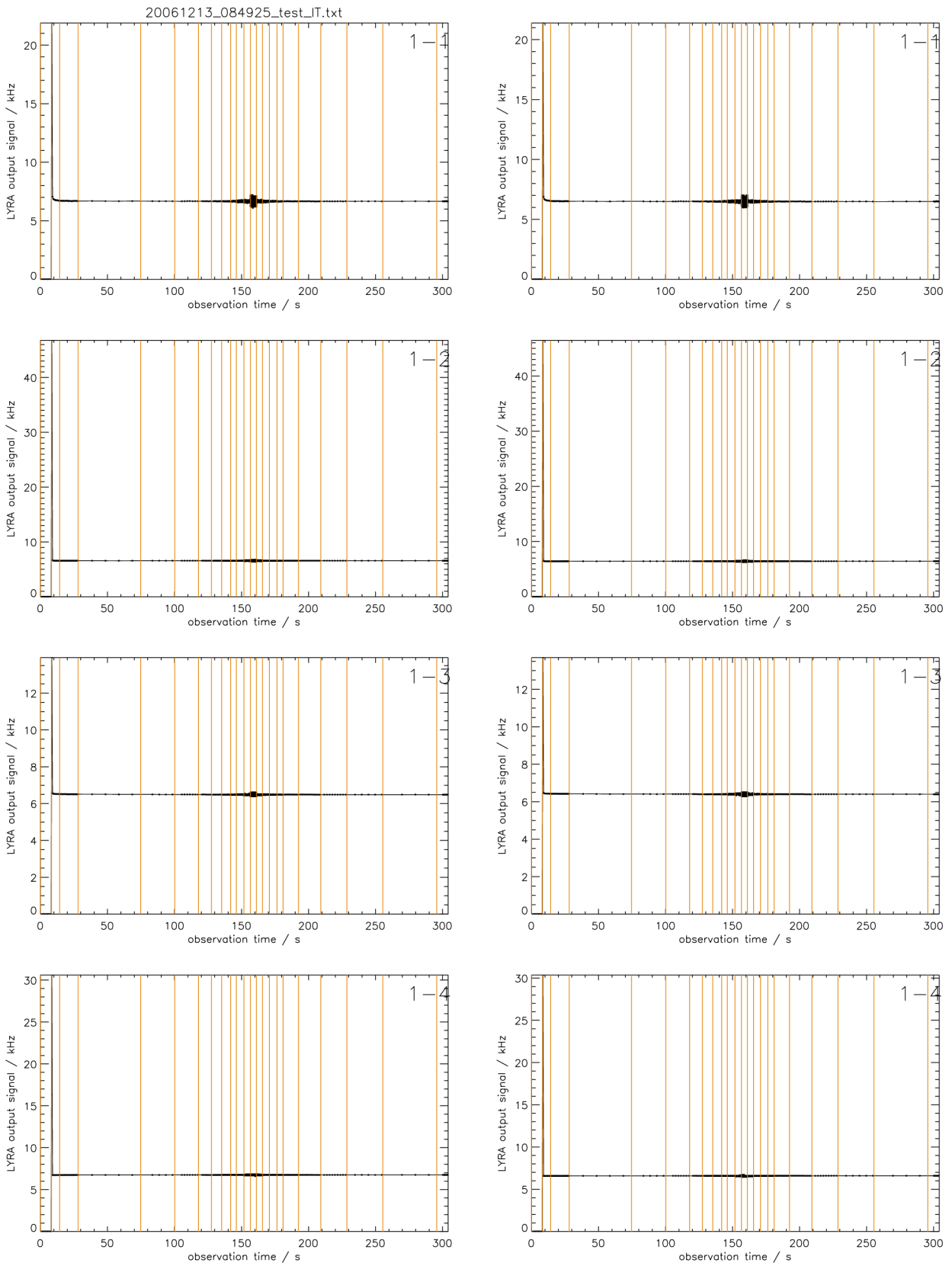


Figure 3: Signal vs. integration time for head 1; only dark currents. Red lines mark changes of integration time, which is stepped down from 10 s to 0.01 s, and up to 10 s again.

First, the beam signals in channels 2-3 and 3-3 were analyzed. Their properties are demonstrated in Figure 4. There is clearly a downward drift in both cases, which is known to be caused by the drift in the beam current, so it says nothing about possible drifts in the LYRA detectors; for this problem, see another document: *LYRA Signal Stability: Report (rev. 04 Dec 2006)*.

Channel 3-3 (Al filter + AXUV detector) shows a higher output level than channel 2-3 (Al filter + MSM detector). This is confirmed by other tests. Channel 3-3 shows irregular fluctuations with a deviation of approx. $\pm 0.05\%$ around the trend, and some degree of noise. Channel 2-3 shows a sinus curve of approx. 20 s period and 0.1 % amplitude around the trend, and also some degree of noise. This sinus type of fluctuation can also be observed in other beam tests taken with channel 2-3, but it can *not* be observed in tests taken with the same beam, on the same day, with channel 3-3, or – so far – in any other channel (more detailed analysis TBD). So it is probably not a fluctuation in the beam signal.

On the other hand, the sinus curve can *not* be observed in the dark current of channel 2-3, or in its reaction to LED signals, nor can it be observed in the reaction to a longer-wavelength beam (BESSY NI campaign). The latter leads to a much lower signal, caused by a much lower responsivity for longer wavelengths. Therefore, it may be concluded that the sinus fluctuation is a property of the MSM detector of channel 2-3 in the presence of a strong signal.

As visible in Figure 4, at integration times shorter than 0.2 s, a different kind of noise takes over. To analyze this type of noise, the values for the shortest integration time, 0.01 s, were adjusted by the trend and fitted to a Gaussian. The results for channels 2-3 and 3-3 are demonstrated in Figures 5 and 6. It can be concluded that the signal values with short integration times roughly follow a Gaussian - or, to be exact, since they are counts, i.e. integer values, a Poisson distribution. The width depends on the count level.

But these findings only hold for sufficiently high count rates and cannot be extended, e.g., to dark currents with just three different output values (see below).

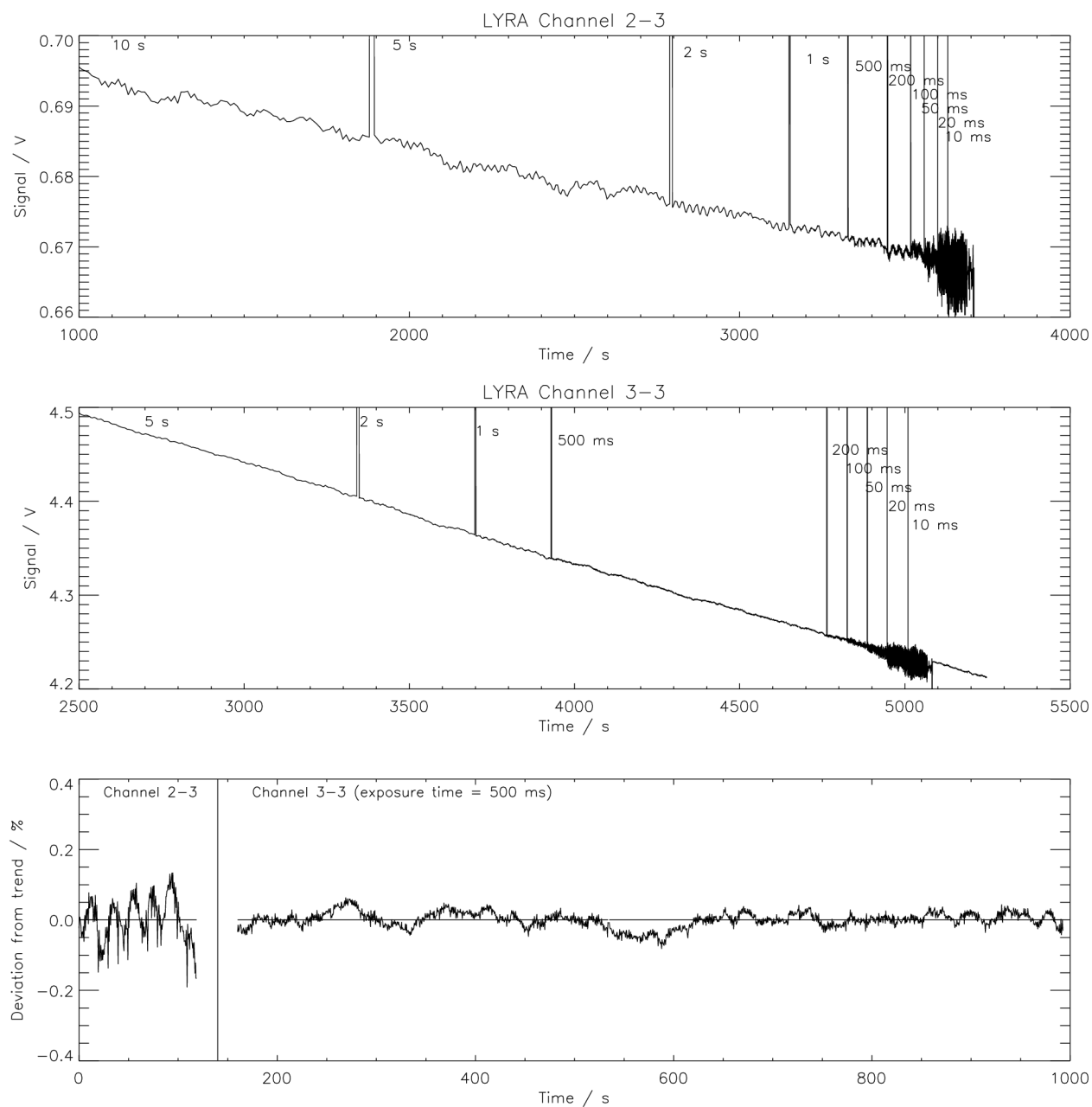


Figure 4: The upper images demonstrate the lower parts of the test data generated with a BESSY beam on channels 2-3 and 3-3. Integration times are marked at the begin of their intervals. - The lower image shows the resp. intervals with 0.5 s integration time, the trend being removed.

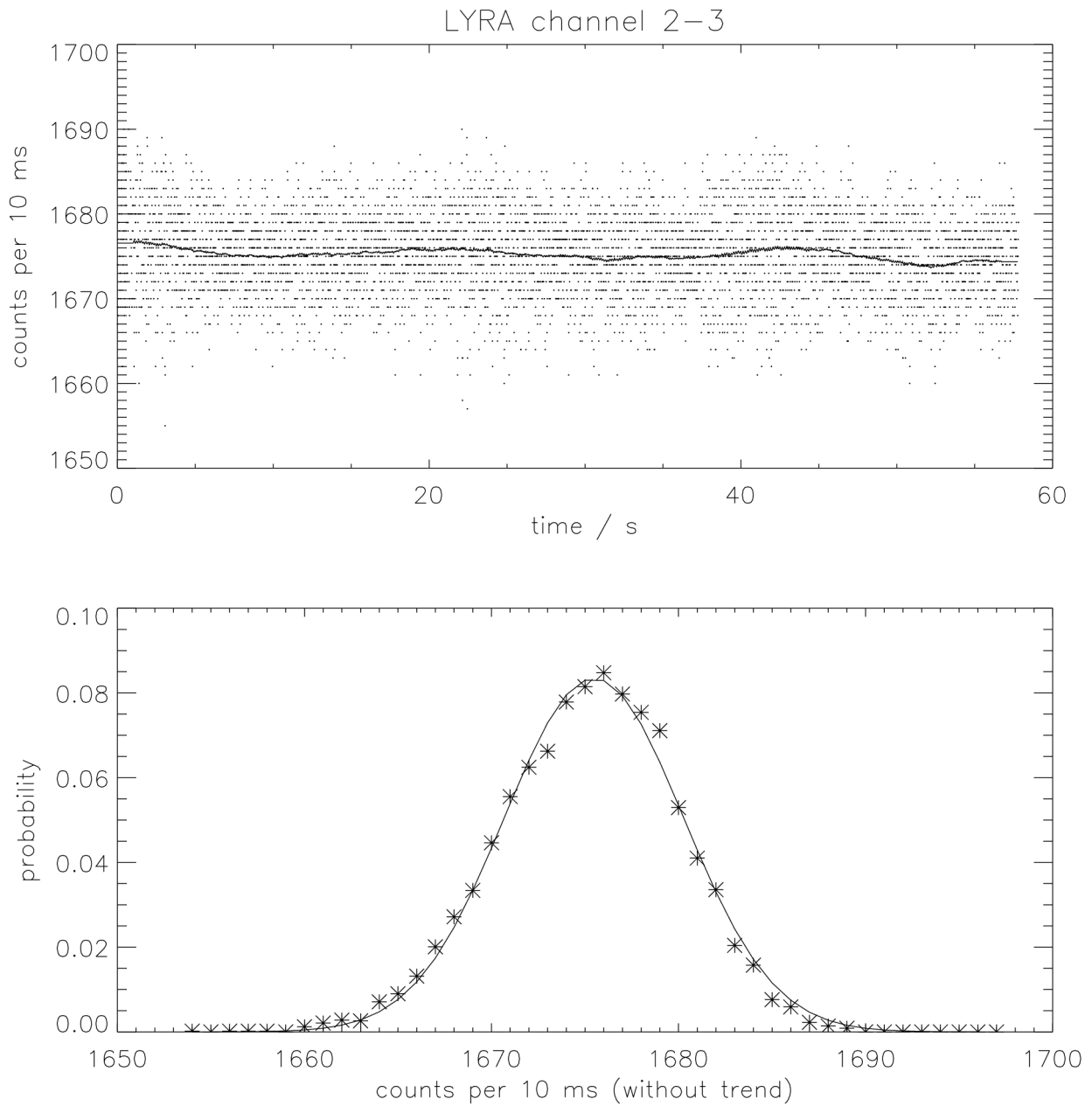


Figure 5: The upper image shows the result of approx. one minute observation of the beam on channel 2-3, with 0.01 s integration time (dots are raw data, the line denotes the trend). - In the lower image, the asterisks denote the histogram of realized counts (trend removed), while the line is a Gaussian fit. The mean of the raw data is 1675.23, the mean of the Gaussian is 1675.48, and the standard deviation is 4.79.

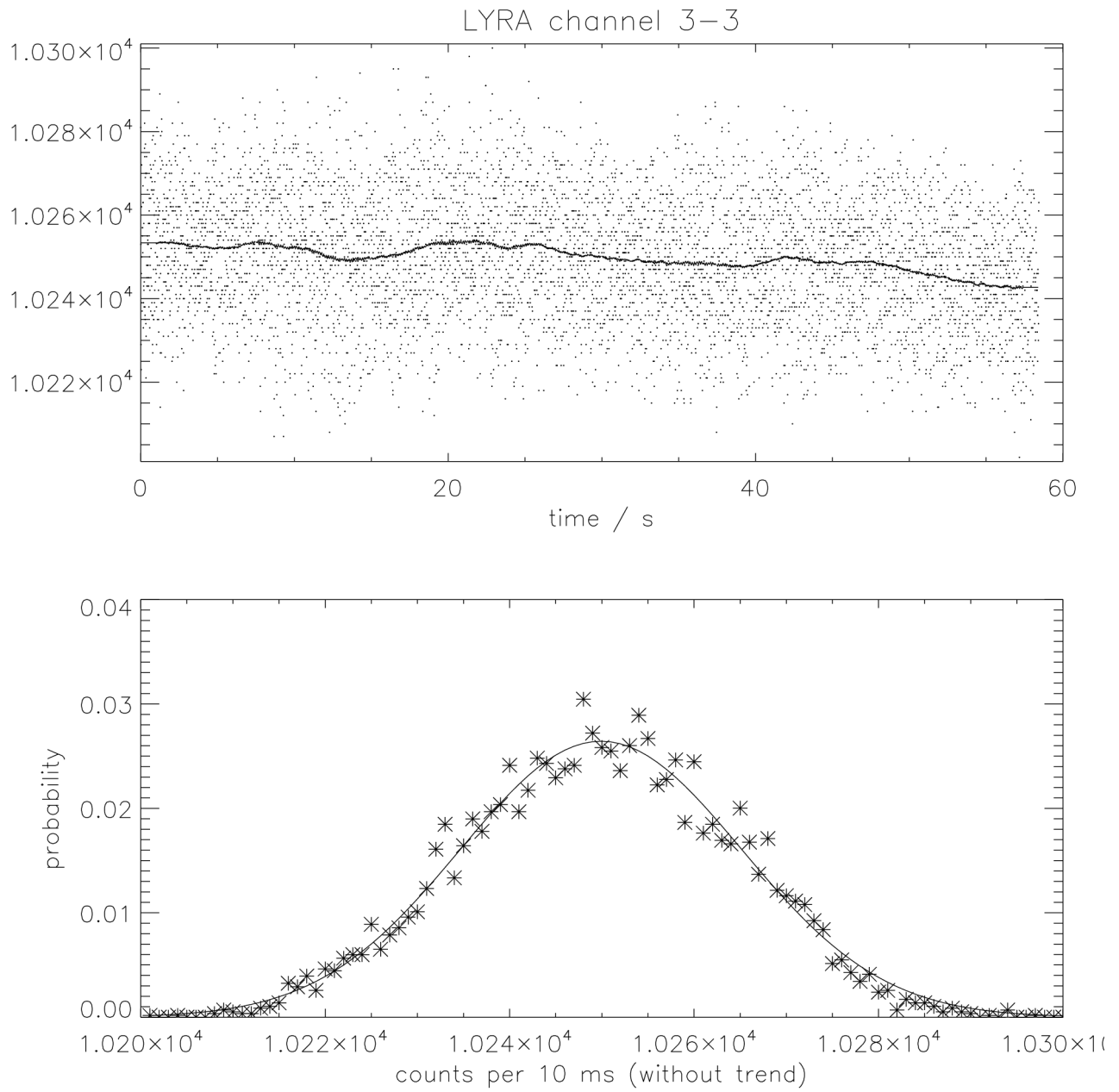


Figure 6: The upper image shows the result of approx. one minute observation of the beam on channel 3-3, with 0.01 s integration time (dots are raw data, the line denotes the trend). - In the lower image, the asterisks denote the histogram of realized counts (trend removed), while the line is a Gaussian fit. The mean of the raw data is 10249.7, the mean of the Gaussian is 10249.9, and the standard deviation is 15.29.

There remains one more problem to be analyzed. Does frequency depend on integration time, or in other words, can LYRA signals be recorded in an arbitrary cadence, and afterwards, for example, can 100 values taken at 0.01 s just be added up to receive the appropriate value for 1 s?

To answer this question, the signal values were averaged within their integration-time bins. As a result, the averages of low integration times (i.e. below 0.2 s) can be observed to drop. This can be explained and corrected with the dead-time value, i.e. the amount of time within the integration interval which is needed to read out the integrated data value. According to PMOD, where LYRA was built, a dead time of 10.5807 microseconds must be removed from the integration times; this dead time is the same for all integration times.

Therefore, it is possible to correct for the dead-time effect in given LYRA frequency values as follows (implying that frequencies are currently calculated as counts per nominal integration time):

$$[\text{corrected LYRA signal} / (\text{count/s})] = [\text{LYRA signal} / (\text{count/s})] * [\text{int.time} / \text{s}] / ([\text{int.time} / \text{s}] - 0.0000105807)$$

where *int.time* can be any possible nominal integration time between 10 s,...,0.01 s. Thus, the highest possible correction – at 0.01 s integration time – is approx. +0.1%.

One example is shown in Figure 7. Other examples appear less smooth, because at the rather low dark-current levels, the output sometimes oscillates between just three or four integer values (counts per integration interval). On the other hand it is also possible that the output oscillates between two clusters of three or four output values each; this was observed for MSM channels 1-1, 2-2, and 2-4.

The general behaviour of the averages – raw and corrected - within their integration-time bins is demonstrated in Figures 8, 9, and 10, for the three test sets. Values of dark currents roughly agree with values found in the previous chapter. - One should also note that the second multiplexer, while reading the same channel (see right sides of Figures 8 and 10), records around 0.1 kHz less than the first one.

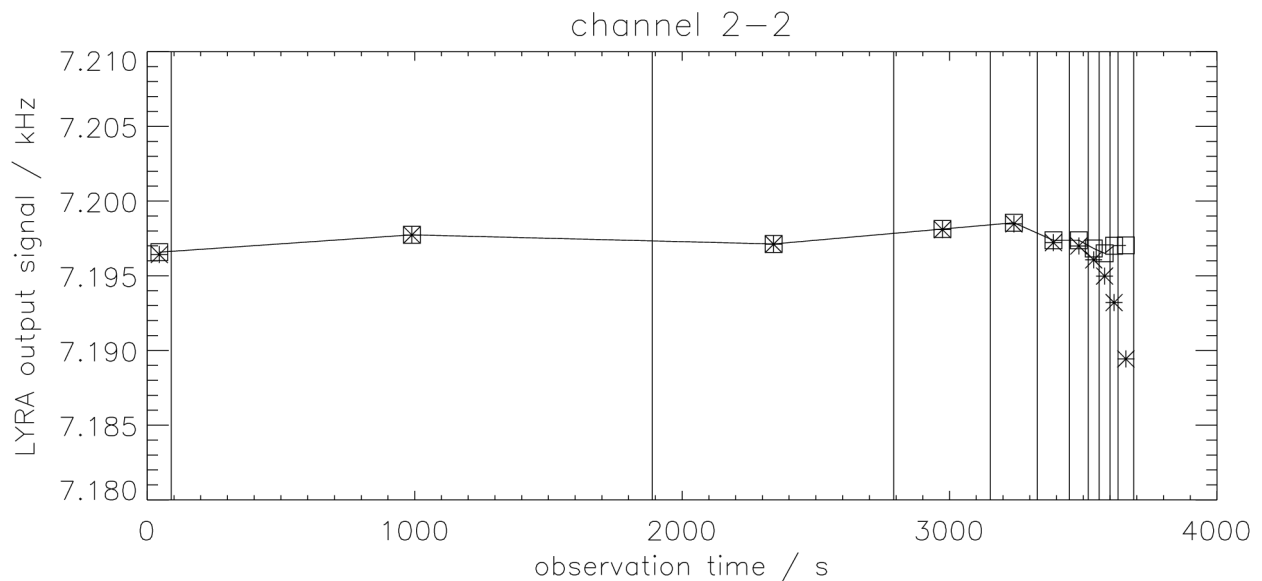


Figure 7: Signal averages in bins of integration time, as calculated for channel 2-2; from left to right, beginning with a short set of 0.5 s, integration times are stepped from 10 s down to 0.01 s. Asterisks mark raw frequency values, squares are corrected for dead time.

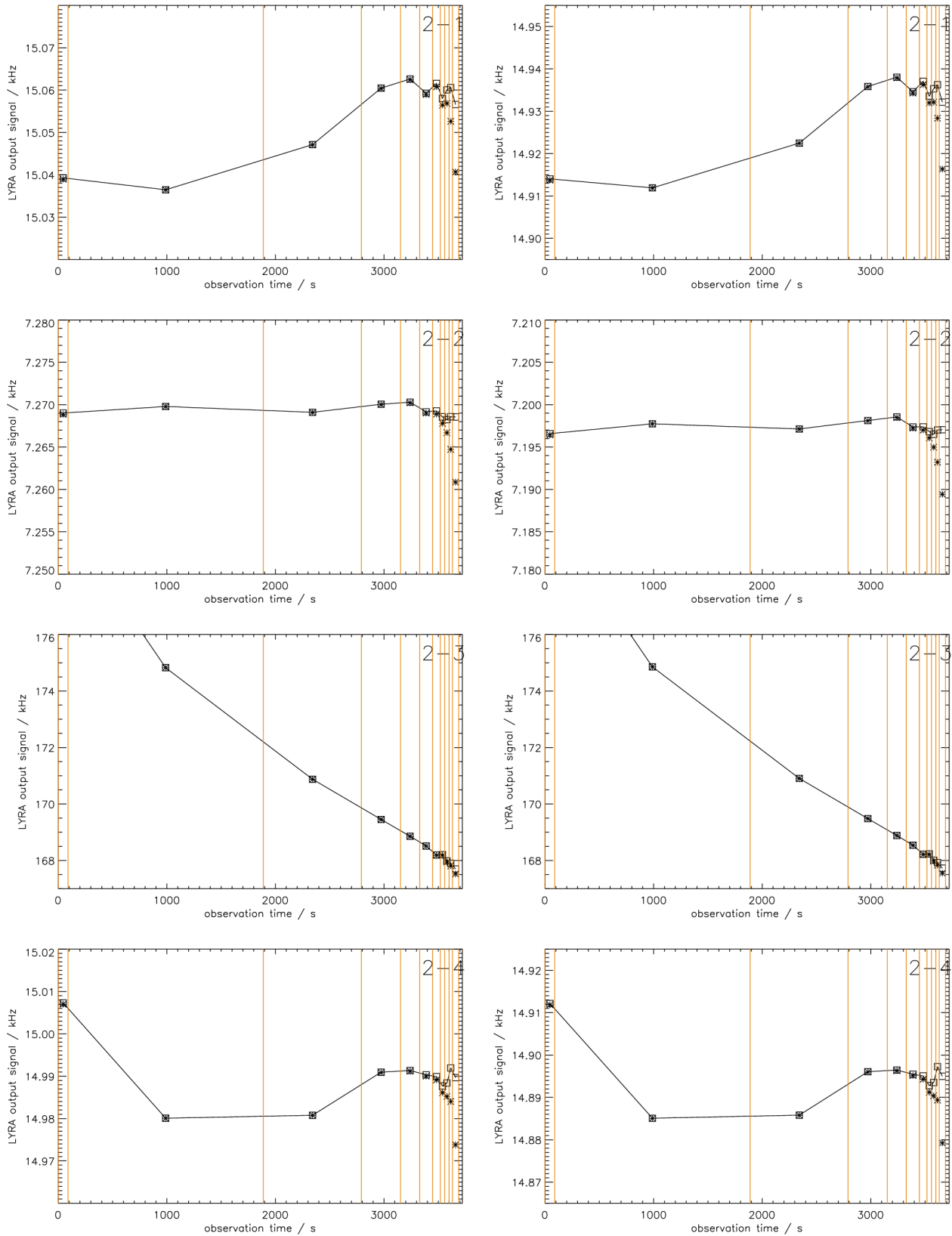


Figure 8: Signal averages in bins of integration time, for head 2; BESSY beam on channel 2-3, dark currents otherwise. Red lines mark changes of integration time, which is stepped down from 10 s to 0.01 s.

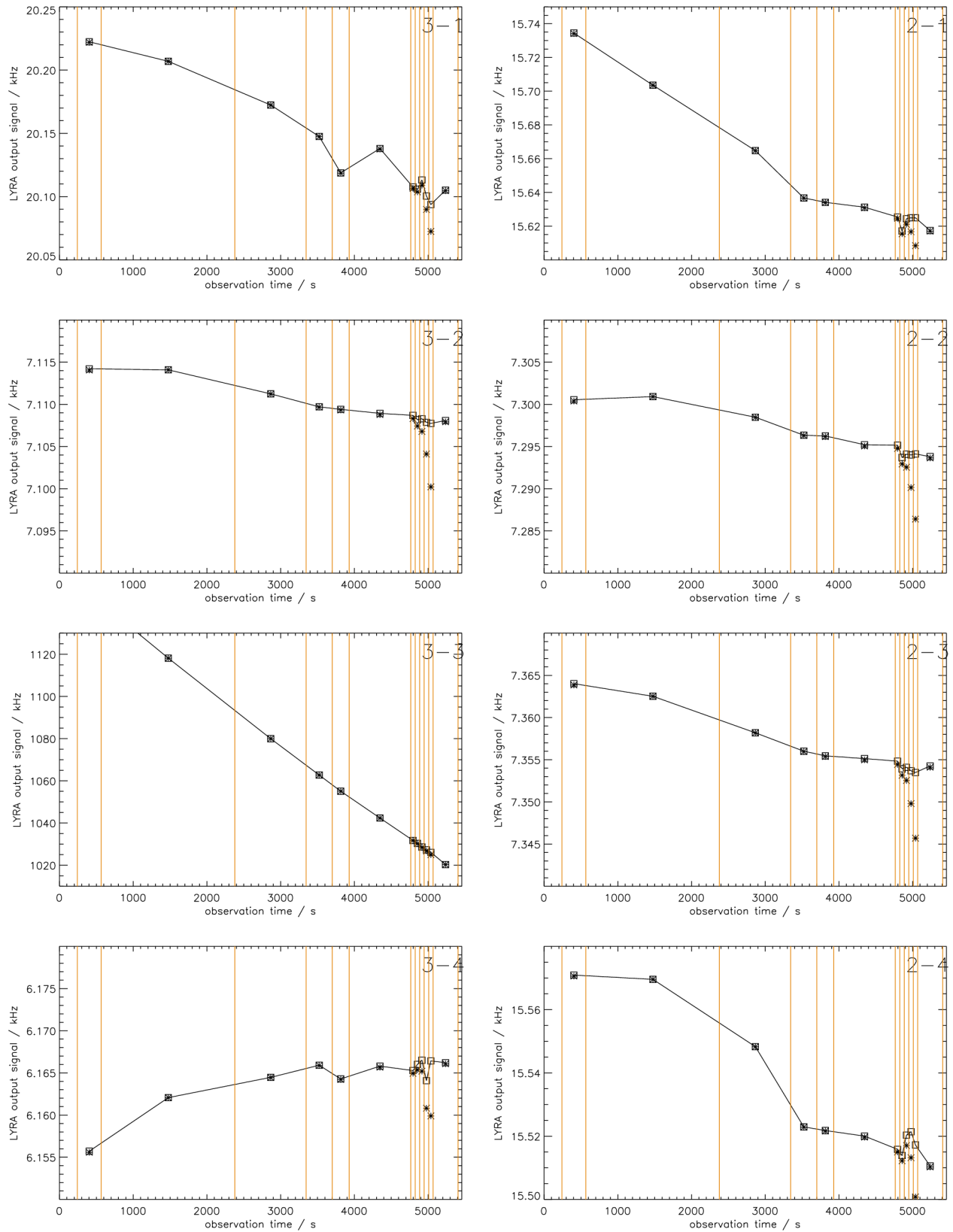


Figure 9: Signal averages in bins of integration time, for heads 3 and 2; BESSY beam on channel 3-3, dark currents otherwise. Red lines mark changes of integration time, which is stepped down from 10 s to 0.01 s.

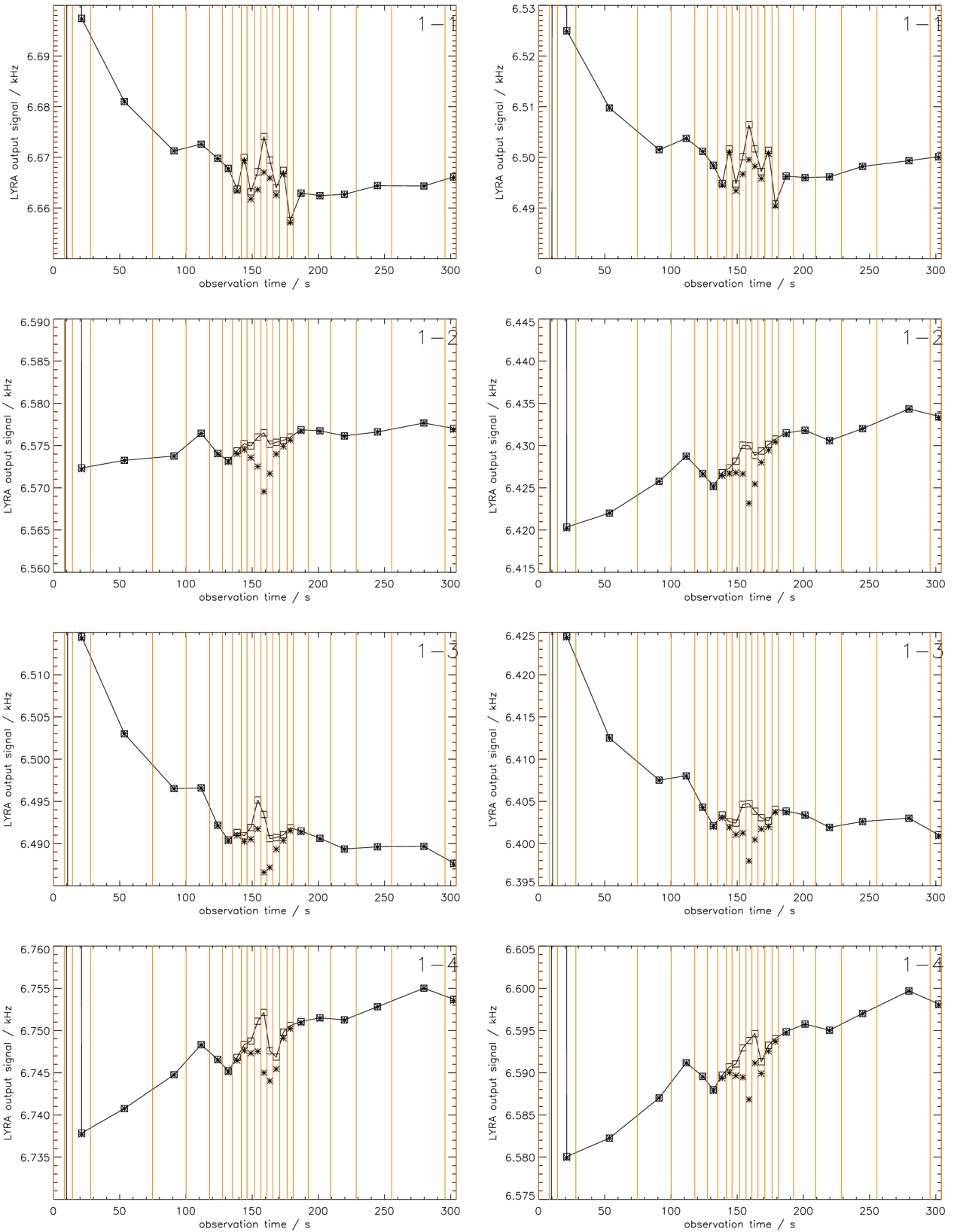


Figure 10: Signal averages in bins of integration time, for head 1; only dark currents. Red lines mark changes of integration time, which is stepped down from 10 s to 0.01 s, and up to 10 s again.